A STUDY OF THE EFFECT OF HARMONICS IN THE SYSTEM ON THE PERFORMANCE OF RESIDUAL CURRENT-OPERATED CIRCUIT-BREAKERS AND ELECTROMECHANICAL OVERCURRENT RELAYS

ASHWIN SASONGKO SASTROSUBROTO

Doctor of Philosophy

THE UNIVERSITY OF ASTON IN BIRMINGHAM

August 1989

THE UNIVERSITY OF ASTON IN BIRMINGHAM

A STUDY OF THE EFFECT OF HARMONICS IN THE SYSTEM ON THE PERFORMANCE OF RESIDUAL CURRENT-OPERATED CIRCUIT-BREAKERS AND ELECTROMECHANICAL OVERCURRENT RELAYS

Summary

Residual current-operated circuit-breakers (RCCBs) have proved useful devices for the protection of both human beings against ventricular fibrillation and installations against fire. Although they work well with currents of a sinusoidal waveform, there is little published information on their characteristics. Due to non-linear devices, not the least of which is the use of power electronic equipment, the mains supply is distorted. Consequently, RCCBs as well as other protection relays are subjected to non-sinusoidal currents. Recent studies have shown that RCCBs are affected by harmonics, however the reasons for this are not clear. A literature search has also shown that there are inconsistencies in the analysis of the effect of harmonics on protection relays.

In this work, the way RCCBs operate is examined, then a model is built with the aim of assessing the effect of non-sinusoidal current on RCCBs. Tests are then carried out on a number of RCCBs and these, when compared with the results from the model showed good correlation. In addition, the model also enables us to explain the RCCBs characteristics for pure sinusoidal current.

In the model developed, various parameters are evaluated but special attention is paid to the instantaneous value of the current and the tripping mechanism movement. A similar assessment method is then used to assess the effect of harmonics on two types of protection relay, the electromechanical instantaneous relay and time overcurrent relay (referred to in BS 142 as an all-or-nothing relay and a single input energising quantity measuring relay with dependent specified-time respectively). A model is built for each of them which is then simulated on the computer. Test results compare well with the simulation results, and thus the model developed can explain the relays behaviour due to harmonics in the system.

The author's models, analysis and tests show that RCCBs and the two protection relays are affected by harmonics in a way determined by the current waveform and the relay constants. The method developed provides a useful tool and the basic methodology to analyse the behaviour of RCCBs and protection relays due to harmonics in the system. These results have many implications, especially the way RCCBs and relays should be tested if harmonics are taken into account.

Keywords : Circuit Breaker, Protection, Relay, Harmonics, Earthing

Author : ASHWIN SASONGKO SASTROSUBROTO

For the degree of DOCTOR OF PHILOSOPHY

1989

Acknowledgement

I would like to express my sincere thanks to my supervisor Dr. A.M. Featherstone for all his advice, suggestions, discussions and especially his continuous encouragements. I would also like to thank those who have given help in this project, particularly my advisor Professor W.T. Norris, Mr. B. James and Mr. B. Davison for all their helpful suggestions and discussions during the project.

I am also grateful to Mr. B. Challenger and his colleagues at Crabtree Electrical Industries Ltd for helpful discussions and guidance.

Many thanks to Mr. B. Harrison, Mr. L. Radford, Mr. C. Hutton and Mr. J. Thomas for all their help in the laboratory work.

I would like also to thank the Government of the Republic of Indonesia for financial support, the Indonesian Institute of Sciences (LIPI) for leave of absence and Aston University for equipment and facilities.

Finally, I would like to thank my wife Yannie and my children Ashni and Ashyafat for all their encouragements, supports and especially for allowing me a lot of their time.

List of Contents

List of Tables

List of Figures

List of Symbols

General :

n = Harmonic number, n = 1 fundamental

f_n = $n f_1$ = Frequency of the n^{th} harmonic, Hz

ω_n = $n\omega_1$ = Angular frequency of the n^{th} harmonic, rad/s

i_n = The current at frequency f_n

I_n = The r.m.s. value of i_n

∂_n = The phase angle between the fundamental and n^{th} harmonic, degree electrical

k_n = Harmonic factor, the harmonic content w.r.t the fundamental; from equation

$$i = I_{(peak)} \{\sin \omega_1 t + \Sigma k_n \sin (n\omega_1 t + \partial_n)\}$$

For RCCBs :

I_Δ = Residual Current (r.m.s.), A

$I_{o\Delta}$ = (Actual) Tripping Current (r.m.s.), A

$I_{o\Delta n}$ = Rated Tripping Current (r.m.s.), A

$I_{\Delta t}$ = Triggering Threshold of RCCB (instantaneous level), A

t_o = Fault time, i.e the time at which the fault is introduced, s

t_s = The time at which the continuous value of I_Δ exceeds the preset value $I_{\Delta t}$, s

t_{st} = The time at which the RCCB senses the fault and starts to carry out the tripping operation, s

t_f = The time at which the circuit breaker opens, s

Note : All instants of time are measured after a residual current zero where current is increasing.

Δt = Total Tripping Time of RCCB, from incidence of fault t_o to the opening of the circuit breaker t_f, s

Δt max = Maximum value of Δt, the total tripping time, for a given residual current, I_Δ, s

Δt min = Minimum value of Δt, the total tripping time, for a given residual current, I_Δ; Normally $\Delta t_{min} = \Delta t_{op}$, s

Δt_{op} = RCCB Operation Time, the time elapsed between the sensing of the fault at t_{st} to the opening of the circuit breaker at t_f, s

Δt_w = Waiting Time; i.e.the time elapsed, from the incidence of fault at t_o to the sensing of fault at t_{st}, s

Δt_a = Arc Extinction Time, from the opening of the circuit breaker at t_f to the extinction of the arc, s

$\Delta t'$ = Total Tripping time, taking into account the Arc Extinction Time. Thus it begins at the incidence of fault t_o continues until the circuit breaker opens and finishes when the arc is extinguished, s

$\delta\Delta t$ = infinitesimal interval of time in the scale of Δt, the total tripping time, s

Δt_{int} = finite interval of time on the scale of Δt, s

$p(\Delta t)$ = The probability of obtaining a tripping time of Δt

$c(\Delta t)$ = The cumulative probability, i.e. the cumulative value of $p(\Delta t)$ over a particular range of tripping time

M = Number of tests

I_p = Primary current of a Core Balance Transformer (r.m.s.), A

I_s = Secondary current of a Core Balance Transformer (r.m.s.), A

$\emptyset_r$ = The flux in the relay of a mechanical type RCCB, Wb

$\emptyset_l$ = The flux produced by the permanent magnet such that when it is counteracted, the relay opens.

N_p = Number of turns of the primary of a CBT

N_s = Number of turns of the secondary of a CBT

X_Δ = The tripping parameter of a RCCB

X_l = Triggering threshold of RCCB w.r.t X_Δ

G_n = The gain of n^{th} harmonic w.r.t the fundamental residual current

θ_n = The phase shift of n^{th} harmonic tripping parameter w.r.t the residual current, degree electrical

For Electromechanical Instantaneous Overcurrent Relay :

N = Number of coil turns

a = Effective core area, m^2

μ_o = Permeability of free space ($4\pi \times 10^{-7}$ H/m)

F_o = Spring force at x=0 (rest position), N

K_s = Spring constant, N/m

K_f = Friction constant, N s m

S_c = Core Reluctance, A/Wb

S_g = Air gap reluctance, A/Wb

S_l = Leakage reluctance, A/Wb

S_o = Closed gap reluctance, A/Wb

S_{log} = S_l in parallel with (S_o+S_g), A/Wb

$\emptyset_c$ = Flux in the core, Wb

$\emptyset_l$ = Leakage flux, Wb

$\emptyset_g$ = Working air gap flux, Wb

x = Armature travel, m

$\emptyset_{c1}$ = the core flux in unshaded pole, Wb

$\emptyset_{c2}$ = the core flux in shaded pole, Wb

i_{sc} = induced current in the shorted coil , A

G_s = conductance of the shorted coil, mho

$ß_s$ = the stopper collision factor

V_{fs} = Armature velocity after collision with the stopper, m/s

V_{is} = Armature velocity before collision with the stopper, m/s

$ß_c$ = the core collision factor

V_{ic} = Armature velocity before collision with the core, m/s

V_{fc} = Armature velocity after collision with the core, m/s

I_a = Attracting current, i.e the minimum current that can attract the armature sucessfully to the core, A

I_o = Tripping current, i.e the minimum current that can attract the armature sucessfully to the core and hold it at the core, A

Electromechanical Time Overcurrent Relay :

K = Relay constant, dependent upon design

N = Number of turns of the coil

S = Reluctance of flux path through the shaded and unshaded pole (assumed the same).

k & a = Disc constants

T_{dn} = The driving torque T_d at frequency nf_1, Nm

T_s = Spring Torque, Nm

T_o = The spring torque at angular displacement of the disc ($x_a = 0$), Nm

$K_{b,s}$ = Spring constant, N m rad^{-1}

x_a = Angular displacement, rad

$\emptyset_{i,j}$ = Flux produced by the current i_j, where $\phi_{i,j} = \emptyset_{i,j} \sin \omega_1 t$, Wb

$T_{b,ij}$ = Braking torque caused by $\emptyset_{i,j}$, Nm

$K_{b,ij}$ = Constants for $\emptyset_{i,j}$

index j can be either 1 for flux in the unshaded pole or 2 for the shaded one.

$T_{b,pm}$ = Braking torque caused by permanent magnet, Nm

$K_{b,pm}$ = Constant for the permanent magnet

$T_{b,f}$ = Braking torque caused by friction, Nm

$K_{b,f}$ = Constant for friction, N s rad^{-1} m

m_I = Moment of inertia of the disc, m^2 kg

CHAPTER 1. INTRODUCTION

1.1. Objective of the work

A literature search has shown that the operating point of residual current-operated circuit-breaker (RCCB) as well as the electromechanical instantaneous overcurrent (EM IOC) relay and the electromechanical time overcurrent (EM TOC) relay are affected by harmonics. Unfortunately, several studies had conflicting ideas about how the RCCB and the relays are affected and how to analyse it. With the increasing use of power electronic equipment that increases the harmonic content in the mains, its effect needs deeper study. The main objective of this study is thus to find out how the effect of harmonics on those RCCB and relays should be analysed and thus to explain the effects. Three protection devices, namely the RCCB, the EM IOC relay and the EM TOC relay were studied. Since many electromechanical relays work with the same principle, the study on these two types of relay also gives an insight into how other relays should be analysed if the system contains harmonics. The characteristics of RCCBs for sinusoidal residual current is also evaluated. This is considered to be important since the RCCB which is designed to protect people against electrocution is widely used, yet their characteristics even for sinusoidal residual current appears not to have been fully studied.

1.2. Background of the work

1.2.1. Residual current-operated circuit-breaker (RCCB)

Since their introduction about 30 years ago, high speed, sensitive RCCBs have proved useful in protecting people against ventricular fibrillation and installations against fire risk (1,4,14,25,26). In the UK, BS 4293 (6) covers RCCBs and their use is recommended in the IEE Wiring Regulation (7). Normally a RCCB is placed before the load. If an earth leakage fault exists, the RCCB may clear the fault, normally in less than 40 ms, even if

the fault current is as low as 30 mA.

Despite the wide use of RCCBs, Morley et al (15) pointed out that there is insufficient explanation about their characteristics and operation. Morley et al (15) and Emmanuel and Dougherty (24) derived the voltage output characteristic of the sensor, i.e. the core balance transformer (CBT) but the secondary current of the CBT is not taken into account. Recently, as reported by Roesch (27) and Electricity Council (28,29), it was observed that periodic non-sinusoidal residual current waveforms, usually caused by the use of power electronic equipment, affected the sensitivity of RCCBs. Some of these breakers became more sensitive while others less. Unfortunately, there is little published information about how harmonics affect the RCCBs (28,29).

1.2.2. Electromechanical instantaneous overcurrent (EM IOC) relay

The EM IOC relay is normally used for overcurrent protection of feeder circuits (37,38). Firstly, the current is sensed by a current transformer (CT). The secondary current is then fed to the relay and if it exceeds the pick up current, the relay trips. This relay is an 'all or nothing' type relay as covered by BS 142 (67). An EM IOC relay may be of a hinged or armature attracted type, and both are covered in this study.

The analytical model of Horton and Goldberg (37) showed that EM IOC relays are not affected by harmonics although their direct measurement showed up to 8% discrepancies, some positive and some negative. It was also questionable whether the hinged and attracted armature type can be treated in the same way. Two studies carried out by IEEE groups (39,48) stated that the above relays are largely independent of frequency effects, however with a very distorted waveform, that may be caused by CT saturation, it was suggested that an instantaneous relay trips provided the given area per cycle of the waveform (i.e., ampere-seconds per cycle) is the same with its rated tripping current. Jost et al (40), cited by an IEEE study committee (36), stated that in a majority of cases,

harmonics will cause relays to exhibit a tendency to operate slower and/or with higher pick up values. Unfortunately, all the above work, with the exception of Horton and Goldberg's model (37), is not thoroughly supported by theoretical analysis. In addition, Horton and Goldberg only considered the r.m.s. value of the current regardless of its waveform.

1.2.3. Electromechanical time overcurrent (EM TOC) relay

Normally the EM TOC relay is used for selective overcurrent protection (3). Firstly, the current is sensed by a current transformer (CT). The output of the CT is then fed to the relay. If the current exceeds the pick up value, the relay starts to trip. The tripping time varies according to the current, thus this relay is a type of 'single input energising quantity measuring relays with dependent specified time' as covered by BS 142 (67). In this work, an EM TOC relay using an induction disc as the rotor is studied. Depending on the relay constants, this relay may have different characteristics such as 'inverse time', 'very inverse time', etc. In the laboratory work, a standard inverse definite minimum time (IDMT) overcurrent relay was used, although the theory developed can be applied to other types of induction disc overcurrent relay.

An IEEE committee study (39) about the EM TOC relay stated that an EM TOC relay using an induction disc as the rotor, tends to operate faster if the current contains higher harmonics, although the relay design may cause it to operate slower. Jost et al (40) concluded that in general, relays exhibit a tendency to operate slower/ or with higher pick up values if the current contains harmonics. Reference (48), which is another IEEE committee study, stated that harmonics may either cause this relay to be more sensitive or less sensitive. The analytical models of Horton and Goldberg (37) and also Saramaga et al (51) showed that harmonics cause an induction disc type EM TOC relay to require a higher pick up current. The test results of Faucet and Keener (50), Saramaga et al (51) and also Chu et al (52) showed that current waveform affects the tripping time of this

relay. Saramage et al's tests showed that harmonics will cause the relay to operate slower. Chu et al and Faucet and Keener' s tests showed that harmonics may cause the relay to operate faster or slower. Unfortunately, with the exception of (37) and (51), the above studies are not supported with a thorough theoretical analysis. In addition, (37) and (51)'s analysis are limited to the pick up current values of the relay only and do not include the operating time, which is of paramount importance in selective overcurrent protection.

It should also be pointed out that despite the growing use of electronic relays, Heising and Patterson (77) stated that electromechanical relays will continue to have a place in many future applications and will be available for years to come due to their proven reliability.

1.3. The approach taken in the study

Since there is disagreement on how the effect of harmonics should be analysed, in this study, the basic construction of the RCCB, the EMIOC relay and the EM TOC relay are firstly examined. A model is then developed for each of them and then simulated on Aston university's VAX CLUSTER. In order to assess how harmonics affect the RCCB and the relays, a waveform with controlled harmonic content was used in the simulation. This will help in understanding how the RCCB and the relays are affected by harmonics and thus give an insight into how they should be analysed if the current contains any harmonics. The analysis is focussed on the effect of periodic non-sinusoidal current waveforms, which is caused by harmonics, but this will also provide a basic methodology on how the effect of non-periodic waveforms should be analysed.

In contrast with other previous work which merely examined the harmonic content of the current, in the model developed the tripping mechanism's movement was evaluated. Thus the instantaneous value of the current was taken into consideration rather than just its

r.m.s. value, and the interaction between the current and the tripping mechanism was evaluated. It was found that the RCCBs and the protection relays are affected by harmonics and that the effect is determined by the shape of the current waveform and the mechanical constants of the relay and not merely by the r.m.s. harmonic content of the current.

To verify the theoretical study, experimental work was also carried out. A waveform generator with controlled harmonic content was developed to test the RCCBs and the relays. A good correlation between the theoretical study and the experimental results was obtained. Some of this work has been published elsewhere (31,32,33,53,54,55,95,97).

1.4. Lay out of the work

Chapters 2 and 3 describe the RCCB characteristics and test results for sinusoidal residual current. Special emphasis is given in these two chapters since the RCCB characteristics for sinusoidal waveform have not been fully explored previously. Chapter 4 presents a theoretical study about the effect of harmonics on the tripping current of RCCBs. A brief review about how harmonics can be produced and fed back to the line is also given in this chapter. Chapter 5 presents the experimental results on the effects of harmonics on the tripping current of RCCBs. In chapter 6, a theoretical study on the effects of harmonics on EM IOC relays is described, followed by the simulation and experimental results which are given in chapter 7. The description of the theoretical study of the EM TOC relay characteristics is given in chapter 8 while the experimental and simulation results are presented in chapter 9. Chapter 10 provides the conclusion to this work which includes the implication of this study in other areas.

CHAPTER 2. THE BASIC CONSTRUCTION AND OPERATION OF RCCBS

2.1. Introduction

In this chapter, the basic construction of RCCBs will be described, followed by the presentation of the standard requirements of their characteristics. The way RCCBs can protect human beings against electrocution is also presented since it helps in explaining the RCCB operation. Based on their construction, the theory of tripping time for sinusoidal current is then derived both for no load and loaded conditions. The theoretical description of RCCB characteristics for sinusoidal current is derived here since there is little published information about it.

2.2. The construction of RCCBs

Although there are many varieties of RCCB, all those examined work on the same principle. The fault current is sensed by a core balance transformer (CBT) using a coil wound around the CBT as shown in Fig.2.1. Under normal conditions, there is no output from the coil because the line current is balanced by the neutral current. However, if a fault current flows to earth, the CBT senses the difference between the line and neutral current. This difference, called the residual current I_{Δ}, which has a similar magnitude to the fault current causes the CBT to send a signal to the tripping mechanism which then opens the switch and trips the circuit breaker. It should be noted that a short circuit fault between the line and neutral that may cause a large current to flow will not trip the RCCB since the CBT will sense no difference between the line and neutral current.

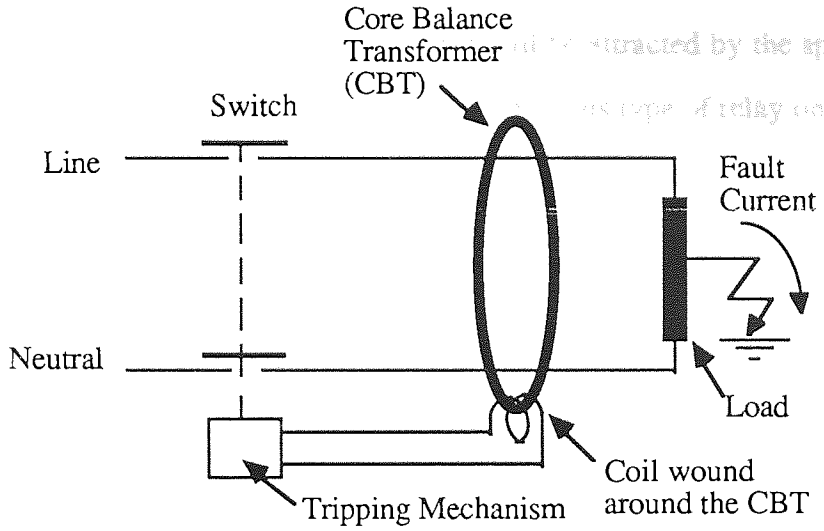

Figure 2.1. The basic construction of RCCBs

Based on the type of tripping mechanism, RCCBs are divided into two classes :

1. Electromechanical. The output of the CBT is fed directly into an electromechanical relay. The relay may be of the more common polarised type and sense only half of the cycle (half wave reaction type), or of the saturation type which senses both halves (full wave reaction type).
2. Electronic. The output of the CBT is amplified and sometimes rectified. The output of the electronic circuit activates a relay. Depending on the electronic circuit, electronic type RCCBs may be of half or full wave reaction type.

The RCCB circuit has been described in many papers (15-22), but a brief review is given below :

Fig.2.2 shows the polarised type of electromechanical relay. During normal operation, the relay is kept closed since the plunger is attracted by a permanent magnet. When a residual current I_Δ flows, the CBT produces I_S which in turn produces $\emptyset_r$, the flux in the relay. As the fault current is increased $\emptyset_r$ reaches a point where it can counteract the effect of $\emptyset_l$, the flux produced by the permanent magnet, such that the permanent magnet

can no longer hold the armature which will be attracted by the spring. At that point the plunger and hence the circuit breaker opens. This type of relay only reacts to one half of the waveform.

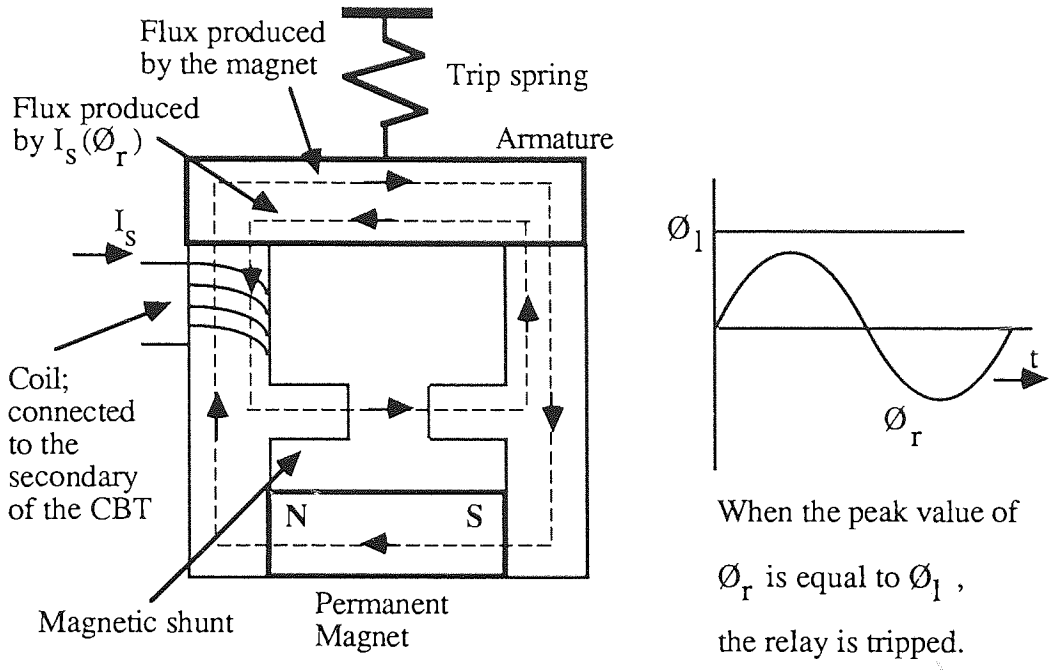

(a) The relay in closed position

(b) The reaction of the fluxes

Figure 2.2. Polarised type relay

Fig.2.3 shows the saturation type of electromechanical relay. As in the other type, during normal operating conditions the relay is kept closed by the permanent magnet. If a fault occurs, I_s drives flux $Ø_r$ around the windows of the core and if $Ø_r$ reaches $Ø_1$, it saturates the region around the windows. The permanent magnet flux is diverted across the central gap and away from the plunger at the top which is thus released and the circuit breaker activated. Since the core can be driven to saturation by both the positive and negative halves of $Ø_r$, this type of relay reacts to both halves of the waveform.

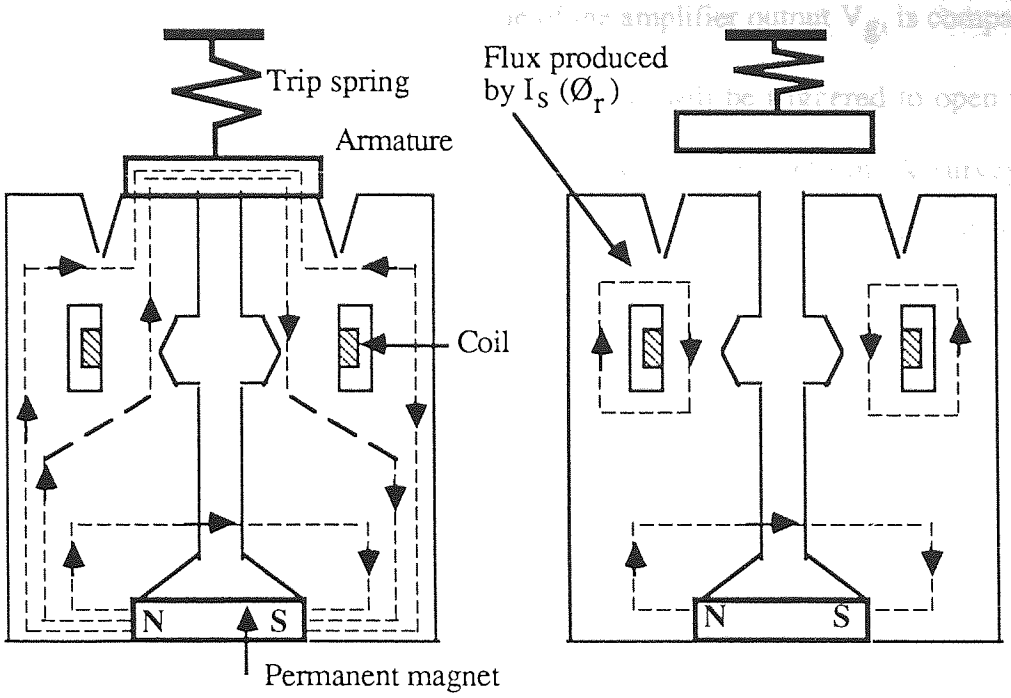

(a) The relay before tripping

(b) The relay after tripping

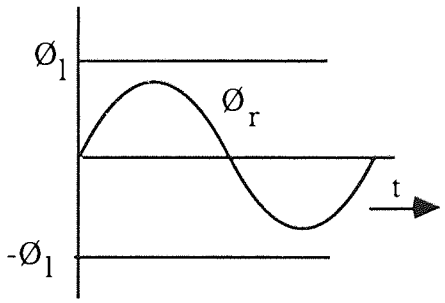

When the peak value of $Ø_r$ is equal to $Ø_l$ or $-Ø_l$, the relay is tripped.

(c) The reaction of the fluxes

Figure 2.3. Saturated type relay

In an electronic RCCB, the output of the CBT is fed to an electronic circuit. The output of the circuit is used to energise a relay. Two block diagrams are shown in Fig.2.4. In Fig. 2.4.a the secondary current of the CBT is directed through a resistor. The voltage is amplified to trigger a thyristor. When the peak of V_g is high enough the thyristor turns on, the relay is energised and the circuit breaker opens. This device responds to only one half of the waveform. In Fig.2.4.b the output of the amplifier is rectified and smoothed.

The d.c. voltage, equal to the peak value of the amplifier output V_g, is compared with a d.c. reference V_1 to determine whether the relay will be triggered to open the circuit breaker. This device responds to both halves of the waveform. A survey of other electronic RCCBs showed that although there are many circuit variations, they work in a similar method.

The above description shows that the residual current I_Δ does not trip the relay directly. A tripping parameter X_Δ can be defined as that which carries out the tripping operation and represents the residual current I_Δ. In the case of mechanical type RCCBs, the tripping parameter is the flux in the relay (Φ_r), while for the electronic type it is the amplified voltage drop across the resistor (V_g). Assuming that the tripping parameter is linearly related to the residual current, then the RCCB will operate if the residual current exceeds a particular value, $I_{\Delta t}$, and based on these explanations, the RCCB characteristics can be derived.

To trip the RCCB, a short but finite 'triggering time' is needed, during which time the tripping parameter should be kept above the threshold value. In the theory its duration is neglected and the relay is assumed to be sensitive only to the peak value of the current. This assumption is supported, as will be seen later, by test results.

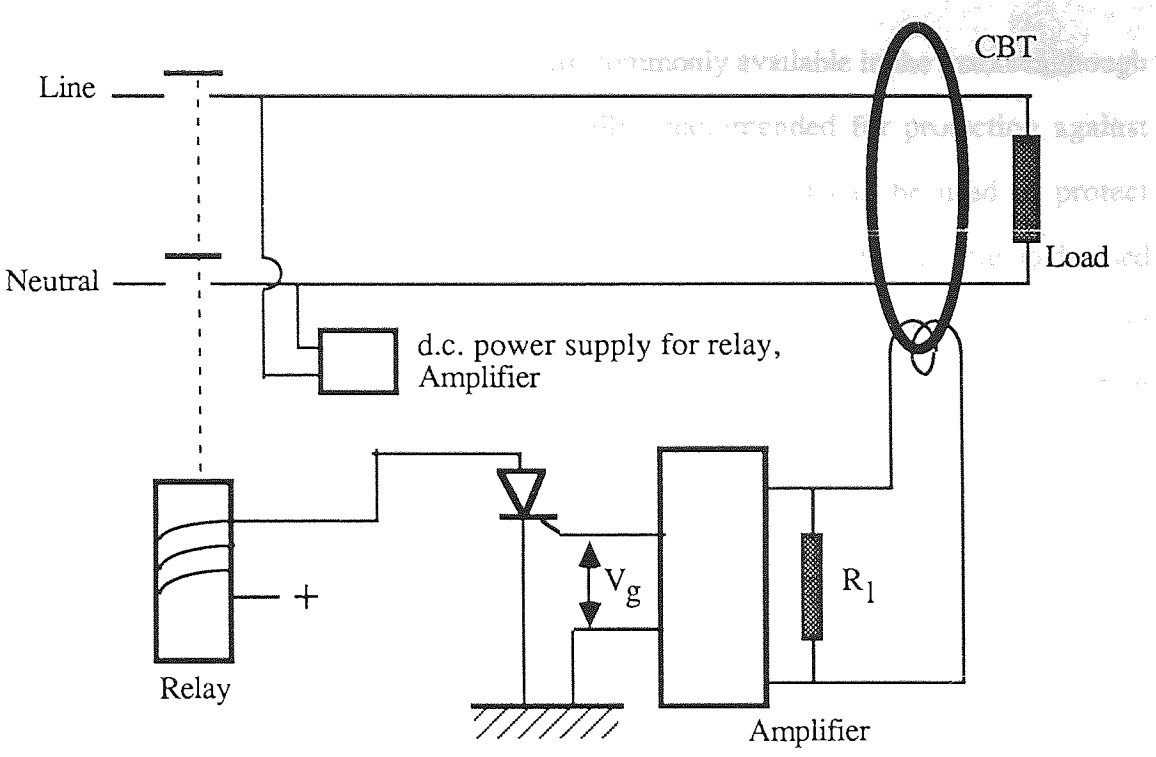

(a) A circuit using a thyristor and an amplifier.

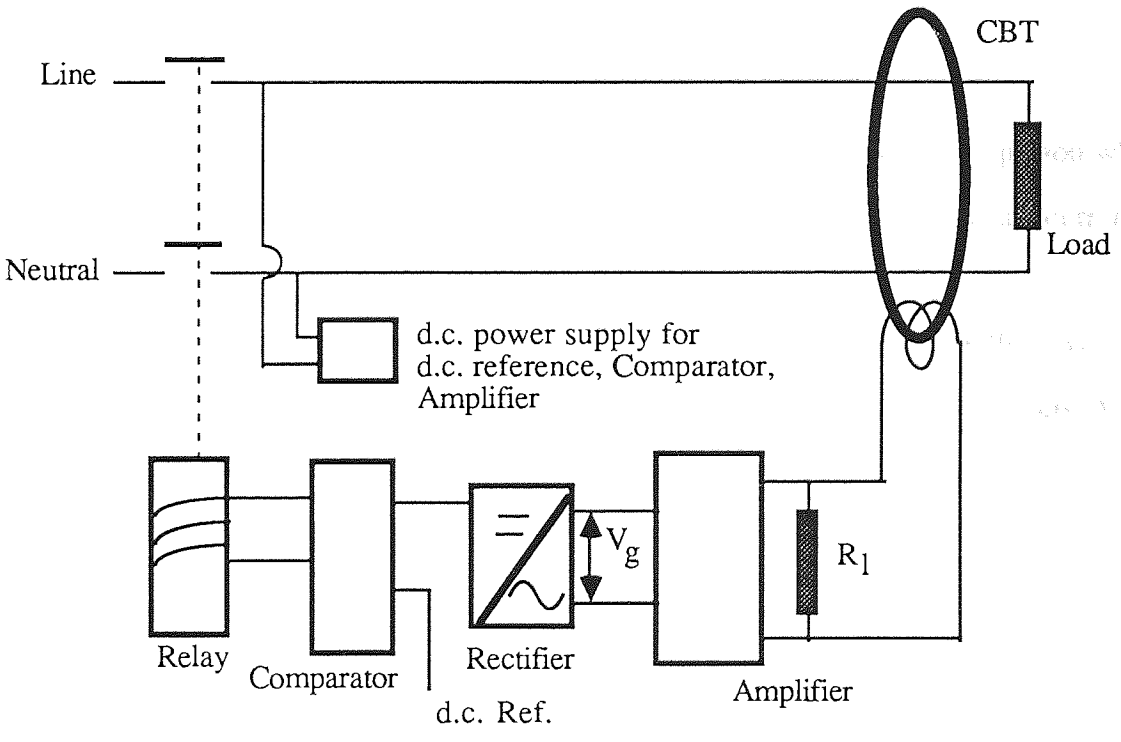

(b) A circuit incorporating an amplifier, a rectifier, and a d.c. comparator.

Figure 2.4. Two typical electronics type RCCBs

RCCBs with a sensitivity as low as 5 mA are commonly available in the market although RCCBs with 30 mA sensitivity are normally recommended for protection against electrocution. This low sensitivity is very useful since it can be used to protect installations against leakage current which may cause fire. Although there are no detailed studies about this fire risk, it is widely believed that a current as low as 100 mA may cause fire (26). This low current may not operate protective equipment such as miniature circuit breakers (mcb) or fuses. On the other hand, due to their sensitivity, RCCBs may sense and clear this fault, but more important is the ability of the RCCBs to protect people against electrocution as a current as low as 30 mA may cause danger to people. While mcbs or fuses may not operate, RCCBs may sense this small current and clear the fault.

2.3. The use of RCCBs to prevent ventricular fibrillation

2.3.1. Electric current in the body

As Ferris et al (8) pointed out, it is the magnitude of current flowing in a person which may be dangerous rather than the magnitude of the applied voltage. If an a.c current of power frequency is passed through the body and increased gradually, the person will eventually feel a tingling sensation. A value of 0.5 mA is taken by the IEC (3) as the threshold of perception. Lower currents have no known long term adverse effects. As the current is increased, the person will feel increasing discomfort accompanied by muscle tightening and at a certain value of current, the subject will be unable to 'let go' the conductor being grasped. The 'let-go current' is defined as the maximum value of current at which a person holding electrodes can release the electrodes (3). IEC Report 479 takes 10 mA as the mean let-go threshold current for adults. As the current is further increased, the person may loose voluntary control over respiratory muscles and breathing may cease. This condition, referred as 'respiratory paralysis', usually ceases if the current is interrupted and no permanent after effects are known (8,11).

At higher levels of current, the normal pumping action of the heart stops and is replaced by a cardiac muscle activity which is fast, irregular and of small amplitude. This condition, called ventricular fibrillation, is accepted as the most common cause of death from low voltage electric shock. The ventricular fibrillation threshold of a human being is obtained from experiments carried out on various species of animal (9,10,11,12,13). The value of current which causes ventricular fibrillation depends on the duration of the current flow.

2.3.2. IEC Specification

The results of the above research are incorporated in the IEC Report 479. Time/current zones of effects for a.c currents (15 Hz to 100 Hz) on a person is described in Fig.2.5. In areas 1 and 2, electric current usually will cause no harmful effects. A current in area 3 may cause 'unwanted effects' such as difficulty in breathing, muscular contraction, etc, although usually no organic damage is expected. Area 4 is a 'dangerous area', since ventricular fibrillation may occur. The possibility increases with current duration and magnitude.

The electrical resistance of the human body limits the current flow. The body resistance (from hand to foot) varies from 500 Ohm to about 7500 Ohm, depending on the voltage, body condition (e.g. wet, dry, etc) and other factors as reviewed by Hammam and Baishiki (12). IEC Report 479 (3) suggests that a body resistance as low as 1000 Ohm can be expected for an applied voltage of 220 V. Thus for the ordinary household voltage of 240 V, as Haseler (23) suggests, a residual current of 240 mA may be expected to flow but higher currents are not likely.

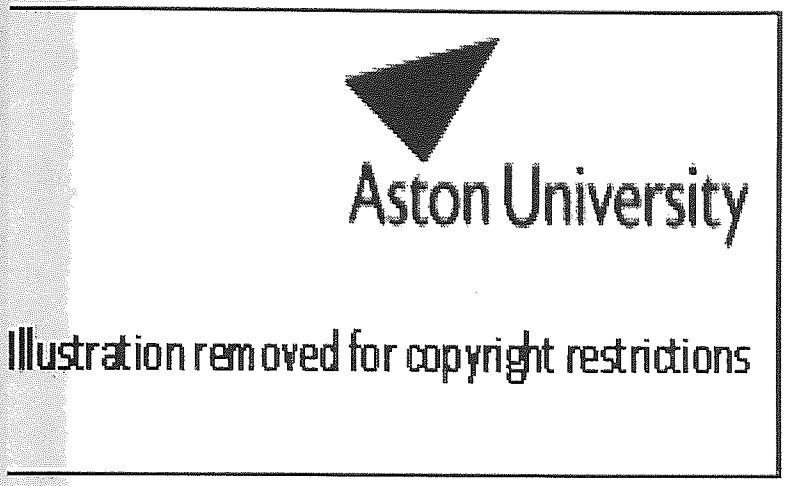

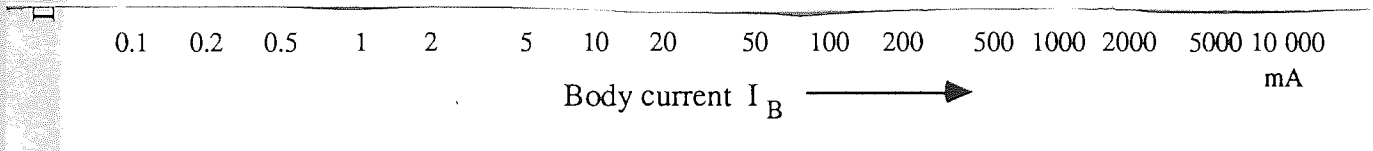

Zones	Physiological effects
1	Usually no reaction effects.
2	Usually no harmful physiological effects.
3	Usually no organic damage to be expected. Likelihood of muscular contractions and difficulty in breathing, reversible disturbances of formation and conduction of impulses in the heart, including atrial fibrillation and transients cardiac arrest without ventricular fibrillation increasing with current magnitude and time.
4	In addition to the effects of zone 3, probability of ventricular fibrillation increases up to about 5% (curve c1), up to about 50% (curve c2), and above 50% beyond curve c3. Increasing with magnitude and time, pathophysiological effects such as cardiac arrest, breathing arrest and heavy burns may occur.

Notes: 1. As regards ventricular fibrillation, this figure relates to the effects of current which flows in the path 'left hand to feet'.
2. The point 500 mA/100 ms corresponds to a fibrillation probability in the order of 0.14%.

Figure 2.5. IEC's time/current zones of effects of a.c. currents (15 Hz to 100 Hz) (taken from IEC report 479-1)

2.3.3. Existing specifications for RCCBs

In the UK, BS 4293:1983 covers RCCBs (6). The 15th Edition of the IEE Wiring Regulations (7), which will be referred to by its common appellation of the '15th Edition', requires the use of RCCBs in a number of circumstances. It calls for the use of RCCBs whose tripping current $I_{o\Delta n}$ does not exceed 30 mA for protection against indirect contact in many applications, while BS 4293 requires 200 ms as the maximum tripping time for an RCCB 'if no intentional time delay is provided'. Such a time delay is sometimes incorporated in the back-up protection.

For overcurrent, BS 4293 and the 15th Edition require that an ordinary RCCB should trip within 40 ms if passing 5 times $I_{o\Delta n}$ (e.g., 5 x 30 mA = 150 mA). An earlier version of the 15th Edition (5) stated that RCCBs may be used to reduce the risk associated with direct contact in the case of failure of other protective measures if this '40 ms criterion' is also achieved with a residual current of 250 mA. This '250 mA requirement' does not appear in the current 15th Edition (7). However, since a residual current of 250 mA is a distinct possibility in practise, the requirement is still taken into account in this work and is implied by BS 4293.

It should be mentioned that during the preparation of this thesis, a new standard for portable residual current devices, BS 7071:1989 (96), was published. The requirement of tripping time and tripping current in this recent standard are similar to BS 4293. However there are some differences concerning the construction, test, etc. This new standard is not taken into account in this work.

2.3.4. Performance of RCCBs to prevent danger

Over the years, RCCBs having $I_{o\Delta n}$ of 30 mA have been ordinarily and widely used

for protecting people against ventricular fibrillation. A study by Laurer (34), also reported by Nowak (14), of 576 fatal accidents due to electricity claimed that 539 of them could have been prevented by the use of a 30 mA RCCB. If an ordinary RCCB is subject to a residual current of 150 mA (BS 4293 and current 15th Edition requirements) or presumably more (c.f.,the early 15th Edition requirement) it should trip within 40 ms. At 30 mA the maximum tripping time is 200 ms. If these points are superimposed on IEC's time-current zone of effects for ac current on a person, and if they are connected by straight lines, as can be seen in Fig.2.6 the RCCB will give protection against most of the 'unwanted area', zone 3, and against most of zone 4, the 'dangerous area' where fibrillation might be induced. A band covering typical RCCB characteristics is also given in Fig.2.6 showing conformance with the standards.

The region B in Fig.2.6 where the RCCB apparently allows zone 4, the dangerous currents to flow, is unlikely to cause trouble in practice because the resistance of the human body limits the current as previously noted. The RCCB also permits zone 3, the unwanted area in region A of Fig.2.6. A low residual current of, say 20 mA, which may not cause a RCCB to trip may cause unwanted effects if it lasts for a long period, say more than about 1 s. However, as Nowak (14) pointed out, a RCCB should prevent body currents which are dangerous to people, whilst avoiding spurious tripping due to excessive leakage current. This aim seems to be just achievable. Biegelmeier (1) expressed the view that 30 mA is adequate for the tripping sensitivity; if 10 mA or even 5 mA are chosen, as in the USA, there is a risk of unnecessary spurious tripping due to leakage current.

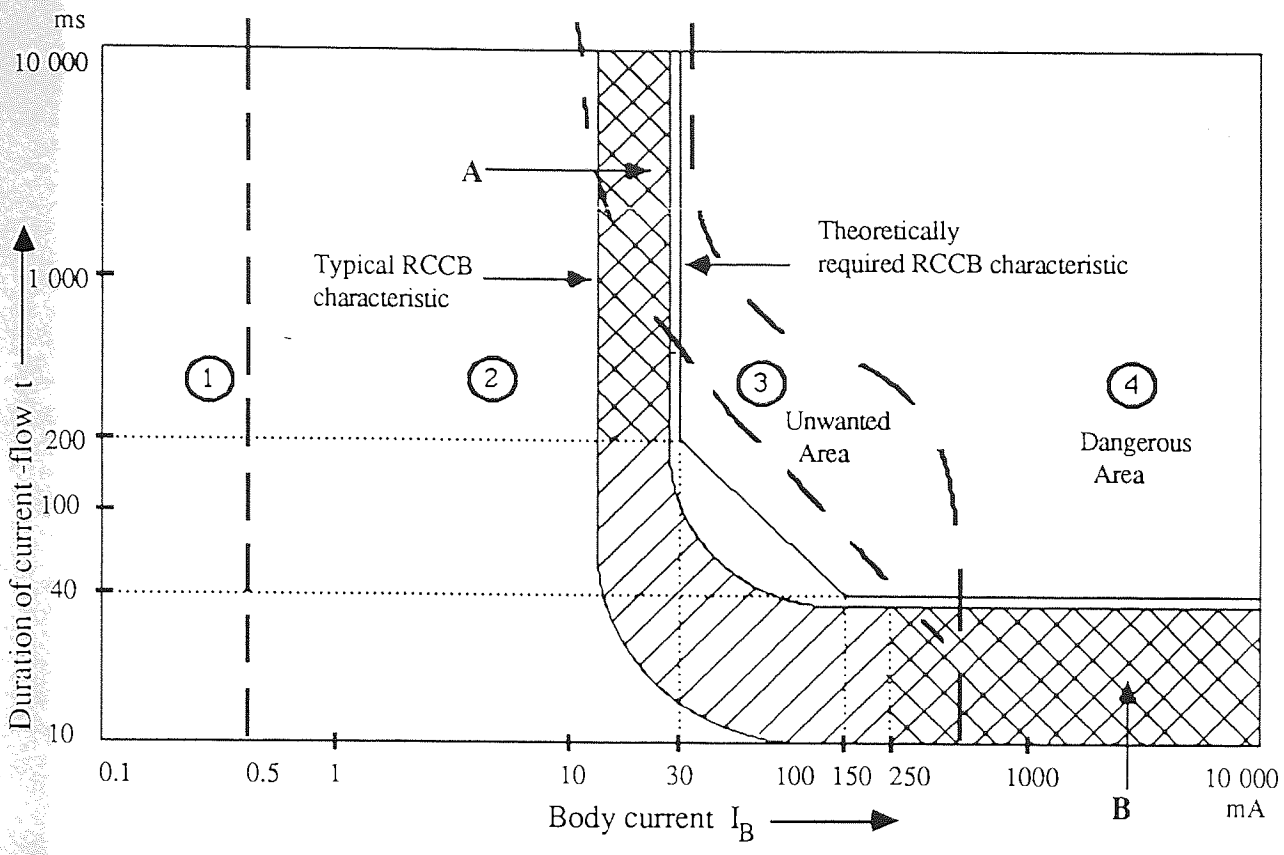

The theoretically required RCCB characteristic is the line produced by connecting all operating points required.

Figure 2.6. RCCBs characteristic and IEC's time/current zones of effect of a.c. currents (15 Hz to 100 Hz) super imposed

2.4. Theory of tripping Time

2.4.1. No load condition

A RCCB starts to operate when the instantaneous value of the residual current I_Δ sensed by the CBT exceeds a particular triggering threshold value $I_{\Delta t}$ at time t_s. This threshold value $I_{\Delta t}$ is thus equal to the peak value of the actual tripping current $I_{o\Delta}$ of the RCCB. Fig.2.7 represents a residual current I_Δ passing through a half wave reaction type RCCB. The fault is introduced at t_o and I_Δ is equal to $I_{\Delta t}$ at time t_s. A frequency of 50 Hz is

taken. Three cases must be considered :

1. The fault occurs at t_o on rising wave before the instantaneous value of I_Δ reaches $I_{\Delta t}$ at t_s. As shown in Fig.2.7.a, $t_o < t_s$ and the RCCB starts to carry out the tripping operation at $t_{st} = t_s$. There will thus be a waiting time of Δtw from t_o to t_{st} that should be added to the RCCB operation time Δtop to obtain the total tripping time Δt. The RCCB operation time is the time between the sensing of excessive current at t_{st}, and the opening of the circuit breaker at t_f. This time, Δtop, is taken as fixed. This assumption is supported, as will be seen later, by experimental results where it was found that normally Δtop has a constant value of around 5 ms. If the zero of time is taken to be when the current passes the zero before the fault is introduced, the following equations hold :

   Operation commence : $t_{st} = t_s$ (2.1)

   Waiting time : $\Delta tw = t_{st} - t_o$ (2.2)

   RCCB operation time : $\Delta top = t_f - t_{st}$ (2.3)

   Total tripping time : $\Delta t = \Delta tw + \Delta top$ (2.4)

   The actual tripping current : $I_{o\Delta} = I_\Delta \sin(\omega t_s)$ (2.5)

2. The fault occurs when the instantaneous value of residual current I_Δ is higher than $I_{\Delta t}$. As shown in Fig.2.7.b, in this case, $t_s \leq t_o \leq (T/2-t_s)$ and

   $$t_{st} = t_o \quad (2.6)$$

   Since in this situation, $\Delta tw = 0$, the RCCB starts to carry out the tripping operation as soon as the fault is introduced.

3. The fault occurs on a falling wave when the instantaneous value of I_Δ is less than $I_{\Delta t}$. For this condition, $(T/2-t_s) < to < (T+t_s)$ as shown in Fig.2.7.c.

   $$t_{st} = T + t_s \quad (2.7)$$

Thus the total tripping time for a half wave reaction type RCCB varies with fault time t_o as shown in Fig.2.8.a. where I_Δ is taken as a parameter. The time - current characteristic can then be derived from this graph and is shown in Fig.2.8.b. where t_o is taken as a parameter.

From Fig.2.8.a, the theoretical longest and shortest tripping times can also be derived as :

$$\Delta t \text{ maximum} = \Delta tw \text{ maximum} + \Delta top$$

$$= (T/2 + 2\, t_s) + \Delta top \qquad (2.8.a)$$

$$\Delta t \text{ minimum} = \Delta top \qquad (2.8.b)$$

t_s varies depending on the residual current I_Δ and the actual tripping current $I_{o\Delta}$ of the RCCB which according to the BS 4293:1983 requirement for a 30 mA (nominal) RCCB may lie between 15 mA and 30 mA. The ranges of t_s and Δtw are given in table 2.1, the total tripping time is obtained by adding Δtop to Δtw.

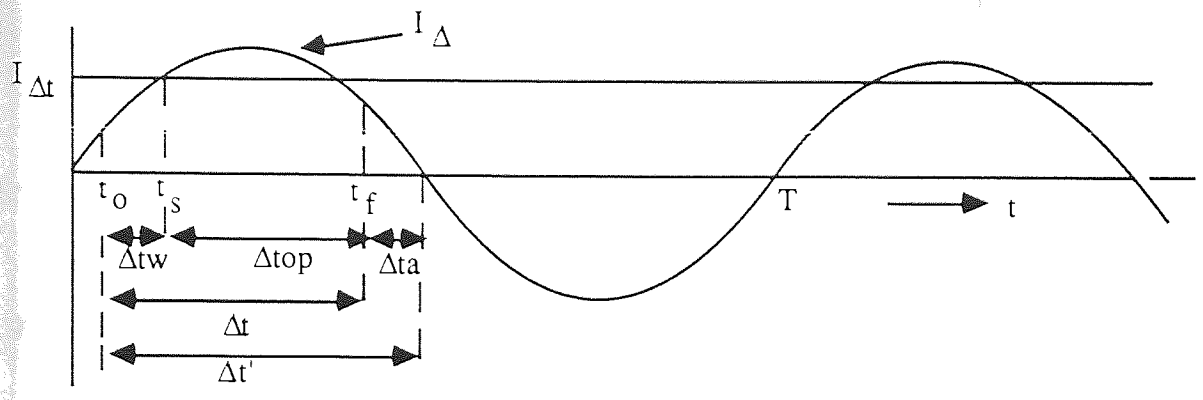

(a) $t_o \leq t_s$

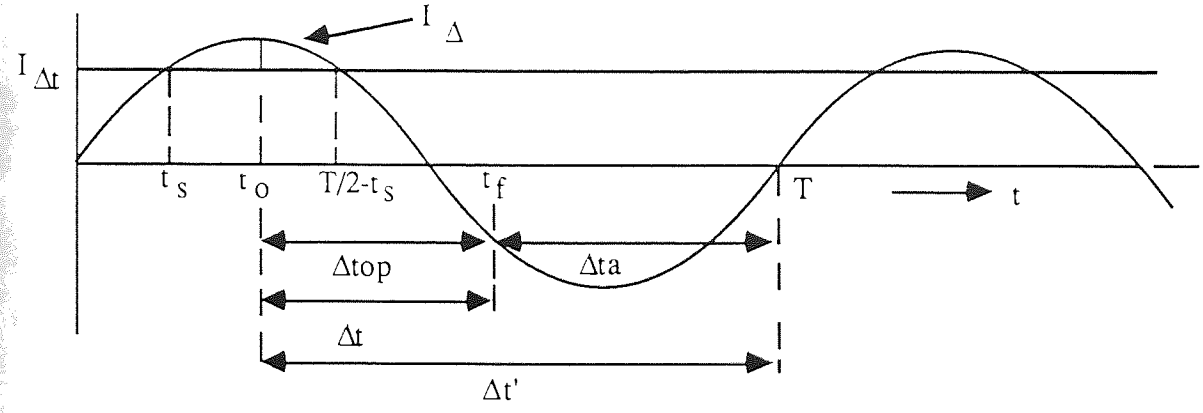

(b) $t_s < t_o < (T/2-t_s)$

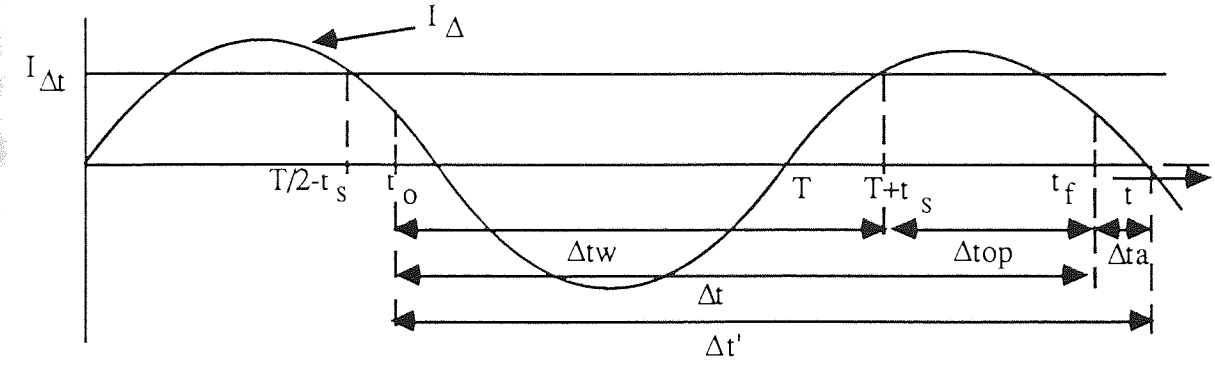

(c) $(T/2-t_s) < t_o < (T+t_s)$

Figure 2.7. Time intervals for a half wave reaction type RCCB.
For reference, t = 0 is taken at the current zero before the fault is introduced.

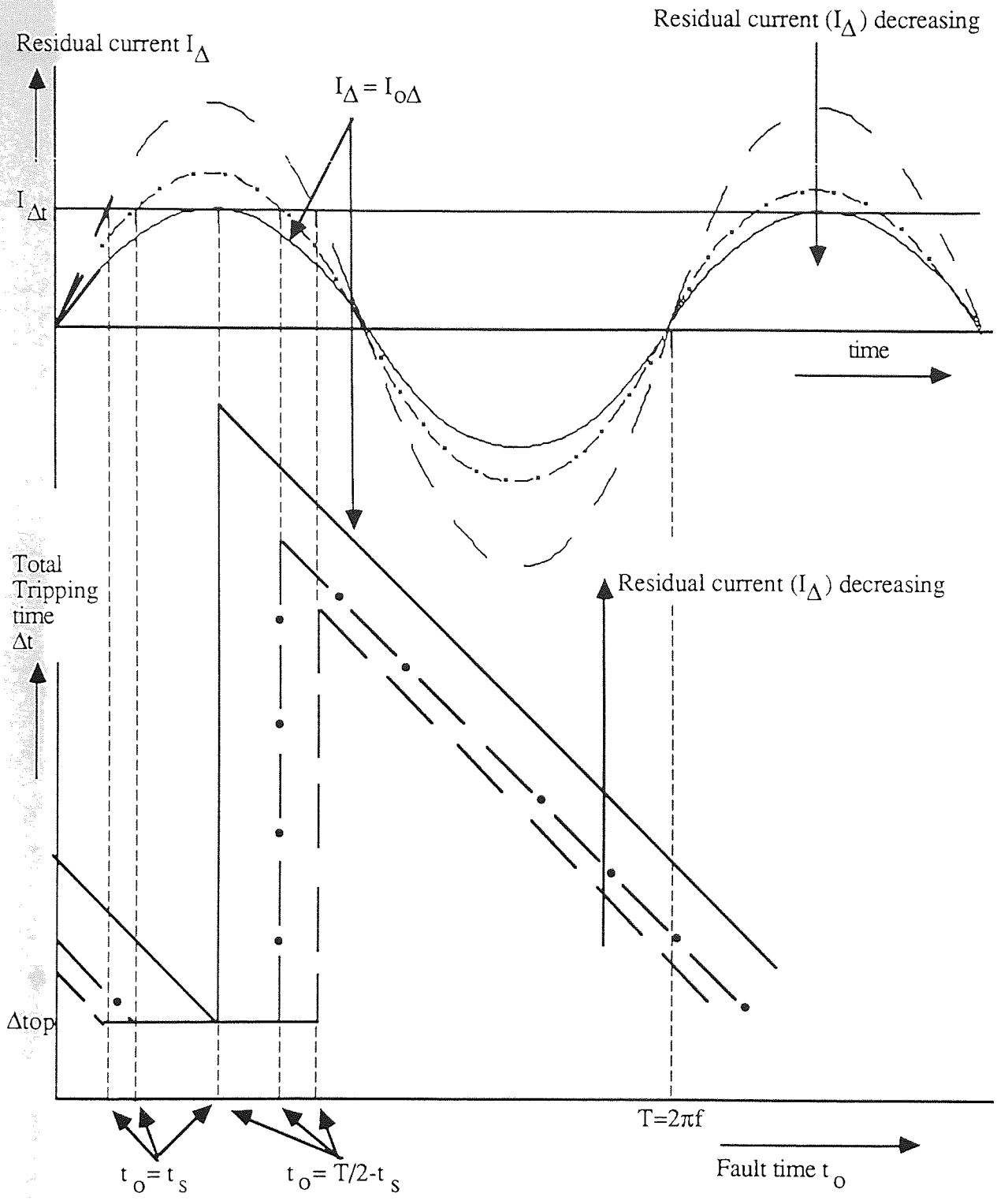

(a) The variation of total tripping time Δt with fault time t_o.
The residual current I_Δ is taken as parameter.

Figure 2.8. The no load characteristics of a half wave reaction type RCCB.

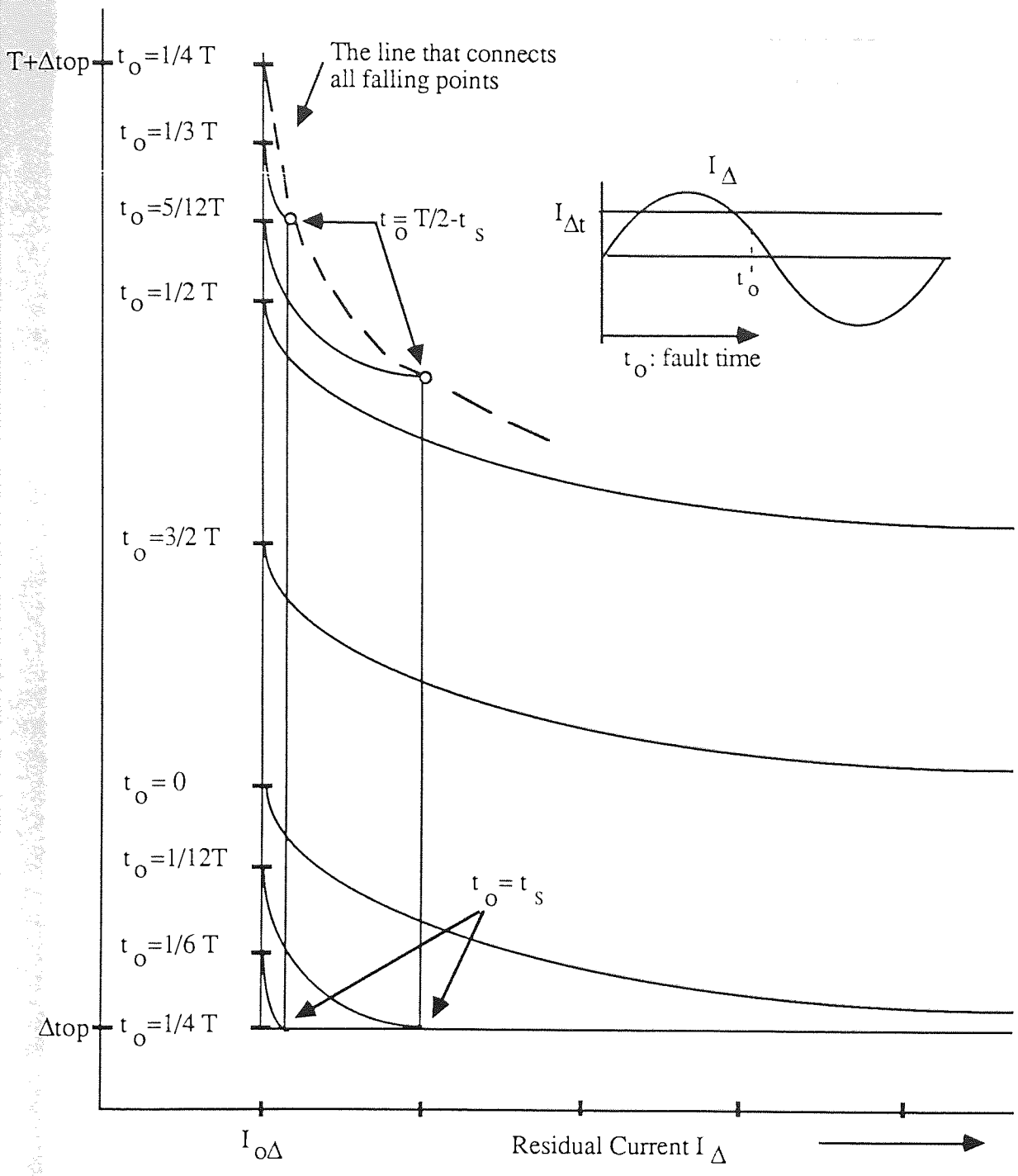

For a particular value of t_o, the waiting time Δtw is maximum when the instantaneous value of I_Δ is slightly less than $I_{\Delta t}$ as described in case 3 Fig.2.7.c. Δtw decreases with the increase of I_Δ and at a particular value of I_Δ, t_o will be equal to $(T/2-t_s)$. At this point $\Delta tw = 0$. Then Δtw falls from $(T/2+2t_s)$ to 0 i.e changes from case 3 (Fig.2.7.c) to case 2 (Fig.2.7.b), causing a 'fall' in the graph. These 'falling points' can then be connected to form the upper boundary of the tripping time.

(b) The variation of the residual current I_Δ and total tripping time Δt.
The fault time t_o is taken as the parameter.

Figure 2.8. The no load characteristics of a half wave reaction type RCCB.

Residual current, mA	Range of t_s , ms	Range of Δtw, ms
30	1.67 - 5.00	0.0 - 20.0
150	0.32 - 0.64	0.0 - 11.28
250	0.19 - 0.38	0.0 - 10.76

Table 2.1 Range of t_s and Δtw

For a full wave reaction type RCCB, the characteristic is similar but the maximum Δtw is reduced by T/2.

2.4.2 The effect of resistive load current

When the fault is introduced while the load current is flowing, the tripping time may be longer. Due to the inductance of the load circuit, an arc is drawn between the contacts of the circuit breaker and only extinguishes at or near current zero. An additional time for this arc extinction (Δta) should be added to get the total tripping time Δt'.

$$\Delta t' = \Delta t + \Delta ta \qquad (2.9)$$

At no load, Δta = 0, and Δt' = Δt if the breaker can chop the residual current and extinguishes the arc directly.

In analysing the effect of resistive load current on the tripping time, assume that :

1. The residual current is also resistive so that both the residual and the load currents are in phase.
2. When the RCCB opens, the residual current still has to flow due to the inductance of the load until the current reaches its natural zero.

Thus, Δta begins at t_f and lasts until the next current zero, its duration depends on t_f. This is shown in Fig.2.7.a to c.

The diagram in Fig.2.9.a shows a residual current I_Δ passing through a RCCB while the resistive load current is flowing. Fig.2.9.b shows the total tripping time $\Delta t'$ as a function of fault time t_o. There are 4 cases to be considered :

1. At $0 \leq t_o < t_s$ there will be a waiting time Δtw, the maximum of which is t_s. Since the RCCB operation time Δtop is taken as constant, an extension of tripping time due to the inductance effect Δta will start from $t_f = (t_s+\Delta top)$ to $t = T/2$, at which point, the arc will be extinguished.
2. For $t_s \leq t_o \leq T/2-\Delta top$, there will be no waiting time, but an arc will persist, it occurs from $t_f = (t_o+\Delta top)$ to $t = T/2$. At $t_o = (T/2-\Delta top)$, there will be no arc since the RCCB opens exactly at current zero. This is why the total tripping time $\Delta t'$, taken when load current is flowing, is always higher than the same graph at no load, and why finally, those two graphs coincide again as shown in Fig.2.9.b.
3. At $(T/2-\Delta top) < to \leq (T/2-t_s)$, although there is no waiting time, the RCCB opens when the current has already passed its zero point, causing a long arc extinction time Δta since the current will be interrupted at $t = T$. The Δta thus increases directly from 0 to T/2 but then decreases as t_o increases. Before Δta reaches 0, t_o reaches a value higher than $(T/2-t_s)$, causing the waiting time to increase from 0 to $(T/2+2t_s)$ directly. This causes two 'jumps' in the total tripping time $\Delta t'$ graph in Fig.2.9.b.
4. For $(T/2-t_s) < t_o < T$, there will be a waiting time of $(T+t_s-t_o)$. At $t = T+t_s$, the RCCB starts to operate and opens at $t_f = T+t_s+\Delta top$. Arcing occurs from t_f to $t = 3T/2$, producing a Δta of $(3T/2-t_f)$, which is constant for case 4. Thus after the second jump, the total tripping time decreases and is a fixed time longer than for the no load condition as shown in Fig.2.9.b.

The theoretical longest and shortest tripping times when a resistive load current is flowing are:

$$\Delta t'\text{maximum} = 3T/2-(T/2-ts) = T-t_S \qquad (2.10.a)$$

$$\Delta t' \text{ minimum} = \Delta\text{top} \qquad (2.10.b)$$

$\Delta t'$max may be shorter in practice since the current may be interrupted before it reaches natural zero.

2.4.3 The effect of inductive load current

It was assumed in section 2.4.2 that both the residual and load currents are resistive and in phase. However while the residual current is likely to be resistive, the load current will probably be not so. This will affect the total tripping time since the time for arc extinction Δta is affected. Fig.2.9.b shows a pure resistive residual current with a pure inductive load current. Since usually the residual current is very small compared with the load current, an arc will be drawn from the time the RCCB switch opens until the natural zero of the load current. The tripping time can be calculated using similar method used to analyse the effect of resistive load current on the tripping time of RCCBs as described in section 2.4.2 resulting in the diagram in Fig.2.9.b. The Fig.2.9.b shows that the maximum total tripping time is 30 ms, i.e., $(5T/4 + t_S)$ when t_S has its maximum value.

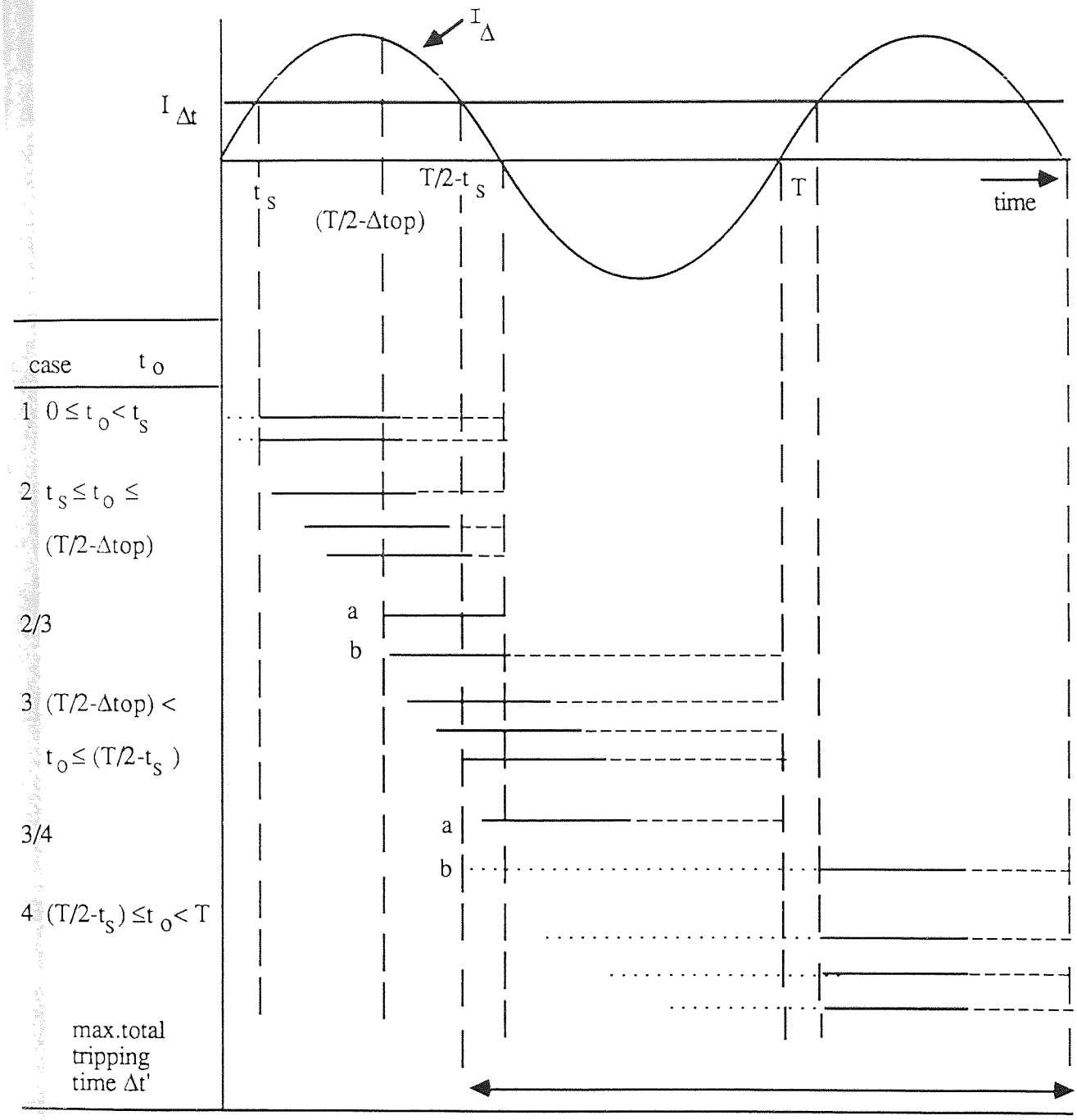

Waiting time : .....
Operating time : _____
Arcing time : ----------

Case 2/3 means the change from case 2 to case 3, i.e. a : case 2 and b : case 3

(a) Operation diagram for resistive load current

Figure 2.9. Effect of load current on the total tripping time

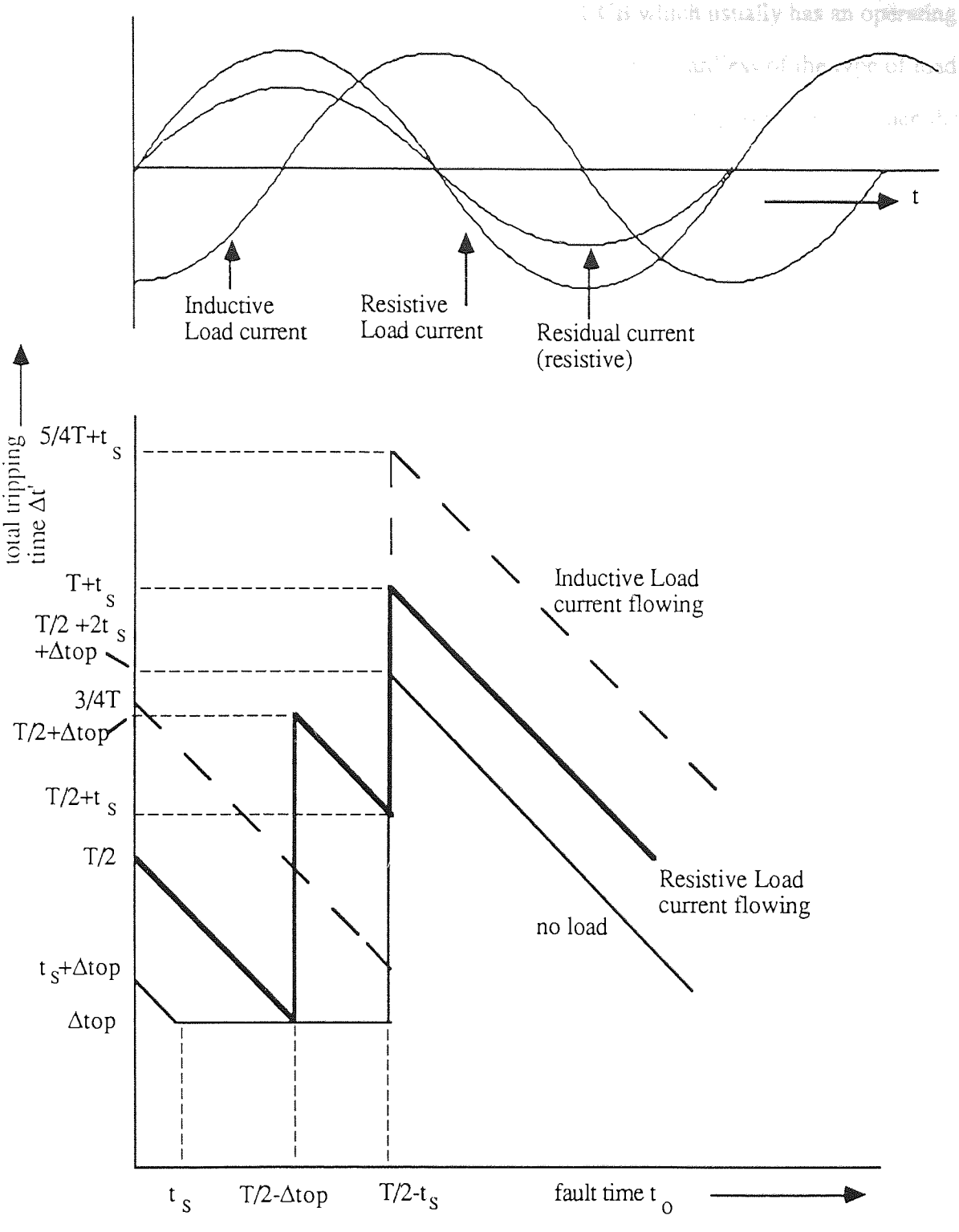

(b) Total tripping time characteristic, taking into account the effect of resistive and inductive load current.

Figure 2.9. Effect of load current on the total tripping time

From this analysis, it can be seen that an ordinary RCCB which usually has an operating time of around 5 ms will clear the fault in less than 40 ms regardless of the type of load current and the fault time, provided it senses the fault at the first opportunity, i.e when the residual current exceeds its threshold of tripping current for the first time.

2.5. Summary

In this chapter, the theoretical tripping time characteristics of RCCBs for sinusoidal current is derived. It should be pointed out that RCCB's tripping time depends on the fault time. Thus if the fault is introduced randomly, the tripping time obtained is also random and the maximum tripping time is unlikely to be obtained. It is also shown that load current may extend the tripping time although it is unlikely to exceed the standard limit. In the next chapter, a series of test is conducted to verify the theoretical description.

CHAPTER 3 EXPERIMENTAL RESULTS AND DISCUSSION OF RCCB CHARACTERISTICS FOR THE FUNDAMENTAL RESIDUAL CURRENT

3.1. Introduction

In this section, several test results using a 50 Hz sinusoidal residual current are presented to verify the theory developed. To demonstrate that the RCCB tripping time depends on the fault time t_o, resistive earth faults were introduced at various points of the current waveform using a point on wave device. The measurements were taken at no load and also when a resistive load current was flowing. It is shown that tripping time varied according to the fault time, thus a fault introduced only once at a random fault time is unlikely to give the maximum tripping time. To obtain the maximum tripping time, a point on wave device is needed. On the other hand, the way to obtain the RCCB tripping time according to the current standard is to introduce a fault at random fault times without specifying the number of tests that should be carried out, this is unlikely to give the maximum tripping time of the RCCB. Since a point on wave device is not normally available, especially in the field, the work is then extended to develop a probability analysis of RCCB tripping time leading to a method of obtaining the maximum tripping time of RCCBs by introducing several faults at random fault times followed by a simple calculation.

3.2. Experimental results

3.2.1. Point-on wave tests

Measurements were made on 2 electromechanical and 2 electronic RCCBs. A 50 Hz sine wave of 240 V was used. Resistive earth faults were introduced at various points on the current wave using a Point on wave device. The test circuit is shown in Fig.3.1. Typical

results for no load condition are given in Fig.3.2, and for loaded condition in Fig.3.3, showing the tripping time for various residual currents and fault time t_o.

Most of the results both for electromechanical and electronic RCCBs follow theoretical predictions fairly closely. However, one of the electronic RCCBs tested departed from the theoretical prediction and as such is discussed later in more detail.

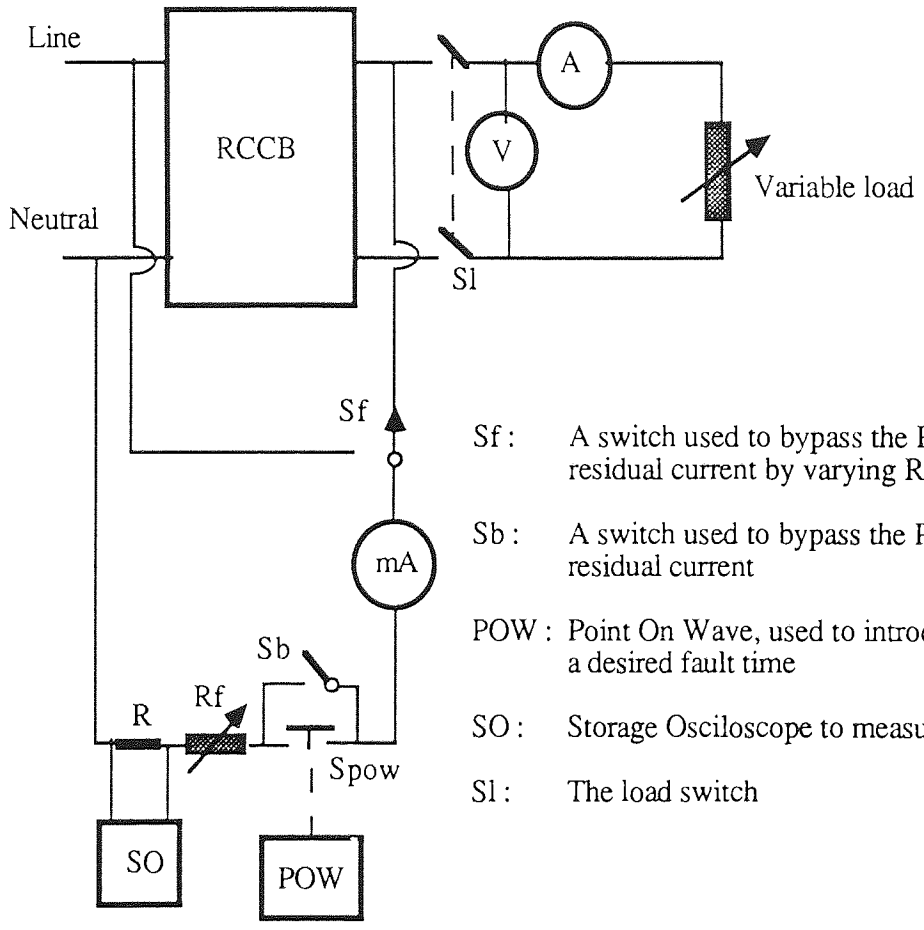

Figure 3.1. The test circuit to obtain the RCCB characteristics for the fundamental residual current

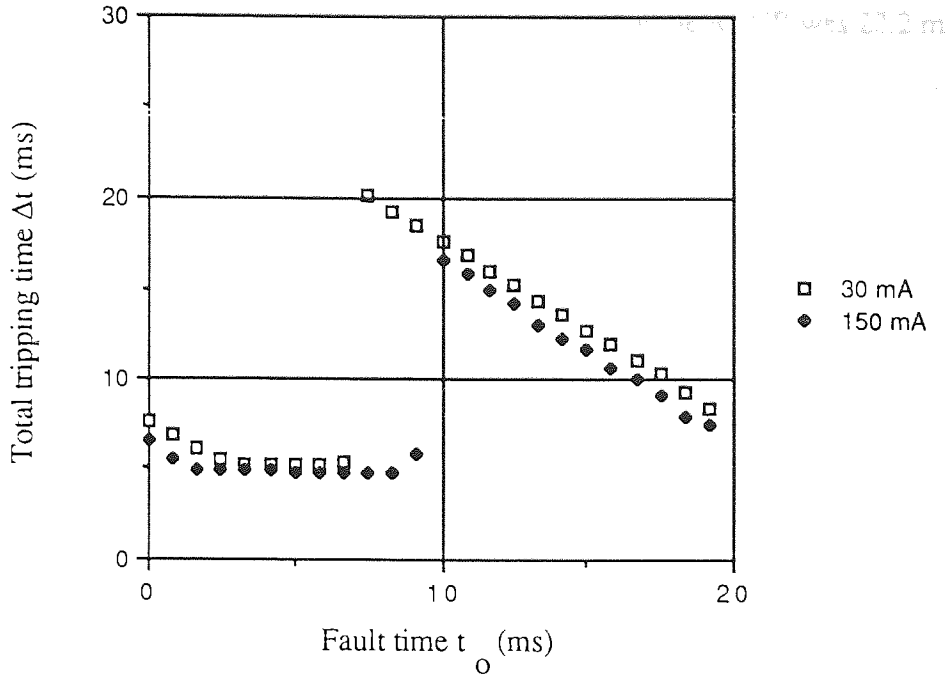

Figure 3.2. Test results at no load for I_Δ of 30 and 150 mA

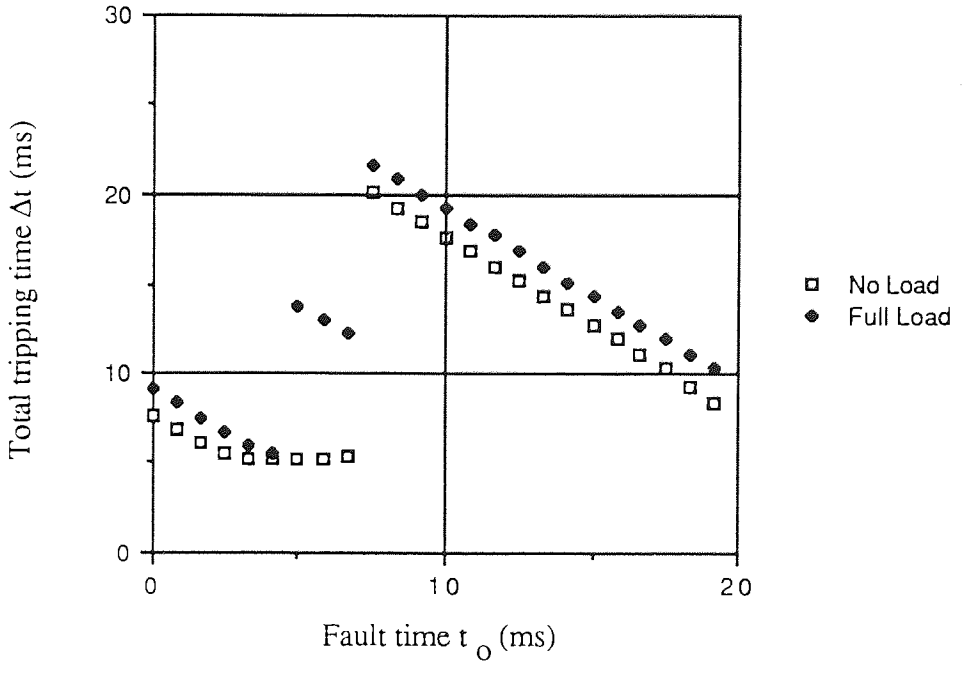

Residual current used was 30 mA

Figure 3.3. Test results at no load and with full load current flowing

Fig.3.2 shows the tripping time for the RCCB at no load condition for a residual current of 30 mA and 150 mA. The actual tripping current $I_{O\Delta}$ of the RCCB was 22.2 mA. It can be seen that the maximum tripping time is lower if the residual current is higher as predicted in section 2.4.1, Fig.2.8.a. The 'jump' of the tripping time due to the increase of the waiting time is also clearly shown.

The effect of load current is shown in Fig.3.3. It can be seen that a longer tripping time was obtained when the load current is flowing. The extra jump in the characteristic caused by the arc when load current is flowing, i.e the first jump, is also clearly shown in Fig.3.3. After the second jump, the total tripping time decreases, and for the loaded condition it is a fixed time longer than for the no load condition. This characteristic follows the theoretical prediction as described in section 2.4.2, Fig.2.9.b.

From Fig.3.2 and 3.3, it can be seen that the RCCB operation time, Δtop, i.e the minimum tripping time observed, is approximately 5 ms. The actual tripping current, $I_{O\Delta}$, of the RCCB was 22.2 mA, and the value of t_S for any residual current I_Δ can be calculated from equation 2.5.

At no load, given t_S and the operating time Δtop, one can use equation 2.8.a to calculate the maximum total tripping time as shown in Table 3.1. For the loaded condition equation 2.10.a can be used and the results are shown in Table 3.2.

Residual Current mA (r.m.s.)	Total Tripping Time, ms	
	Observed	Calculated
30.0	21.0	20.3
150.0	16.0	16.0
250.0	16.0	15.6

Table 3.1. Comparison of total tripping times, observed and calculated. No-load condition.

Residual Current mA (r.m.s.)	Total Tripping Time, ms	
	Observed	Calculated
30.0	22.0	22.6
150.0	20.0	20.5
250.0	19.0	20.3

Table 3.2. Comparison of total tripping times, observed and calculated. Resistive load current flowing.

3.2.2. Current interrupting characteristics

Fig.3.3 shows how the tripping time is extended when the load current is flowing. Fig.3.4 shows that if the RCCB opens when the current is far from the current zero (which exist at 180^{o}), at around 200^{o}, the circuit inductance and current between them sustained an arc, causing the residual current to flow until near the next current zero. In Fig.3.4, one can also see the current is interrupted just before it reaches current zero.

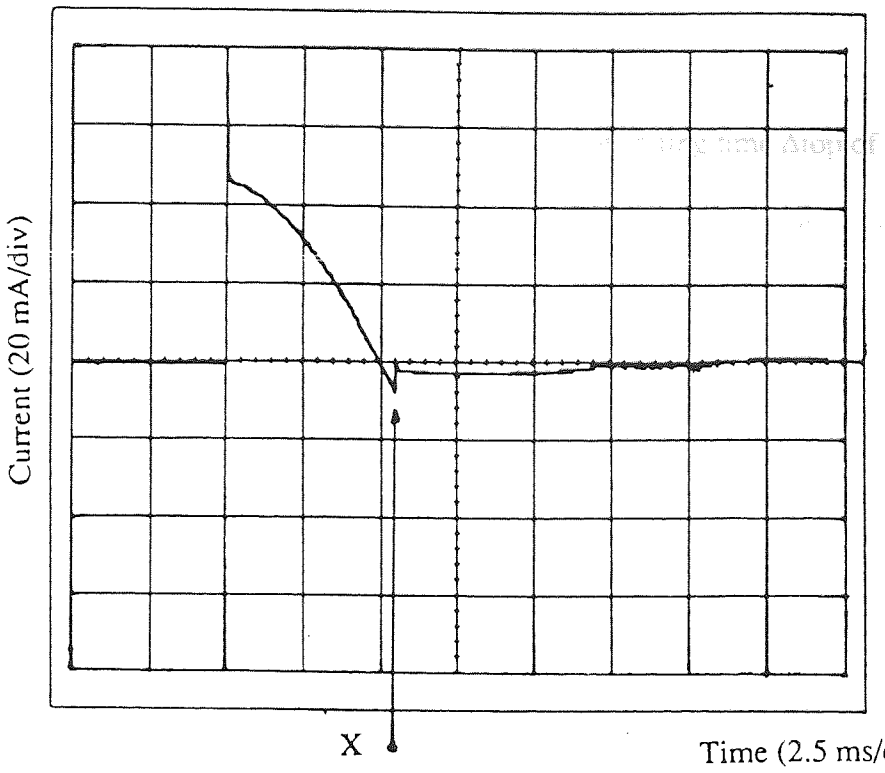

(a) The cessation of the residual current at no load.

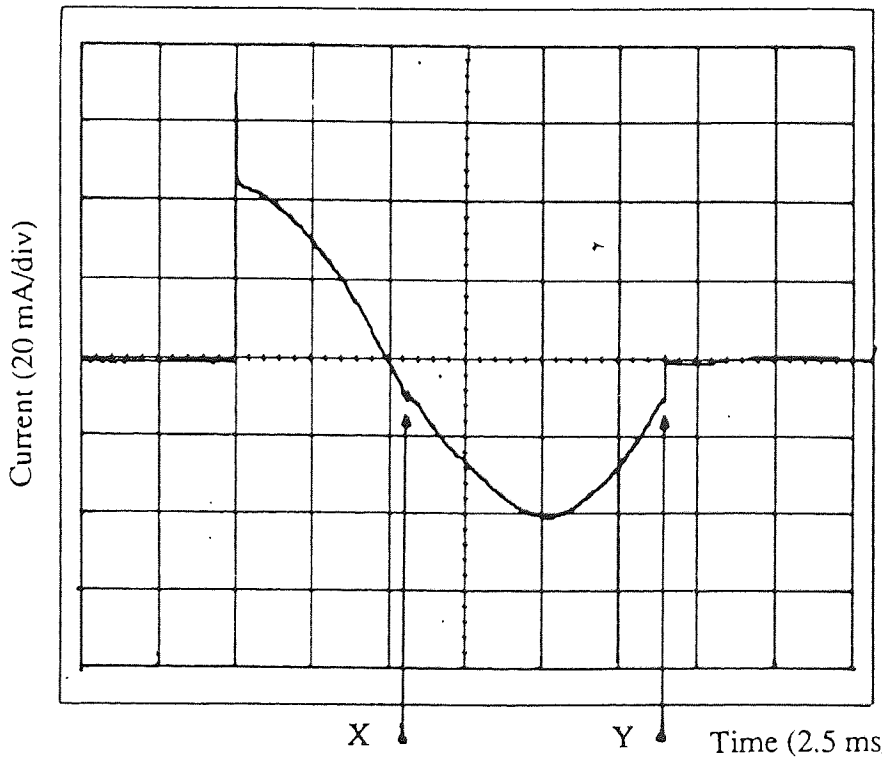

(b) The cessation of the residual current when full load current was flowing

At no load (a), the RCCB opened when the current angle was approximately 200°, and the current could be chopped directly at point X. When the load current was flowing (b), arc existed from point X until the next current zero (point Y).
The residual current used was 30 mA.

Figure 3.4. The extension of tripping time due to the existence of the arc

Examination of Fig.3.2 and 3.3 shows that the operating time Δtop of the RCCB is about 5 ms, and that the residual current I_Δ does not affect this time perceptibly. Hence the waiting time Δtw is a significant proportion of the total tripping time Δt as predicted in the theoretical analysis. It can thus be concluded that if the fault is introduced randomly then, on most occasions, the longest tripping time will not be obtained. To find the longest tripping time faults should be introduced at various angles.

3.2.3. Failure to meet the theoretical prediction

The results from one of the electronic RCCBs tested did not agree with the theoretical predictions for a residual current I_Δ of 30 mA but did so for I_Δ = 150 mA and 250 mA. At 30 mA the RCCB did not trip at the first opportunity, i.e when the instantaneous value of the residual current I_Δ exceeded the threshold value $I_{\Delta t}$ for the first time, but only at the second opportunity. This resulted in the characteristic shown in Fig.3.5. The maximum tripping time was still lower than the 200 ms limit and this deviation does not of itself seem to be harmful. It seems that the electronic circuit needs time before it can sense the fault.

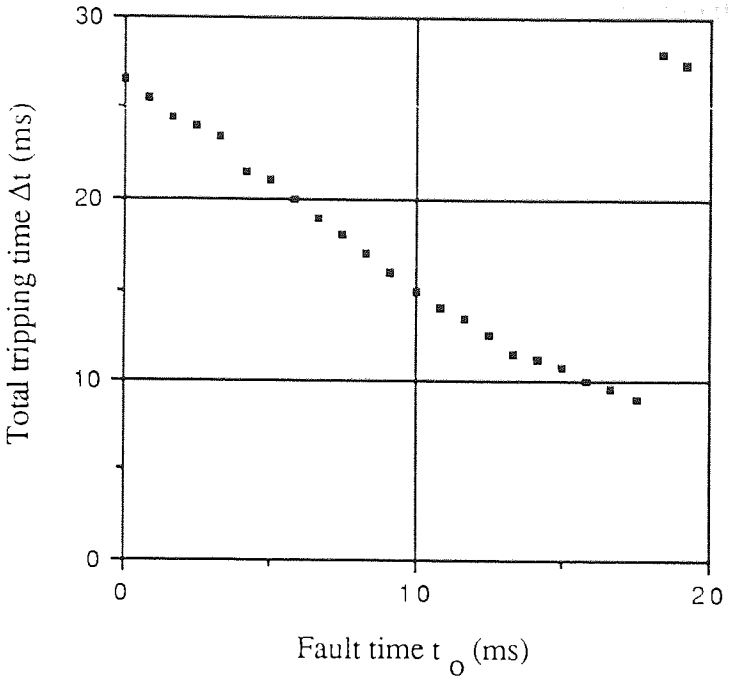

Actual Tripping current $I_{O\Delta}$ of the RCCB is 22.0 mA
Residual current I_{Δ} = 30 mA

Figure 3.5. Test results for the RCCB that failed to react at the first opportunity, i.e when the residual current exceeds its threshold value for the first time.

3.2.4. Effect of standing fault

A standing fault, i.e a fault which already exists before the RCCB is connected to the supply may affect the tripping time of the electronic RCCB. Electronic RCCBs have an auxiliary power supply to energise the amplifier, comparator and relay which are only in action when the RCCB itself is connected to the mains. A finite time is needed for the RCCB to get into a fully operational state in which it is able to sense and trip the relay. An experiment was set up so that the power supply and the RCCB itself were switched on to a standing fault. Such a situation may occur when a person holds equipment which is faulty before the RCCB and the power are switched on.

It was found that the two electronic RCCBs failed to react to the fault current when the instantaneous value of the residual current I_Δ exceeded its threshold value $I_{\Delta t}$ for the first time, but did react when the residual current exceeded its threshold for the second time. Total tripping times of up to approximately 45 ms were observed for I_Δ = 250 mA. Similar tests carried out on electromechanical RCCBs showed that their performance was not impaired in the same way.

Figs.2.5 and 2.6 show that failure to meet the 40 ms criterion pushes the tripping point at I_Δ = 250 mA from zone 2 to zone 3 of the IEC chart but not to zone 4 where ventricular fibrillation might be expected.

The number of RCCBs tested was limited, and more experiments would give greater confidence in application of the results. The theory developed however does seem to offer a basic frame work for such further study.

3.3. Random phase test method

3.3.1. Theory

The work so far shows that a fault introduced at a random phase angle is unlikely to yield the longest total tripping time, i.e Δt_{max} of the RCCB. Based on the RCCB characteristics however, it is possible to relate the number of tests and the probability of reading the maximum Δt.

Fig.2.8 shows that if a residual current I_Δ is passed through a RCCB at no load condition, the total tripping time Δt is a function of fault time t_0. If the fault is introduced randomly, a probability function $p(\Delta t)$ is obtained. From Fig.2.8, it can be found that the

minimum Δt is obtained for a fault delay between t_s and $(T/2-t_s)$. Thus the probability of obtaining the minimum total tripping time (Δt min.) is :

$$p(\Delta t = \Delta t \text{ min.}) = \{(T/2-t_s)-t_s\}/T$$

$$= (T/2 - 2\,t_s)/T \qquad (3.1)$$

From the same figure, one can also find that :

$$p(\Delta t < \Delta t \text{ min.}) = 0$$

$$p(\Delta t > \Delta t \text{ max.}) = 0$$

and that the probability of obtaining a value of between Δt and $(\Delta t+\delta\Delta t)$ in the range Δt minimum to Δt maximum is given by combining and extending equations 3.1 and 2.8 :

$$p(\Delta t \text{ min.} < \Delta t+\delta\Delta t \leq \Delta t \text{ max.}) = \frac{1- p(\Delta t = \Delta t \text{ min.})}{\Delta t \text{ max.} - \Delta t \text{ min.}} . \delta\Delta t$$

$$= (1/T).\ \delta\Delta t \qquad (3.2)$$

The probability function is shown in Fig.3.6.a.

If the integral of the function is taken as the cumulative value $c(\Delta t)$, where :

$$c(\Delta t) = \int_{\Delta t}^{\Delta t \text{ max.}} p(\Delta t)\, d_{\Delta t} \qquad (3.3)$$

a steep straight line is obtained as shown in Fig.3.6.b, $c(\Delta t)$ is thus the probability of obtaining a particular total tripping time Δt or higher.

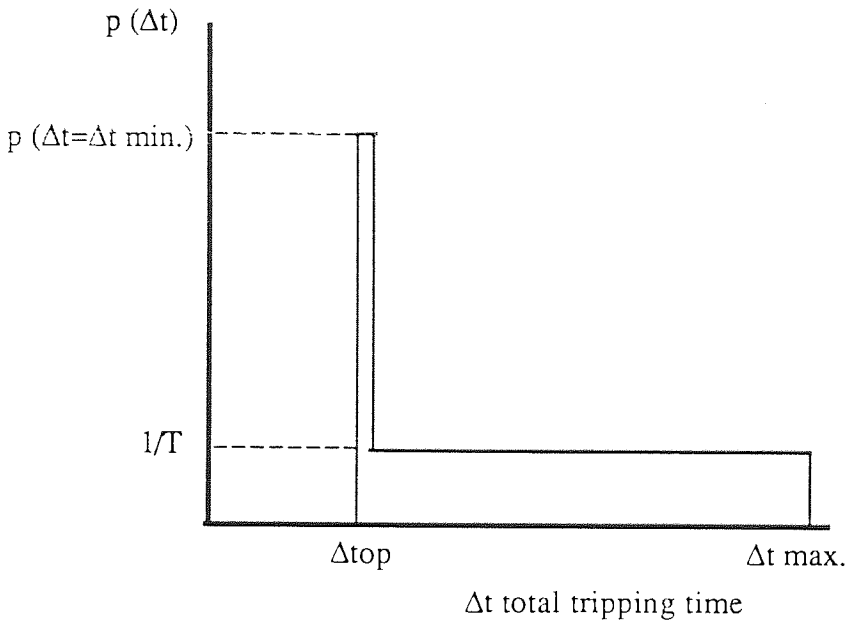

(a) The probability p(Δt) function

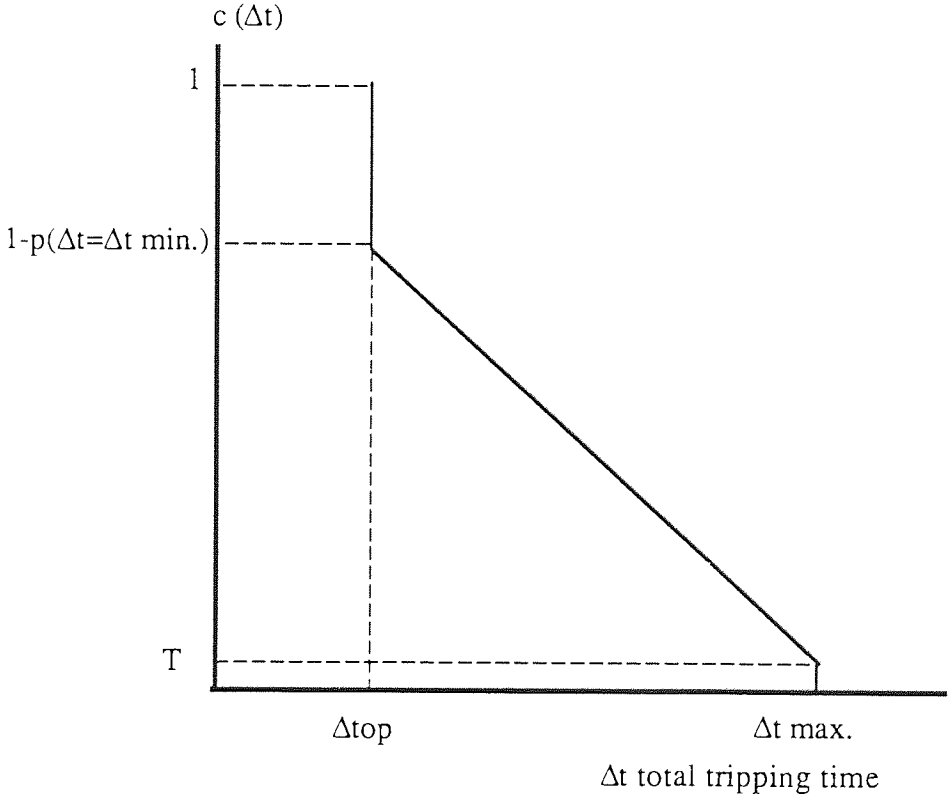

(b) The cumulative probability c(Δt) function

Figure 3.6. The probability and cumulative probability characteristics of RCCB's total tripping time Δt at no load

3.3.2. Random phase test results

A RCCB was tested with random faults using a 30 mA residual current at no load. Faults were switched using a triac rather than a contactor to eliminate contact bounce and improve the sharpness of the fault application, 30 readings were taken. The times were put in descending order and plotted as shown in Fig.3.7, and the points should approximate the cumulative probability curve. The similarity between the test results and the theoretical prediction gives confidence to this work.

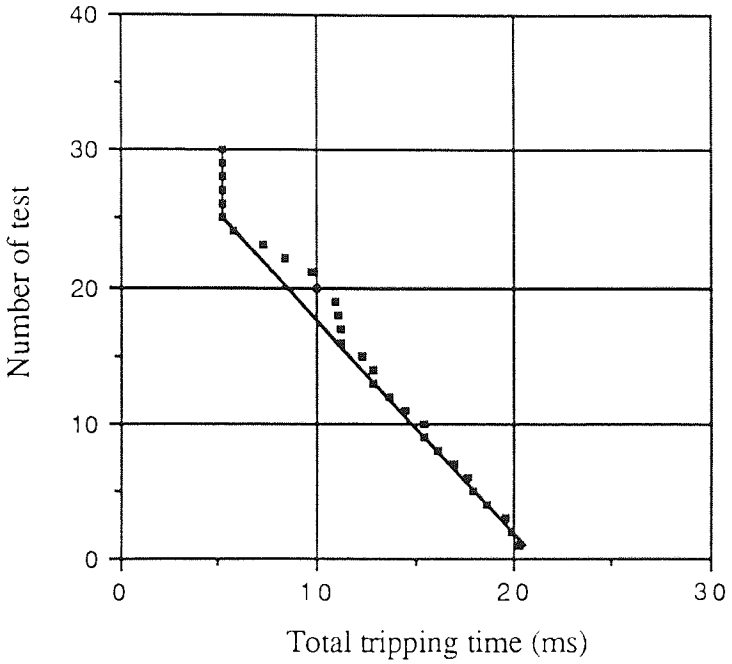

Total number of tests M : 30
Residual current I_{Δ} = 30 mA.
Actual tripping current $I_{O\Delta}$ = 22.2 mA.
____ : theoretical calculation.

Figure 3.7. Cumulative probability of the number of tests taken from a series of random tests at no load

3.3.3 Confidence levels on estimates of maximum tripping time

If the scale of Δt is divided into intervals of $\Delta tint$, then the probability of observing a tripping time in the interval $\Delta tint$ centred around Δt ($\neq \Delta t$ min.) is : $\Delta tint/T$

For a RCCB tested with random fault angles, the outcome of each test can be assigned into one of two possibilities :

a. $\Delta t = \Delta t$ max., the probability is $\Delta tint/T$

b. $\Delta t < \Delta t$ max., the probability is $1-(\Delta tint/T)$

The distribution is binomial, so for M tests, the probability that any $\Delta tint$ including the maximum Δt may not be obtained is :

$$F(0) = \{1-(\Delta tint/T)\}^M \qquad (3.4)$$

and the probability of obtaining at least one maximum total tripping time is $1-F(0)$.

From equation 3.4 the number of random fault angle tests that must be carried out to obtain the maximum total tripping time with 95% confidence can be calculated as shown in Table 3.3. To obtain an accurate measurement without having to perform too many tests 30 tests is suggested as giving the maximum tripping time to within 2 ms with 95% confidence.

The maximum and minimum tripping time should be related to each other by

$\Delta tmax - \Delta tmin = T/2 + 2t_S$, where the range of t_S is shown in table 2.1, and so :

$$t_S = (\Delta t \text{ max.} - \Delta t \text{ min.} - T/2)/2 \qquad (3.5)$$

$$I_{O\Delta} = I_\Delta \sin [\, \omega (\Delta t \text{ max.} - \Delta t \text{ min.} - T/2)/2] \qquad (3.6)$$

Thus given Δt maximum and Δt minimum for one value of trial residual current I_Δ, one

may calculate $I_{O\Delta}$, the actual tripping current. Conversely, given the actual tripping current and the maximum tripping time Δt max., the operating time Δtop can be calculated.

Time interval, Δtint (ms)	Number of test
0.5	118
1.0	59
1.5	39
2.0	29
2.5	23
3.0	19
3.5	16
4.0	14

Table 3.3 Relation between time interval and the number of tests for a 95% confidence level.

It should be pointed out that if the load current is taken into account, a rather different probability function is obtained from the no-load case as shown in Fig.3.8. The important point to note is that the probability of obtaining the maximum $\Delta t'$ is the same, that is 1/T, although the value of $\Delta t'$ maximum itself is greater. Consequently the probability analysis developed for the no load case above can also be applied, and the same number of tests should be performed to obtain the maximum total tripping time.

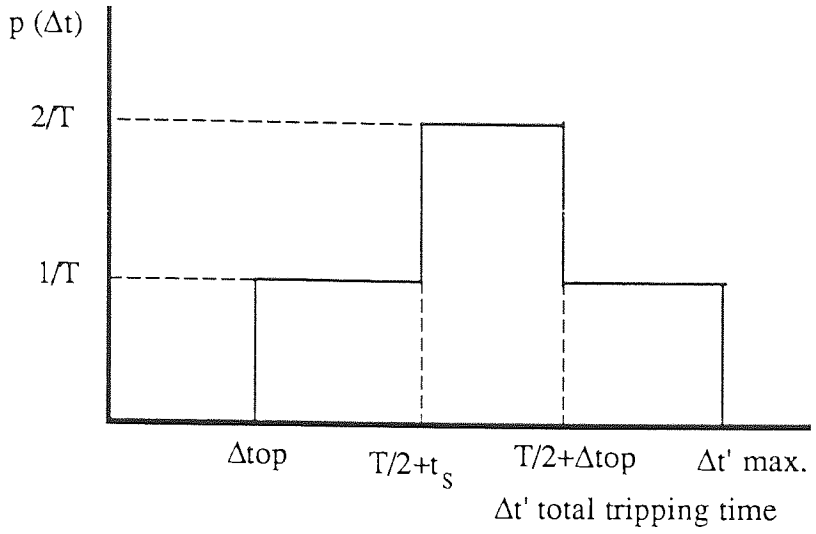

(a) The probability p(Δt) function

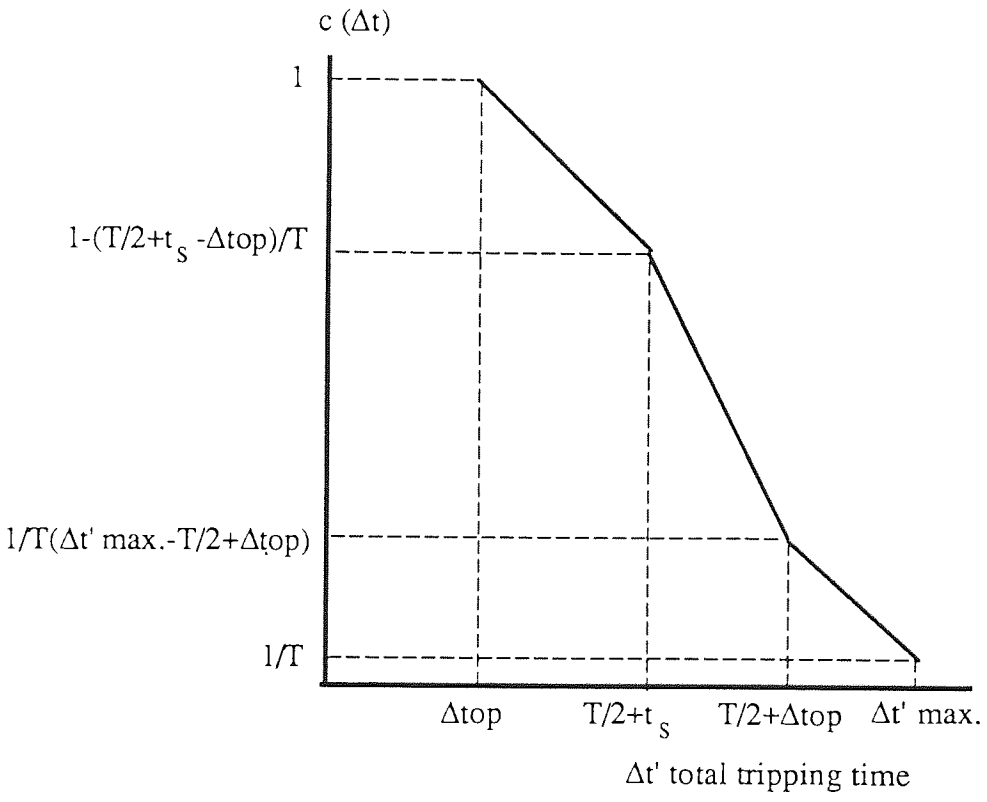

(b) The cumulative probability c(Δt) function

Figure 3.8. The probability and cumulative probability characteristics of an RCCB's total tripping time with load current flowing.

3.4. Summary

There are several important points to note about the RCCB characteristics for sinusoidal current. Firstly, as described in the theory and verifed by test results, the tripping time of the RCCB is a function of fault time, and that the load current may extend the tripping time due to the existence of the arc. Thus a fault introduced only once at no load will rarely measure the maximum tripping time that can be encountered in practice. The maximum tripping time can be obtained by using a point on wave device which unfortunately is not normally available especially in the field. Based on the probability study however, it is possible to obtain the maximum tripping time by carrying out random tests several times. If a 2 ms interval resolution is taken, then the random test should be repeated 30 times in order to obtain the maximum tripping time with 95% confidence level. The maximum value, and not the average should be taken as the maximum tripping time. A similar analysis can also be used if the load current is flowing to obtain the maximum total tripping time. Finally, it should be mentioned that a longer maximum total tripping time, in excess of the standard limit, may be obtained in electronic RCCBs if they are switched onto a standing fault (Note, this may not be as dangerous as it appears).

CHAPTER 4. THE EFFECT OF HARMONICS ON RCCB CHARACTERISTICS

4.1. Introduction

In the beginning of this chapter, a brief introduction about how the harmonics are generated as well as the harmonic content of the mains supply is presented. Since RCCBs are mainly used to protect people against ventricular fibrillation, then the effect of harmonics on ventricular fibrillation is also briefly described. It is then followed by the theoretical description of the effect of harmonics on RCCBs.

4.1.1. The harmonic content in the mains supply

Basically harmonics are produced by non-linear loads and especially power electronic devices. Although the system generators also produce some harmonics, their value is negligible. The main sources of harmonics, as pointed out by the Mc Graw Edison team are (56) :

1. Ferromagnetic devices such as distribution transformers.
2. Arcing loads such as arc furnaces, fluorescent lighting.
3. Electronic and power electronic devices such as oven controls, rectifier circuits on TVs, battery chargers, etc.

The last two are the dominant sources of harmonics (56).

Since RCCBs are used to protect a particular installation or a particular load, they are subject to harmonics produced by the particular load, or in case of an installation, the summation of harmonics produced by all devices within the installation. Protection relays, which will be described in the next chapters, are connected to the distribution or transmission line via current or voltage transformers and are thus subject to the summation of harmonics of all devices supplied by the line. Fortunately, as Crucq and Robert (57) pointed out, the resulting harmonic level is lower than the arithmetic sum of

the individual contributions .

In the UK, and also in other countries, the harmonic currents that may be fed into the electricity supply system by the consumers' electrical equipment are governed by regulations (58,59,83). The harmonic content in the mains line and the way it should be measured are still being extensively studied (57,58). One of the most important features is the 'time interval' of the measurement, since an installation which has a negligible harmonic content over a long period, say one week, may produce a high harmonic content during a very short period, say 1 s. The following time intervals for measurement have been proposed for an IEC guidelines (60) :

1. Very short interval : 3 s
2. Short interval : 10 minutes
3. Long interval : 1 hour
4. One day interval : 24 hours
5. One week interval : 7 days

Another important feature is the parameter that should be measured. EPRI report (70) stated that conventional statistical measurement of amplitude does not adequately describe harmonic levels because of frequent abrupt changes in harmonic and noise amplitudes with time at a fixed location. A similar view was also expressed by Orr and Cygorski (84). In order to present the information about the non-sinusoidal waveform, the amount of distortion can be expressed in several ways (48,77). One way is to define the distortion factor as the ratio of the r.m.s. value of the harmonic only to the the r.m.s. value of the waveform. Another way is to express the distortion factor as the ratio of the r.m.s. value of the harmonics only to the r.m.s. of the fundamental. The above expressions about distortion give information about the harmonic content but not how the waveform itself looks like. Recently, Crucq and Robert (57) started to present harmonic content in a probability diagram which includes both magnitude and phase angle of the harmonic current/voltage. In the light of my study as reported previously (32,53,54,55),

this method of presentation seems to be preferable since phase angles affect the tripping value of RCCBs as well as the two types of protection relays studied.

Although it is not the intention of this work to study the harmonic content in the mains, it should be pointed out that at the moment many measurements of harmonic content of a particular installation or load have been reported (70,71,82). In particular, attention should be paid to the high harmonic content in some plants where it was observed that the harmonic currents exceed the magnitude of the fundamental currents as described by an IEEE committee study (48).

4.1.2. The effect of harmonics on ventricular fibrillation

Concerning the effect of harmonics on ventricular fibrillation, after an extensive literature survey, it was found that several vague points exist. Although Dalziel (63) showed that the threshold of let go current varies with frequency, it is not yet known whether the effect on the human body of a periodic non-sinusoidal current waveform can be considered the same as the effect of each individual frequency component summed appropriately (64). On the other hand, Dalziel (66) also showed that for a periodic non-sinusoidal current waveform, it was the peak of the waveform which determined the let go threshold.

Despite a broad literature survey, no complete information was found concerning the effect of a periodic non-sinusoidal waveform on the threshold of ventricular fibrillation. Morley (15) calculated the effect of frequency on the threshold of ventricular fibrillation based on Geddes and Baker's results (65). However it is not known how the human body, especially the heart, will react to the effect of the summation of those waveforms. There is no confirmation as to whether Dalziel's experimental results concerning the threshold of let go current for non-sinusoidal waveforms (66) is also applicable to ventricular fibrillation. Although not accepted unanimously, Bernstein (64) stated that it

was widely agreed that the energy in the current determined the threshold of ventricular fibrillation. However, Bridges et al pointed out that a full and complete understanding on how human body will react to non-sinusoidal current was still some time away (26).

Despite the lack of complete understanding, in the middle of 1987, IEC published the electrocution criterion for a.c. current above 50 Hz and 3 types of non sinusoidal waveform (3) :

- Alternating Sinusoidal Currents with a d.c. component.
- Alternating Sinusoidal Currents with phase control.
- Alternating Sinusoidal Currents with multicycle control.

Other types of waveform are still under consideration.

Fig.4.1 shows the effect of frequency on the threshold of ventricular fibrillation.

In general it can be concluded that the effects of periodic non-sinusoidal current waveforms on the human body is a field that needs further works (NB: Outside the scope of this work).

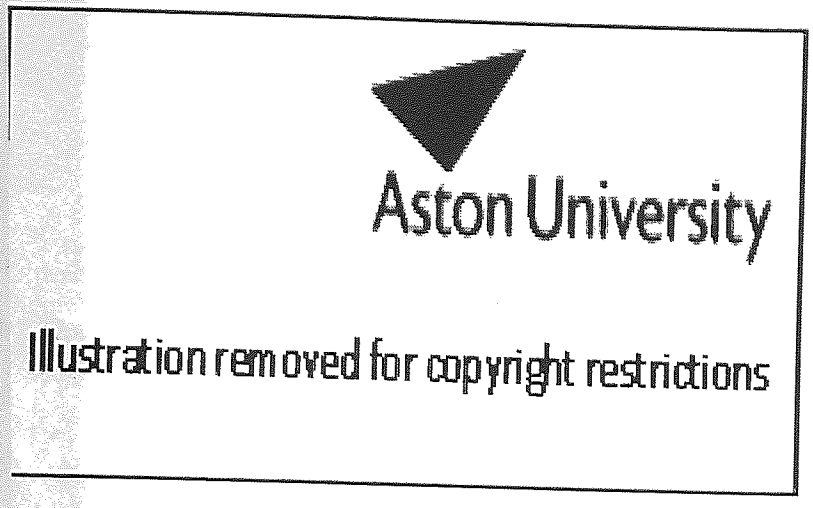

Variation of the threshold of ventricular fibrillation within the frequency range 50/60 Hz to 1000 Hz, shock durations longer than one heart period and longitudinal current paths through the trunk of the body.

Note.- For shock-durations shorter than one heart period, other curves are under consideration.

Frequency factor F_f is the ratio of the threshold current for the relevant physiological effects at the frequency f to threshold current at 50/60 Hz.

Figure 4.1. The Effect of frequency on the threshold of ventricular fibrillation; Taken from IEC report 479-2 (3)

4.1.3. Approach taken in analysing the effect of harmonics

In the previous RCCB model described in section 2.2, the tripping parameter X_Δ is assumed to be linearly related to the residual current I_Δ. Consequently, RCCBs start to operate when the instantaneous value of the residual current I_Δ sensed by the CBT exceeds a particular triggering threshold value $I_{\Delta t}$. The theoretical prediction of an

RCCBs performance based on the above model compared well with the experimental results in the case of a pure sinusoidal residual current. If the residual current contains harmonics, i.e it is not sinusoidal, then every single sinusoidal component frequency of the residual current will be affected by the RCCB differently. The inductance of the CBT for example will have different effects on each frequency. Thus the effect of the RCCB on each sinusoidal component of the periodic non-sinusoidal residual current waveform should be firstly considered, then the effect of the non-sinusoidal waveform will be considered.

4.2. Frequency response analysis

4.2.1. The effect of the CBT

Firstly, the effect of frequency on RCCBs will be considered, since any periodic waveform can be divided into a series of sinusoidal waveforms. If a CBT is connected to a relay which acts as a burden as shown in Fig.2.1, a residual current I_Δ passing through the CBT will act as the a primary current of a current transformer I_p. This current will cause a secondary current I_S to flow. Ideally, based on the equation :

$$N_p I_p = N_S I_S \qquad (4.1)$$

I_S is not a function of frequency and depend only on I_p, N_p and N_S. If the core losses, magnetising flux and other constants are taken into account as discussed below, I_S will vary with frequency. Fig.4.2 shows the model of the CBT and Fig.4.3 shows its phasor diagram.

As frequency increases, core losses will increase. On the other hand, I_{mp} will decrease

since the impedance ωL_{mp} increases. The decrease in I_{mp} will also decrease V_s and I_s. The increase in frequency will also increase V_s since it is directly proportional to frequency, and will tend to increase I_s. Morley (15) showed that although V_s increases proportionally with frequency, at even higher frequencies, the voltage tends to level off due to increasing losses. Since both the secondary winding and the burden contain some inductance, the total secondary winding impedance Z_s will increase with frequency. This effect will decrease I_s. All the above effects will affect the variation of the secondary current I_s with frequency. Depending on which effects are dominant, I_s may either increase or decrease. It is thus clear that the output of the CBT and hence the RCCB will exhibit a 'Gain Response'.

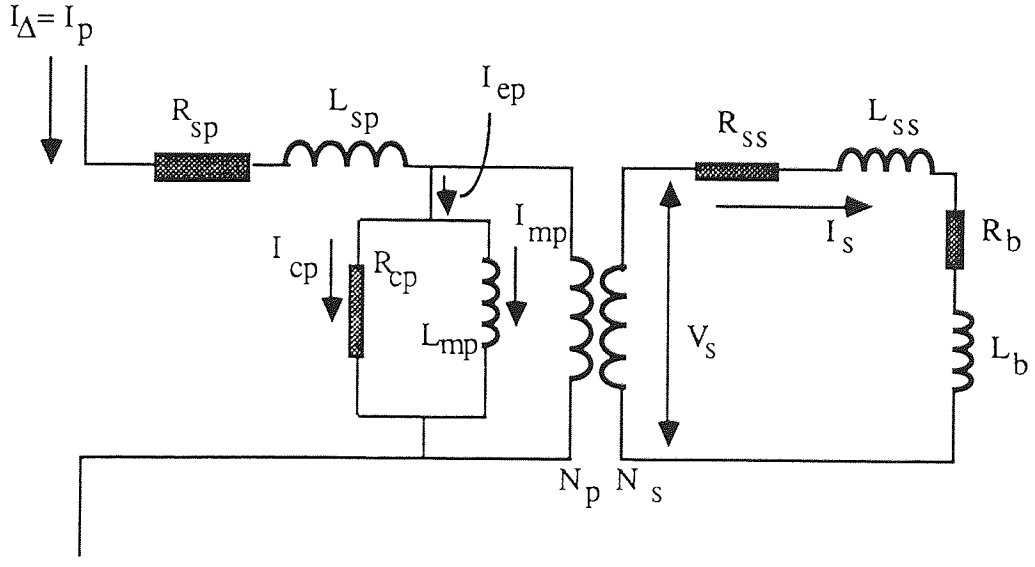

$R_{ss} + R_b = R_s$
$L_{ss} + L_b = L_s$
$Z_s = R_s + j\,\omega\,L_s$

Figure 4.2. The CBT model

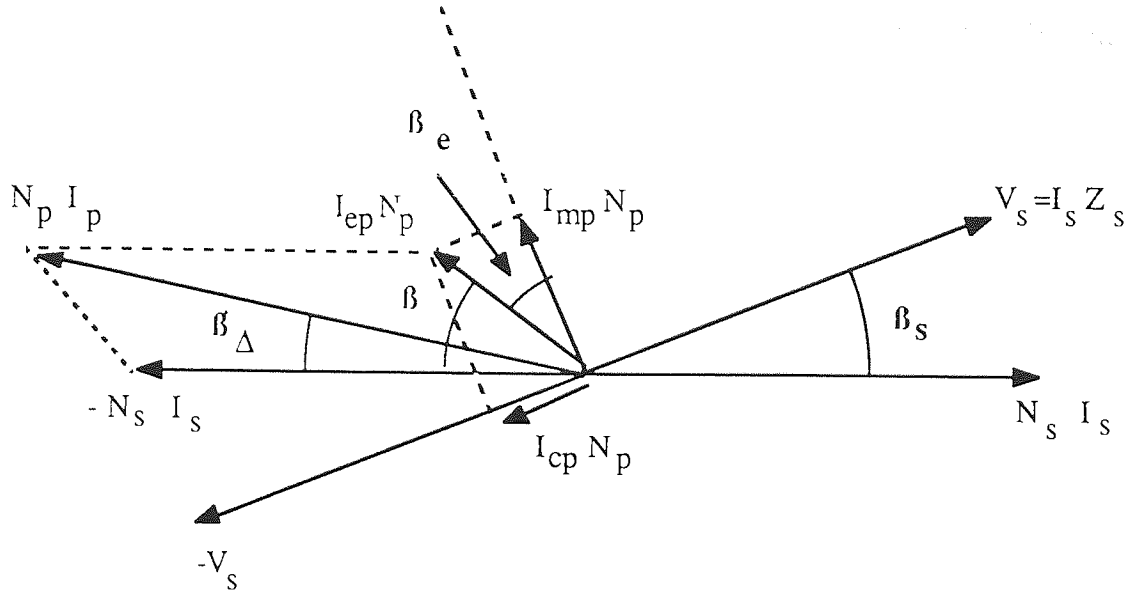

Figure 4.3. Phasor diagram of the CBT model

The electromechanical relays as shown in Fig.2.2 and Fig.2.3, which are the tripping mechanisms of electromechanical RCCBs, are the burden of the CBT. The relay opens the circuit breaker provided the flux in the relay produced by I_S can overcome the effect of flux produced by the permanent magnet. Assuming that the flux is linearly related to I_S then the relay will open when the peak value of I_S reaches the threshold value. If I_S decreases when frequency increases, then in order to trip the RCCB, the residual current I_Δ should be increased to increase I_S such that its peak value reaches the threshold value, causing the relay to open. Consequently, the RCCB's tripping current $I_{o\Delta}$ will increase with frequency. Similarly, if I_S increases with increasing frequency, the tripping current $I_{o\Delta}$ decreases.

For the electronic RCCBs as shown in Fig.2.4, the load resistor R_L is the burden of the CBT. Provided R_L is a pure resistor and the amplifier gain is independent of frequency,

then the amplifier output voltage V_g, which is the tripping parameter of the RCCB, will be linearly related to I_s. The relay will be energised whenever the peak value of V_g reaches V_l which is a constant value. Consequently, the analysis of the variation of RCCB's tripping current $I_{o\Delta}$ with frequency for electromechanical RCCBs is also applicable to electronic RCCBs.

In addition to 'gain response' as discussed above, Fig.4.3 shows that RCCBs also exhibit 'phase shift'. From this figure it can be seen that I_s is not necessarily in phase with I_p. The phase difference $ß_\Delta$ is dependent upon Z_s, R_{cp}, and L_{mp}, and as Wright (30) shows, $ß_\Delta$ can be negative although in most cases it is positive. If the frequency is varied, $ß_\Delta$ will vary .

$$ß_e = \tan^{-1}(I_{cp}/I_{mp})$$

$$= \tan^{-1}(\omega L_{mp}/R_{cp}) \qquad (4.2)$$

As frequency increases, then the ωL_{mp} reactance and the core losses increase, and change the value of $ß_e$ and hence $ß_\Delta$.

$$ß_s = \tan^{-1}(\omega L_s/R_s) \qquad (4.3)$$

hence with the increase in frequency, $ß_s$ increases, causing ß and $ß_\Delta$ to decrease. The combination of the above effects will either increase or decrease $ß_\Delta$ (depending which of the effects dominate).

4.2.2. The effect of the relay

The relay may affect electromechanical RCCB characteristics since the relay flux, $\emptyset_r$, is not necessarily linearly related to the secondary current I_S. Hence, the increase in frequency may affect the relationship between $\emptyset_r$ and I_S as discussed below. The flux in the relay $\emptyset_r$ is related to I_S since :

$$\emptyset_r = I_S/S_{rl} \tag{4.4}$$

$$S_{rl} = \mu_{rl}\, l_{rl}/A_{rl} \tag{4.5}$$

where S_{rl} is the relay reluctance, l_{rl} is the relay length, μ_{rl} is the relay permeability and A_{rl} is the cross sectional area of the relay. Ideally, the frequency does not affect the relationship between the current and the flux. However, as the frequency is increased, the core loss of the relay becomes more significant and the magnetising component of the current decreases, hence flux $\emptyset_r$ decreases and consequently, the tripping current has to increase. Thus in mechanical RCCBs, the tripping current $I_{O\Delta}$ is affected by both the CBT and the relay. Consequently, the flux in the relay $\emptyset_r$, which is actually the tripping parameter X_Δ of the RCCB, exhibits both gain and phase shift with respect to the residual current I_Δ even though the core operates in its linear region. As a consequence, the waveform of the tripping parameter X_Δ differs from the waveform of I_Δ and varies with frequency.

For electronic RCCBs, normally the relay has no effect at all since it is not energised directly by the secondary current I_S of the CBT. The secondary current is normally used to trigger an electronic circuit and the relay itself is energised by a separate power supply

which draws the power from the mains (see section 2.1).

4.2.3. The effect to the RCCB tripping current

Normally, RCCBs are adjusted for residual current at power frequency, i.e 50 Hz. If the residual current at 50 Hz reaches the tripping current $I_{O\Delta}$, the RCCB will trip. However, if the frequency increases, the relationship between the tripping parameter X_Δ and the residual current I_Δ also changes since their relationship is a function of frequency. Consequently the RCCB is more sensitive if X_Δ increases with the increase of frequency and vice versa.

Depending on the RCCB constants, the increase in frequency may increase or decrease the sensitivity of RCCBs. This may explain the Electricity Council test results (see Ref.29), where it was found that harmonics may increase or decrease the sensitivity of RCCBs.

4.3. Effect of harmonics

A periodic non-sinusoidal residual current can be split into its sinusoidal components. As described in section 4.2 above, each component is affected differently, i.e. each frequency may have a different tripping current since the relationship between the residual current and the tripping parameter X_Δ may be different for each frequency. Consequently, the waveform of the tripping parameter will be different to that of the residual current. A periodic non-sinusoidal residual current can be represented as :

$$I_\Delta = \sum_{n=1}^{\infty} I_{\Delta n} \sin(\omega_n t + \partial_n) \qquad (4.6)$$

Then the tripping parameter waveform is :

$$X_{\Delta} = \sum_{n=1}^{\infty} (G_n I_{\Delta n}) \sin (\omega_n t + \partial_n + \theta_n) \qquad (4.7)$$

provided the CBT and the relay work in their linear region. G_n and θ_n are the gain and phase shift of the tripping parameter $X_{\Delta n}$ for the n^{th} harmonic residual current $I_{\Delta n}$.

Equations 4.6 and 4.7 show that if the frequency response of a RCCB is known, it is possible to calculate its tripping current for non-sinusoidal waveforms. Firstly, the non-sinusoidal waveform should be split into its fundamental and harmonics, then the peak of the triggering parameter X_{Δ} can be determined. Since the RCCB trips once this peak reaches X_1, then the tripping current $I_{O\Delta}$ of the waveform can be calculated.

4.4. Other considerations

It has been described that the sensitivity of RCCBs is affected by harmonics and for sinusoidal residual current it is also affected by the frequency of that residual current. The effects depend on the RCCB constants. On the other hand, ventricular fibrillation is also affected by the frequency of sinusoidal currents and in the case of non-sinusoidal current, by its harmonics content although the effect is not completely clear. It is important to point out at this stage that the effect of harmonics on RCCBs is not necessarily similar to that on ventricular fibrillation. Thus a RCCB that may provide protection against ventricular fibrillation may not do so if the current contains harmonics. A RCCB however may be designed with an additional filter which has a similar frequency response to that of a body as developed by Morley et al (15). However, while the response of such a filter to a periodic non-sinusoidal waveform can be calculated, the response of the same waveform to our heart is still unclear and as such this deserves more study (outside the

scope of our work).

Although BS 4293 (6) only considers sinusoidal residual current, other standards such as West Germany 's VDE 0664 (72) includes non-sinusoidal residual current requirements. In this standard (72) only pulsating d.c. currents, e.g the waveform that occurs at half wave rectification, are included in the requirement. This work however focusses on the effect of harmonics on RCCBs used for sinusoidal residual current as laid down by BS 4293 although the brief discussion below on the RCCBs that follow VDE 0664 shows that they are also affected by harmonics.

In order to enable a mechanical RCCB to sense pulsating d.c. residual current, usually a magnetic material which has high 'flux charge' as described by Meir (73) and Roesch (74) is used. In addition, a capacitor is placed in series with the electromechanical relay to make the trip circuit resonant (73,74). Roesch (74) showed that this capacitor may increase the phase shift between the secondary current (I_S) and the primary current (I_p) of

the CBT. Thus while an ordinary RCCB may have negligible phase shift θ_n, a RCCB fitted with a capacitor, which are widely used in order to fulfill the requirement of a standard such as VDE 0664, may not. However, since the construction of the d.c. sensitive RCCBs are similar to the ordinary RCCBs, the effect of harmonics on them can be analysed in the same way.

4.5. Summary

This theoretical description shows that sinusoidal residual currents with different frequencies have a different tripping current which depends on the RCCB constants. Since a periodic non-sinusoidal current can be split into its sinusoidal components, then each components is affected differently. However, if the frequency response of the RCCB is known, then the tripping current for the non-sinusoidal current waveforms can

be calculated. Depending on the RCCB constants, harmonics may increase or decrease the sensitivity of RCCBs.

Another important point to note is that the effect of non-sinusoidal current on the human heart is still largely unknown. Thus although the RCCB behaviour due to harmonics is known, its effectiveness in protecting people against ventricular fibrillation still has to be found which is outside the scope of this work.

CHAPTER 5. EXPERIMENTAL RESULTS AND DISCUSSION OF THE EFFECT OF HARMONICS ON RCCB CHARACTERISTICS

5.1. Introduction

In this chapter, some test results are presented. Firstly, the tripping currents of the RCCB for sinusoidal current at various frequencies were obtained. Then the tripping currents of the RCCB if the current contain harmonics were measured. A waveform generator that could generate a waveform with controlled harmonic content was built and used to test the RCCB. In order to see the effect of the waveform on the tripping current, several currents which have the same harmonic content but different waveforms due to different phase angle ∂_n were used to trip the RCCB.

5.2. Frequency response tests of RCCBs

Following the previous theoretical analysis in chapter 4, two mechanical and one electronic RCCB were tested using sinusoidal current waveforms with frequencies from 50 to 1000 Hz. A signal generator was used coupled to a high power amplifier and the output was connected through the RCCB tested to a resistive load as shown in Fig.5.1. Both the amplifier gain and load can be varied to increase the current.

The tripping current of the RCCB, $I_{o\Delta}$, and the relay magnetising current, i.e the secondary current of the CBT, I_s, were measured. The phase shift between the primary

(I_p) and secondary (I_s) current, θ_n, was also measured. I_s and I_p were passed through a linear resistor of low resistance and the phase shift between the two voltage drops was measured using an oscilloscope. In the case of the electronic RCCB, the voltage drop across the resistance, V_g, could be measured directly. It was found that in one

electromechanical RCCB, I_s decreased with an increase in frequency, causing $I_{o\Delta}$ to increase as predicted previously in the theoretical work in chapter 4. In another electromechanical RCCB however, it was found that although I_s increased, $I_{o\Delta}$ increased as well, suggesting that the suppression caused by the electromechanical relay was dominant in comparison to the gain caused by the CBT. Thus the effects as described in the theory took place as predicted. For the electronic RCCB, it was found that the tripping current $I_{o\Delta}$ increased while V_g decreased as predicted in the theory.

Fig.5.2 shows the effect of frequency on the tripping current of a RCCB. The figure shows that the frequency affects the tripping current significantly. The measurement on the phase shift θ_n shows that its value is quite small, around 5^o, as predicted.

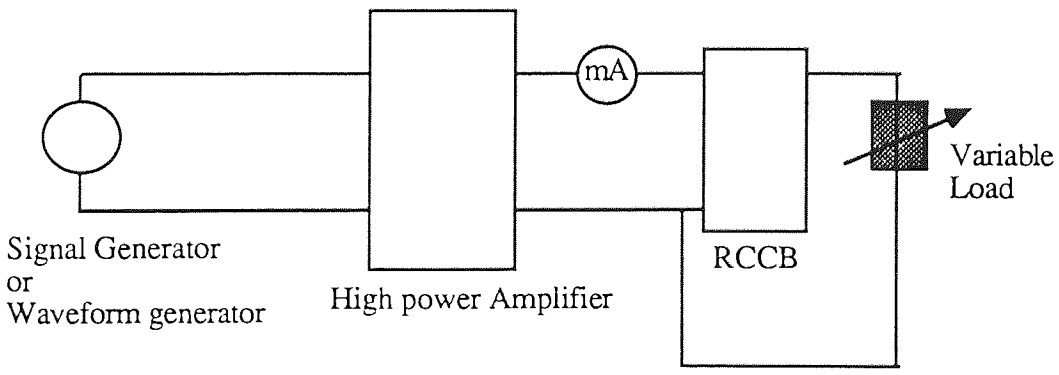

Figure 5.1. The test circuit to obtain the effect of harmonics on RCCB characteristics

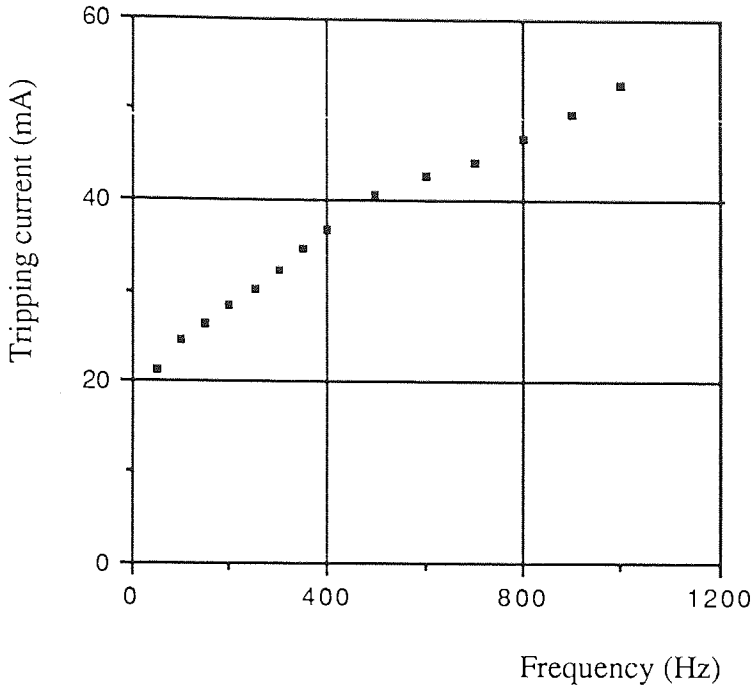

Figure 5.2. Experimental results of the effect of frequency on the tripping current of a RCCB.

5.3. Effect of harmonics

Based on the test results of the RCCB tripping current for sinusoidal waveform at various frequencies, the tripping current $I_{o\Delta}$ of various non-sinusoidal current waveforms can be calculated based on equation 4.7. Since the phase shift θ_n was small, its value was neglected in the calculation. The predictions of the RCCB tripping current for non-sinusoidal waveforms were then compared with direct measurements.

A waveform generator that can produce a waveform with a controlled harmonic content was built. Appendix 1 gives the details of the generator. The generator was coupled to a high power amplifier and connected to the load through the RCCB as shown in Fig.5.1.

The waveform generator was used to obtain the tripping current of the RCCB for a non sinusoidal waveform. A residual current of :

$$i_\Delta = I_\Delta \{\sin(\omega_1 t) + k_n \sin(n\omega_1 t + \partial_n)\} \qquad (5.1)$$

was passed through the RCCB, and increased gradually until the RCCB tripped and the tripping current was measured. In the test, n = 3 and n = 5 were used. In order to vary the waveform, ∂_n was varied. As long as k_n is kept constant, the variation of ∂_n will only affect the waveform but not the harmonic content which depends only on k_n. The same method will also be used for relay testing in the next chapters.

Figure 5.3 shows the test results and the predictions. It can be seen that peaky waveforms have a lower tripping current since the RCCB is sensitive to peak values (see Chapter 2). All the test results correlated well with the theoretical predictions and discrepancies obtained for all RCCBs tested were below 7.5 %. All calculations were carried out using a computer program written for this purpose.

The computer program written consists of 2 different programs. The first program can be used to calculate the r.m.s. value of a waveform provided its harmonics content is known (odd only, up to 7^{th}). The second program is used to find the tripping current of a RCCB provided the harmonic content of the waveform is known. To do this, the program will find the peak of the waveform then increase the value such that the peak reaches the threshold value of the RCCB. Once the waveform value is known, the first program can be used to find the r.m.s. value of that waveform. All these programs are given in appendix 2. Aston University's VAX CLUSTER was used to write, run and store all the programs described in this chapter as well as all those in the next chapters.

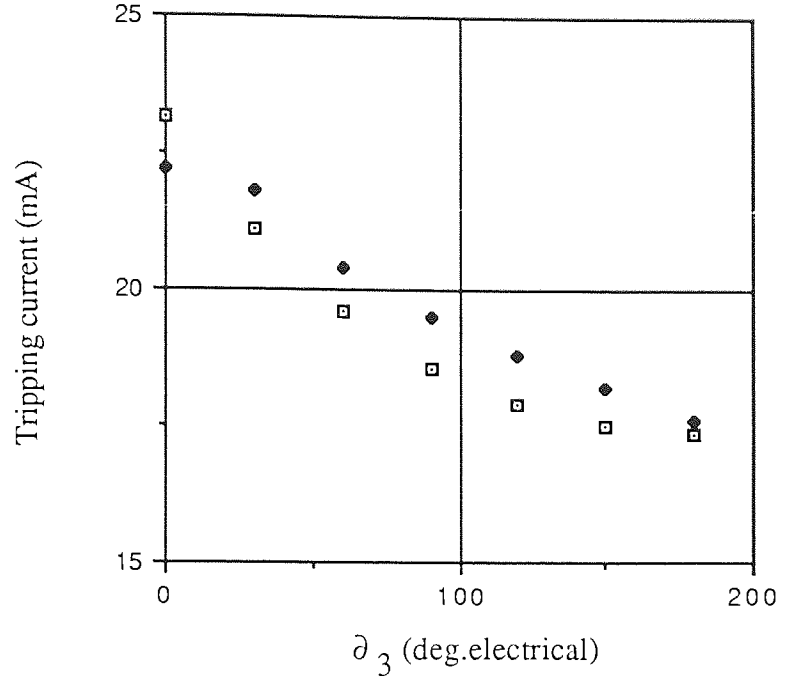

(a) For harmonic order n = 3

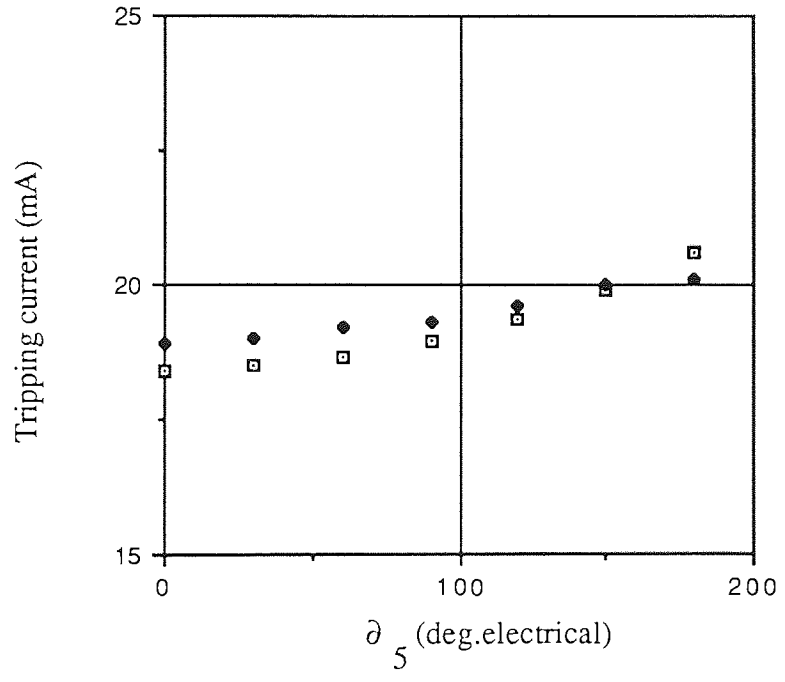

(b) For harmonic order n = 5

Note : A residual current of $i_\Delta = I_\Delta \{ \sin(\omega_1 t) + \sin(n\omega_1 t + \partial_n) \}$ was used.

- ▫ Theoretical result
- ● Experimental result

Figure 5.3. Comparison of experimental and calculated (theoretical) results

5.4. Summary

In this chapter, the comparison between the theory and the experimental results of the effect of harmonics on the tripping current of the RCCB is presented. The theoretical results compare well with the experimental results.

An important point to note is the way the effect of harmonics is assessed. The interaction between the tripping parameter and the relay mechanism that carries out the tripping operation, i.e the armature, is evaluated. Consequently, the waveform of the tripping parameter and the relay constants should be taken into account. This method demonstrates that two waveforms having the same harmonic content but different waveform shapes may have different tripping currents. A similar method will be used to asses the effect of harmonics on electromechanical overcurrent relays in the next chapters.

CHAPTER 6. THE BASIC CONSTRUCTION AND OPERATION OF EM IOC RELAYS

6.1. Introduction

In this chapter, the basic construction and the operation of EM IOC relays are assessed theoretically. This is considered important since there are somewhat contradictory views about the effect of harmonics on this type of relay. Horton and Goldberg's model (37) showed that EM IOC relays should not be affected by harmonics provided the current and the flux are linearly related and independent of frequency. In their work, it was assumed that the relay tripped if the average force produced by any waveform had the same value as the average force produced by the rated tripping current of the fundamental sinusoidal current. Since it could be shown mathematically that the average force was linearly related to the r.m.s. current value, then this relay would trip provided the r.m.s. value of any current waveform exceeded its rated tripping current. Two other studies by IEEE groups (39,48) stated that although EM IOC relays were largely independent of harmonics, a very distorted waveform might affect the tripping current. Linders in his discussion (37) also stated the fact that some distorted waveforms might affect the tripping current of this relay. Unfortunately, no reasons were given as to why the EM IOC relay, which was theoretically unaffected by harmonics, may or may not be affected by harmonics.

The method taken to asses the effect of harmonics on the characteristics of EM IOC relays in this work is similar to the method used to assess the effect of harmonics on RCCBs. Thus the basic construction of the EM IOC relay is analysed then the movement of the armature is evaluated. To do this, the equations that govern the armature movement are derived. The relay is said to trip if the current can attract the armature from its rest position to its operating position and hold it at that position.

6.2. The basic construction of an EM IOC relay

The basic construction of an EM IOC relay is shown in Fig.6.1, Fig.6.1.a. is the attracted armature type and Fig.6.1.b is the hinged armature type. As shown by Peek and Wagar (41) and also derived in appendix 3, the armature movement of both relays can be analysed using similar equations.

In the UK, BS 142 covers the requirements of this relay which is grouped as an 'all or nothing' type relay. Thus this relay should be energised when the the energising quantity, in this case the current, exceeds the pick up value. Normally, the rated tripping current can be set at various values by means of a plug setting bridge which has a single insulated plug. When the relay trips, i.e the armature is attracted to the operating position, the armature actuates several switches which can be of normally open or normally close types.

Although the relationship between the current passing through the relay winding and the flux produced by the core is not generally linear, in this analysis it will be assumed that they are linearly related. This assumption is a fair representation of reality due to the air gap, and is normally taken (37,41). An examination of Fig.6.1.b, taking $x = 0$ at rest position and $x = X_o$ (or $x = X_o/2$ for Fig.6.1.a) at the operating position, shows that the relay's magnetic circuit can be represented by the circuit in Fig.6.2.

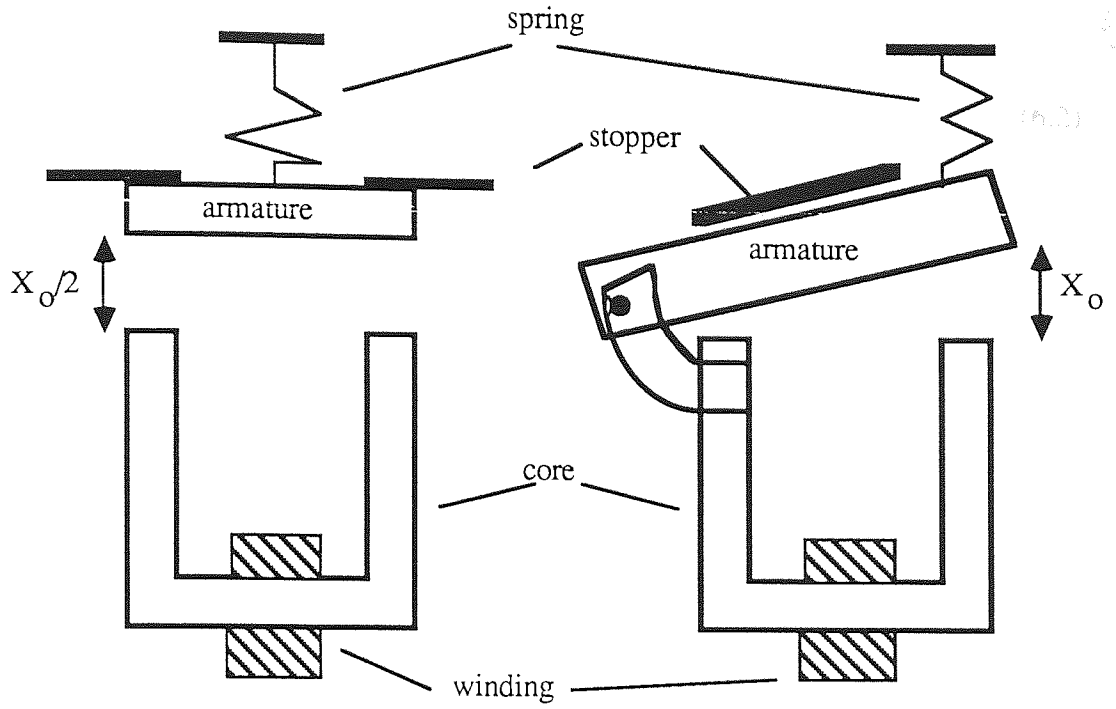

a. Attracted armature type b. Hinged armature type

Figure 6.1. The basic construction of an EM IOC relay.

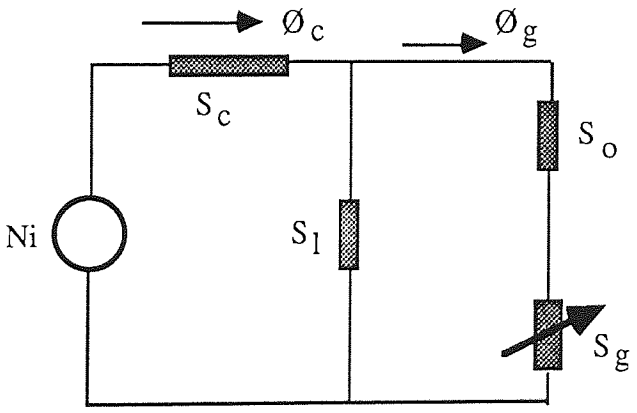

Figure 6.2. The magnetic circuit of an EM IOC relay

Based on the magnetic circuit, the armature movement as discussed in detail by Peek and Wagar (41) and also by Karo and Dhar (42) will be governed by the following forces :

Pulling Force : $F_p = \emptyset_g^2 / 2 \mu_o a$ (6.1)

where :

$$\emptyset_g = \frac{S_l}{S_l+(S_o+S_g)} \emptyset_c \qquad (6.2)$$

$$\emptyset_c = Ni / (S_c+S_{log}) \qquad (6.3)$$

$$S_{log} = \frac{S_l (S_o+S_g)}{S_l+(S_o+S_g)} \qquad (6.4)$$

$$S_g = (X_o-x) / \mu_o a \qquad (6.5)$$

The restraining force consists of :

Spring Force : $F_s = F_o + K_s x$ (6.6)

Friction Force : $F_f = K_f \, dx/dt$ (6.7)

The movement of the armature is then governed by :

$$F_p - F_s - F_f = m \, d^2x/dt^2 \qquad (6.8)$$

By using the above equations, the armature movement, x, can be obtained.

From the above equations, it can be seen that the current produces a pulling force that attracts the armature and thus trips the relay. The armature movement is significantly affected by the relay constants. To determine the tripping current, the interaction between the pulling force F_p and the tripping mechanism should be evaluated as will be described later in section 6.5.

6.3. Effects of the shaded pole

In order to prevent an a.c. relay from vibrating, it is usual to split the magnetic pole into two sections and surround one half with a copper band (38). This is known as shading

the pole. The equations that governs the armature movement of a relay with shaded pole for a current $i = \sqrt{2}\, I \sin(\omega_1 t)$ is given below.

$$F_{pi} = \emptyset_{gi}^2 / 2\,\mu_o\, a_i \tag{6.9}$$

$$\emptyset_{gi} = \frac{S_{li}}{S_{li}+(S_{oi}+S_{gi})}\,\emptyset_{ci} \tag{6.10}$$

$$\emptyset_{c1} = \frac{N(\sqrt{2}\, I)\sin(\omega_1 t)}{S_{c1}+S_{log1}} \tag{6.11}$$

$$\emptyset_{c2} = \frac{N(\sqrt{2}\, I)\sin(\omega_1 t+\gamma)}{\left[(S_{c2}+S_{log2})^2 + (\omega_1 G_s)^2\right]^{0.5}} \tag{6.12}$$

$$\gamma = -\tan^{-1}\{(\omega_1 G_s)/(S_{c2}+S_{log2})\} \tag{6.13}$$

$$S_{logi} = \frac{S_{li}(S_{oi}+S_{gi})}{S_{li}+(S_{oi}+S_{gi})} \tag{6.14}$$

$$S_{gi} = (X_o - x)/\mu_o\, a_i \tag{6.15}$$

Index 1 and 2 in all equations are used in conjunction with $\emptyset_{c1}$ and $\emptyset_{c2}$ respectively, and index i represents either 1 or 2. A complete derivation of the above equations is shown in Appendix 3. The total pulling force is the summation of the pulling force produced by the shaded and unshaded poles ;

$$F_p = F_{p1} + F_{p2} \tag{6.16}$$

Equation (6.8) can then be used to evaluate the armature movement. If the current contains harmonics, then the pulling force produced by each individual frequency component caused by the shaded and unshaded poles should be obtained and then summated to obtain the total pulling force.

6.4. Effects of the stopper

Depending on the mechanical constants, applied frequency and the current passing through the relay, the armature may be fully attracted directly. In general however, it will be only partially attracted before being fully attracted. The initial pulling force is unable to overcome the restraining force, causing the armature to collide with the stopper before it is attracted again. This collision may happen several times before the armature is fully attracted. Consequently, the collision between the armature and the stopper should be taken into account.

Assuming a head on type of collision and that the stopper has a much bigger mass than the armature, so that it is always in a stable/ rest position before any collision, than the armature will have :

1. Zero final velocity for a completely inelastic collision, i.e. where the kinetic energy decreases.
2. Final velocity = Initial velocity but with negative sign for completely elastic collision, i.e. where the kinetic energy is conserved.
3. Final velocity is a fraction of its initial velocity but with negative sign for a partially elastic collision.

In short :

$$V_{fs} = - \beta_s . V_{is} \qquad (6.17)$$

where β_s is the collision factor and it has a value between 0 and 1, V_{fs} = final velocity

and V_{is} = initial velocity of the armature before and after the collision with the stopper.

6.5. Tripping requirements

When a current is passed through the relay, the armature will be attracted towards the core. It should be pointed out that once the armature is attracted, it doesn't necessarily mean that the core will also be able to hold the armature successfully.

A typical instantaneous overcurrent relay of hinged armature type is shown in Fig.6.3. It can be seen that the relay switch is on even when the armature has not been completely attracted, and it is still on even when the armature is just separated from the core. Thus an armature vibration can be accepted as long as it does not cause the relay switch to vibrate. A relay can thus be said to trip if the armature can be successfully attracted and held by the core. Thus the attracting current I_a can be defined as the minimum current that can attract the armature successfully to the core, while the tripping current I_o is the minimum current that can attract and hold the armature successfully.

Since a collision may occur between the armature and the core, then assuming a head on type of collision and that the armature has a negligible mass compared with the core, a collision coefficient $ß_c$ should be considered such that :

$$V_{fc} = -ß_c \cdot V_{ic} \qquad (6.18)$$

where V_{ic} and V_{fc} are the velocity of the armature before and after collision with the core, $ß_c$ is the collision factor.

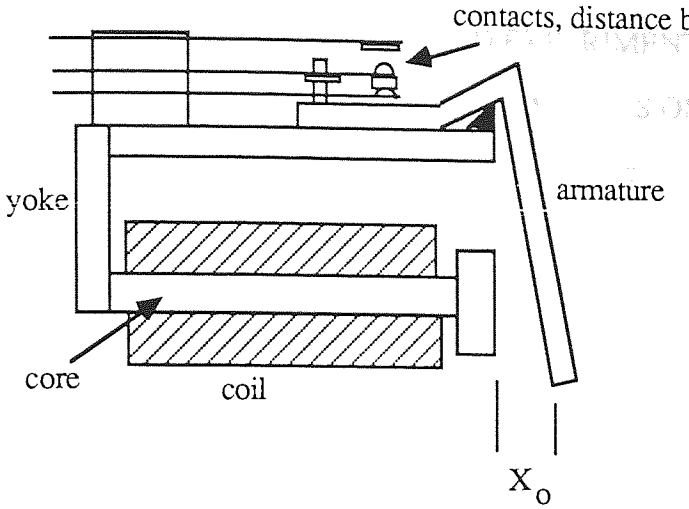

Note : Since the contacts travel (X_1) is shorter than the armature's (X_o), then the contacts are still on even if the armature vibrates slightly.

Figure 6.3. An EM IOC relay and its contacts.

6.6. Summary

In this chapter, equations that govern the armature movement are derived, taking into account the effect of the shaded pole. It is important to note that in order to trip the relay, the armature should be attracted and held at the operating position. The next step is then to simulate all the above equations in a complete computer model to obtain the tripping current of the EM IOC relay and compare the results obtained from this model with experimental results.

CHAPTER 7. SIMULATION AND EXPERIMENTAL RESULTS OF THE EFFECT OF HARMONICS ON THE OPERATING POINT OF AN EM IOC RELAY

7.1. Introduction

The simulation results of both the attracting current and the tripping current of the EM IOC relay are presented in this chapter. The simulation to obtain the attracting current, i.e the current that can attract the armature to the operating position, was carried out to compare the results with the theoretical model of Horton and Goldberg (37). This comparison is considered important since in their model, the vibration of the armature was not taken into account, i.e. the relay tripped when the armature could be attracted to the operating position. Note that in the theoretical description in chapter 6, the current is also assumed to be linearly related with the flux as was also taken in the other model (37). The next step is to carry out the simulation to obtain the tripping current of the EM IOC relay, taking into account the vibration of the armature.

In the simulation, the effect of frequency on the tripping current of the relay was also obtained in addition to the effect of harmonics. This was carried out mainly for two reasons. Firstly, if the relay can really trip provided the r.m.s. value of the current exceeds the rated tripping current irrespective of the waveform, then frequency should not have any effect on the tripping current. Secondly, it is also important to see whether superposition can be applied to this type of relay. Experimental results concerning the effect of frequency as well as harmonics on the tripping current of the relay are also presented and compared with the simulation results.

7.2. Preparation of the simulation

To find out the effect of frequency and harmonics on the relay operation, the equations

that govern the armature movement were simulated. It can then be shown whether different waveforms having similar r.m.s. values will be able to attract the armature successfully and thus trip the relay. The attention of the simulation is thus focussed more on the effect of the current waveform rather then only on the r.m.s. of the harmonic content. For this exercise, the relay constants were taken from reference (42).

The simulation was carried out using an ACSL (Advance Continuous Simulation Language) package program. ACSL is a simulation language which is designed for modelling continuous systems. The system can be described by time dependent, non linear differential equations (69). A special feature of this package is its integration operator, which is the heart of the simulation. To use the package, all the differential operators should be changed to integration. This is carried out by expressing the highest derivative of a variable in terms of lower order derivatives and other variables.

In the simulation, several assumptions were made :

- The flux is considered to be linearly related to the current, independent of frequency.
- The relay is subject to overload current, hence transients are not considered.
- The fault is introduced at current zero when current is increasing.
- Constant core permeability μ and leakage reluctance S_l .

In the first simulation, the effect of harmonics in attracting the armature successfully to the core is evaluated as presented in section 7.3. Then the effect of harmonics on the tripping current is analysed and presented in section 7.4.

7.3. The simulation of an EM IOC relay to evaluate the attracting current

7.3.1 Non-shaded pole

A sinusoidal current of 50 Hz was used to obtain the attracting current I_a. It was carried out by passing several gradually increasing currents through the relay when it was in a non-operating position. The minimum current value able to attract the relay can then be obtained. Fig.7.1 shows the simulation of the armature travel, x, for several values of current at $ß_S = 0.5$. It shows that the armature moves from the rest position at the stopper i.e. $x = 0$ to the operating position i.e. $x = X_O$ (see also Fig.6.1) and that collision between the armature and the stopper may take place before the armature reaches the operating position. Fig.7.2 shows the minimum a.c. attracting current for several values of $ß_S$. Appendix 4.1 gives the complete computer program.

7.3.2. Effects of shaded pole.

The effect of the shaded pole on the attracting current is also shown in Fig.7.2. In the simulation, it was assumed that one half of the pole is surrounded by one turn of copper, so that all the reluctance due to the flux in the unshaded pole is equal to that in the shaded pole. It can be seen that this shaded pole effect increases the attracting current. This is apparently caused by the short circuited coil, since the current induced in it (I_{SC}) will produce a flux opposing the flux caused by the main current (I). Consequently, the attracting current will increase. Since an a.c. relay usually has a shaded pole to prevent the armature from vibrating, in all further simulations, a shaded pole is always assumed to be used. Fig.7.3 shows the pulling force produced by the current. Due to the shaded pole, the pulling force (F_p) never reaches zero, and thus avoids the vigorous armature vibration.

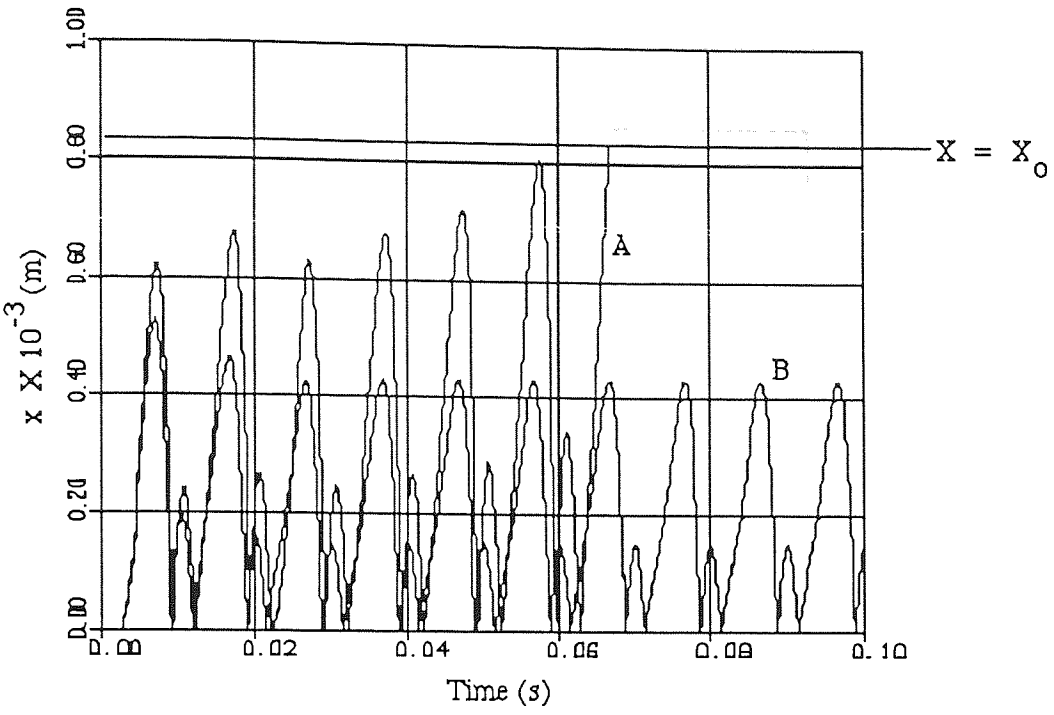

A : The armature is successfully attracted, NI = 137.5 A . Since $ß_S$=0.5, it can be seen that the armature may collide several times with the stopper before it is fully attracted.

B : The armature cannot be attracted, NI = 134.35 A. During the time when $F_p < F_o$ the armature will be attracted toward the stopper. However, since $ß_S$=0.5, the bouncing effect takes place causing the armature to move toward the core again.

$ß_S$ was taken as 0.5

Figure 7.1. Simulation results of the armature travel, x, for fundamental current.

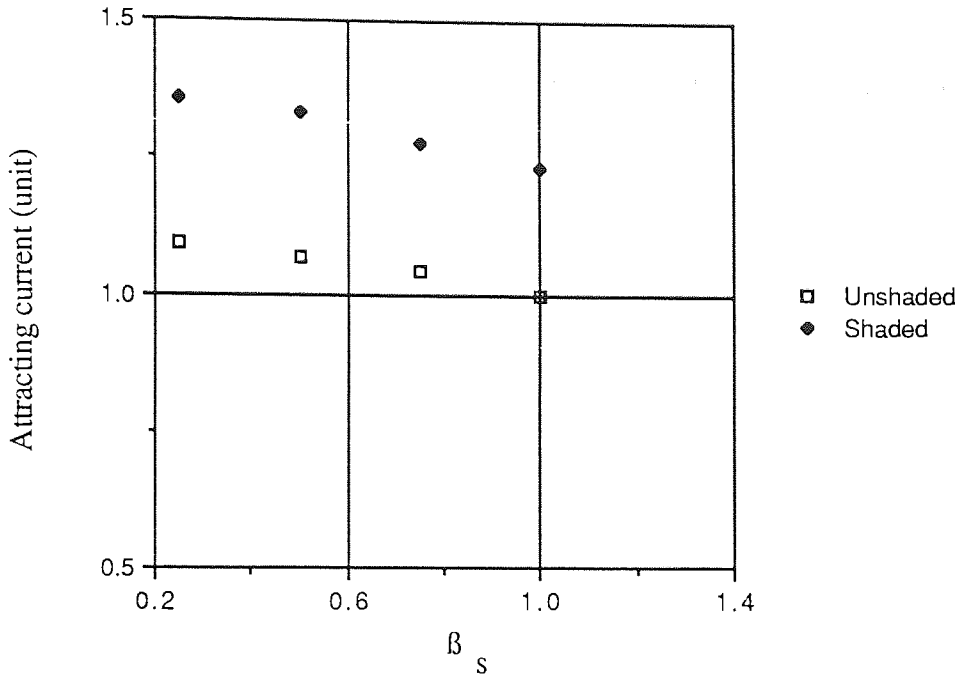

f = 50 Hz (sinusoidal),
The value of the unshaded type at $ß_S = 1$ was taken as 1 unit.

Figure 7.2. Simulation results of the attracting current for several values of $ß_S$, showing the effect of shaded pole.

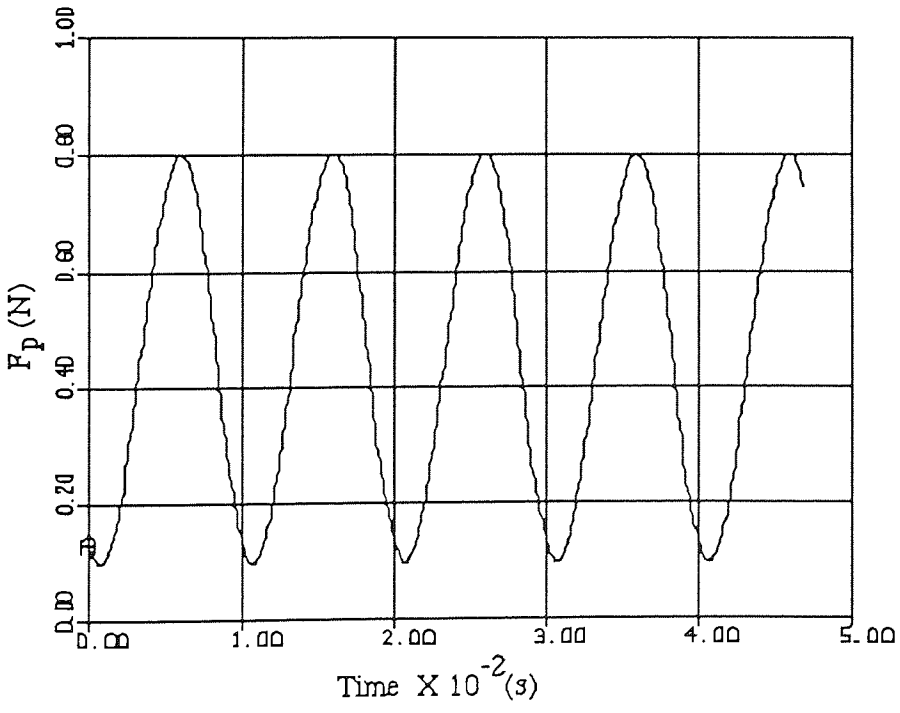

Figure 7.3. Simulation results of the pulling force F_p for a shaded pole relay at fundamental current.
F_p is always greater than 0 due to the shaded pole.

7.3.3. Effects of harmonics.

The next simulation was designed to assess the effect of harmonics on the attracting current. A current of :

$$i = I\{\sin(\omega_1 t) + k_n \sin(n\omega_1 t + \partial_n)\} \qquad (7.1)$$

was used in the simulation where ∂_n and k_n were varied. A change in ∂_n while maintaining k_n constant results in a change in the waveform of the current while maintaining the harmonic content constant. The results are shown in table 7.1. The figure shows that two waveforms which have a similar harmonic content, say 3rd harmonic ($n = 3$) with $k_3 = 1/3$, will have different attracting currents if their waveforms are different because of different phase angles ∂_3. This result shows that the attracting current is affected by the shape of the waveform of the current.

7.3.4. Discussion.

This preliminary simulation shows that the current needed to attract the armature to the core successfully depends on the waveform of the current. However, table 7.1 shows that the attracting current values for non-sinusoidal waveforms do not differ very much from the 50 Hz pure sinusoidal waveform. This can lead to the conclusion that although theoretically the EM IOC relay's tripping current depends on the current waveform, the difference is negligible, thus Horton and Goldberg's theoretical results (37), i.e that harmonics do not affect the tripping current of an EM IOC relay at all, can be accepted. Similarly, references (39) and (48) 's suggestion that EM IOC relays characteristics are largely independent of harmonics can be accepted. It should be pointed out however, as described in section 2.5, that although the armature is attracted successfully, it does not necessarily mean that the relay trips. In the next simulation, where the tripping current

will be assessed, the simulation results show that different waveforms having a similar harmonic content may have significant differences in their tripping currents, and this is supported, as will be seen, by the experimental results.

Waveform	Attracting current (unit)
Sinusoidal, 50 Hz	1.0
n = 3, k_3 = 1/3	
∂_3 = 0°	1.062
∂_3 = 90°	0.939
∂_3 = 180°	0.917
n = 3, k_3 = 1	
∂_3 = 0°	1.128
∂_3 = 90°	0.968
∂_3 = 180°	0.929
n = 5, k_5 = 1/3	
∂_5 = 0°	0.996
∂_5 = 90°	1.039
∂_5 = 180°	1.094

$ß_S$ was taken as 0.5;

The attracting current for the fundamental is taken as 1 unit.

The current used was $i = I\{\sin(\omega_1 t) + k_n \sin(n\omega_1 t + \partial_n)\}$

Table 7.1. Simulation results of the effect of harmonics on EM IOC relay's attracting current I_a.

7.4. The simulation of an EM IOC relay to evaluate the tripping current

This simulation took into account the ability of the core to hold the armature after it was successfully attracted. It was assumed that a small vibration, taken as 20 % of X_O was permitted. All the equations that govern the armature movement, including the ability of the core to hold the armature were simulated with an ACSL package program. The complete program is given in appendix 4.2.

In order to obtain the tripping current I_O, a similar method to that used previously for assessing the attracting current was used. Thus the current passing through the relay was gradually increased until the armature can be attracted and held at the operating position. Fig.7.4 shows a typical simulation of the armature travel, x. It shows that the armature moves from the rest position at $x = 0$ to the operating position at $x = X_O$. Although a small vibration occurs, it was less than 20% and the contact still closed, i.e the armature was attracted and sucessfully held at the operating position. The other simulation results are presented and discussed below.

7.4.1. Effects of frequency

A shaded pole relay was simulated using sinusoidal currents at several frequencies and the results are shown in Fig.7.5. It can be seen that the tripping current I_O was affected by frequency. As frequency increased, so did the tripping current. At around 150 Hz however, it started to level off. Firstly, higher frequencies caused a higher induced current I_{SC} in the short circuited coil (see Appendix 3) which would increase the tripping current. On the other hand, at low frequencies the armature followed the pulling force movement easier than at a higher frequency due to its inertia. As a result, a smaller tripping current was needed at higher frequencies. It is the combination of these two

effects that determines the tripping current. The first effect caused increasing I_o at the beginning, however at even higher frequencies, the second effect took place causing I_o to level off and decrease.

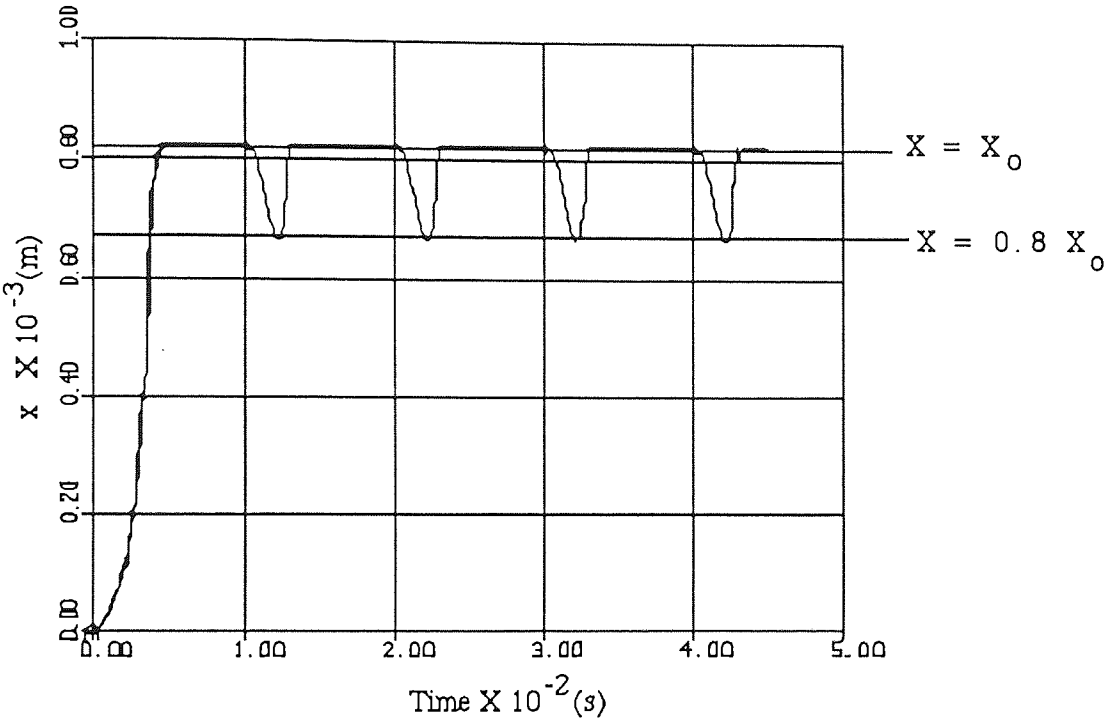

The armature is attracted and held successfully. Small vibration causing it to move towards the stopper occurs but since it is less than 20% X_o, the contacts is still closed, NI_o = 330.2 A (sinusoidal) , $ß_s$ and $ß_c$ were taken as 0.5, f = 50 Hz

Figure 7.4. A typical simulation result of the armature travel, x.

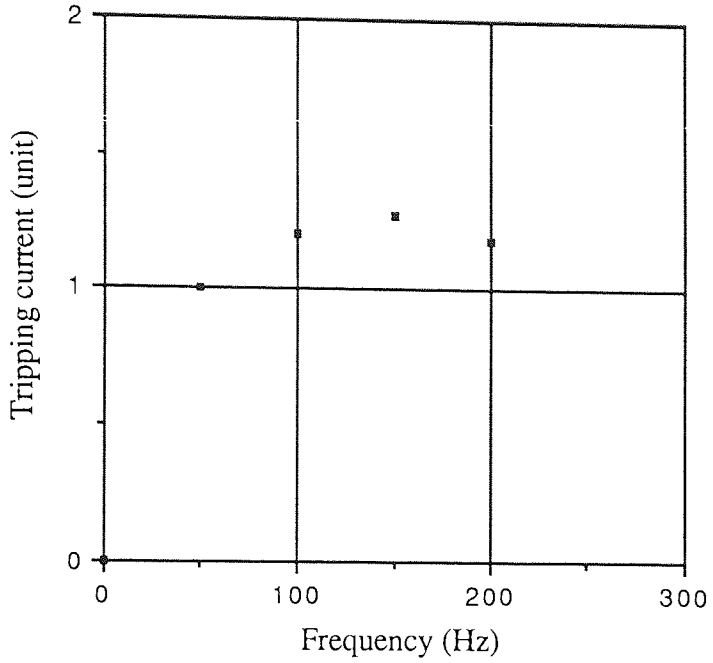

$ß_S$ and $ß_C$ were taken as 0.5.
The value of tripping current at 50 Hz is taken as 1 unit.

Figure 7.5. Simulation results of the effect of frequency on the tripping current.

7.4.2. Effects of harmonics

In this simulation, a current similar to that described in equation 7.1 was passed through the relay. k_n and ∂_n were varied for n = 3 and n = 5 to find out their effect on the tripping current I_O. The results are shown in Fig.7.6.

Firstly, as ∂_n increased so did the tripping current. At a particular value of ∂_n, the tripping current increased rapidly before finally decreased again. The variation of the tripping current due to the phase angle ∂_n was less significant for higher order of harmonics due to the inertia of the armature. At low order harmonics content, the

armature can follow the pulling force easier then at higher order harmonics.

To explain the rapid increase in I_o, see Fig.7.7.a which shows the simulation of the pulling force F_p for $\partial_3 = 180^o$, $k_3 = 0.5$. The figure shows that within 1 cycle, this force has 1 high peak and that between 2 peaks, the force is very small compare with the one shown in Fig.7.7.b. This small pulling force value is unable to hold the armature. Hence the current should be increased until it is high enough to hold the armature. Fig.7.7.b shows the simulation of the pulling force F_p for a similar value of current at $\partial_3 = 0^o$. It can be seen it has 2 peaks and that the pulling force never reaches a very small value as that reached in Fig.7.7.a. Hence, less current is needed at $\partial_3 = 0^o$ to hold the armature successfully.

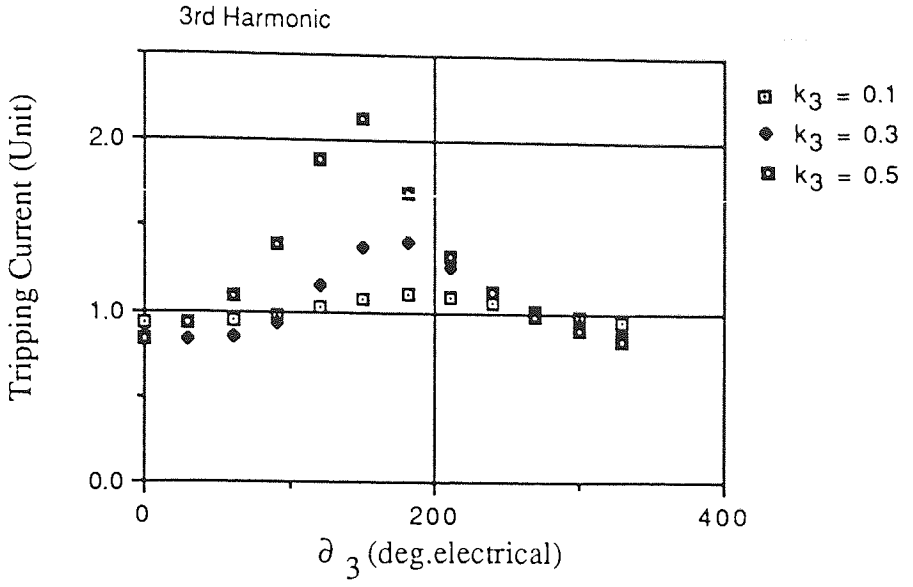

(a) Harmonic order n = 3

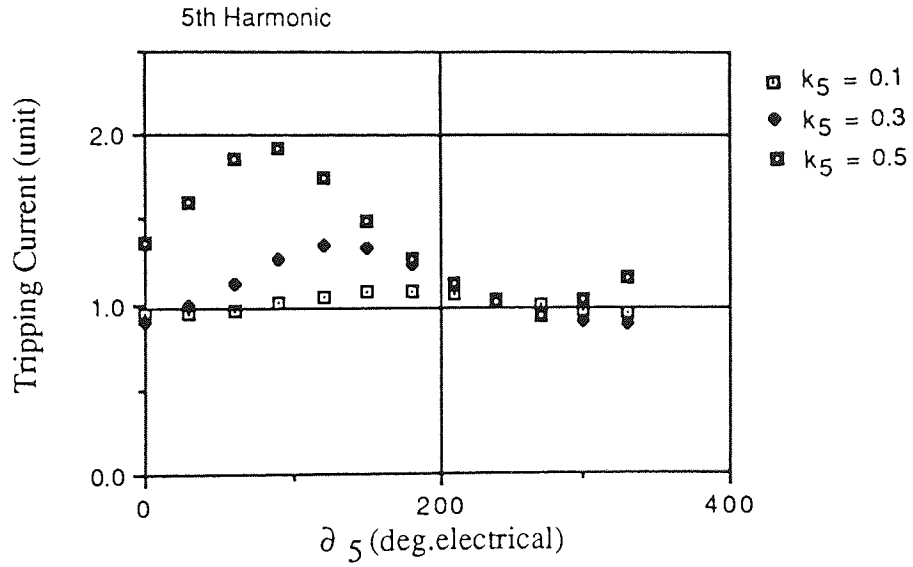

(b) Harmonic order n = 5

The current used was $i = I\{\sin(\omega_1 t) + k_n \sin(n\omega_1 t + \partial_n)\}$.
The tripping current for the fundamental is taken as 1 unit.

Figure 7.6. Simulation results of the effect of harmonics on the tripping current of an EM IOC relay

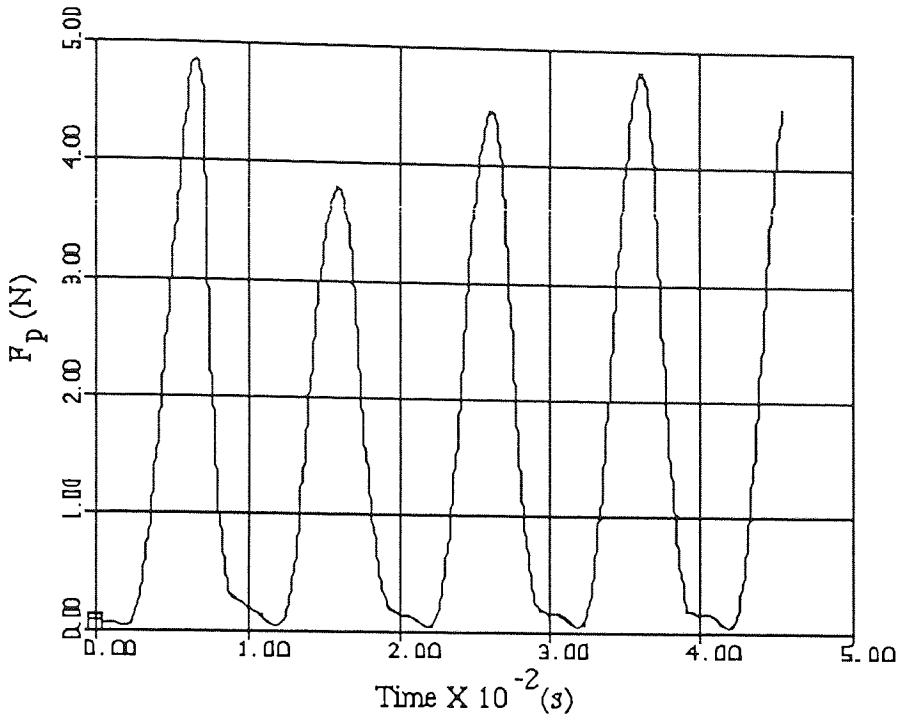

(a) The phase angle $\partial_3 = 180^o$

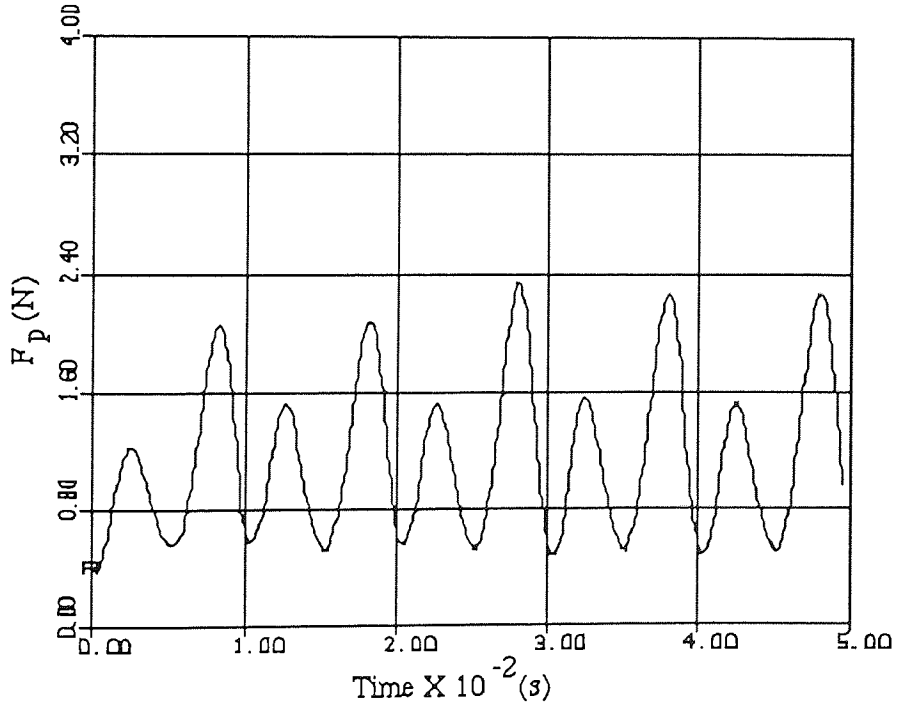

(b) The phase angle $\partial_3 = 0^o$

The current used was $i = I \{\sin \omega t + 0.5 \sin (3\omega t + \partial_3)\}$

Figure 7.7. Simulation results of the pulling force, F_p, for $\partial_3 = 0^o$ and 180^o.

7.5. Experimental results

Following the preliminary simulation results above, a series of direct measurements were carried out. A 2 Ampere instantaneous overcurrent relay was used. Firstly, the tripping current for sinusoidal current of various frequencies was obtained. Then the tripping current of the relay if the fundamental current contains harmonics was obtained.

A signal generator was used in the test to provide sinusoidal waveforms with various frequencies. The waveform generator built was used to produce a waveform with controlled harmonic content (See appendix 1). A high power amplifier was coupled to the generator and the output was connected to the relay and a large resistor. The value of the resistor was approximately 12 - 15 times the relay impedance. As Marshall (85) pointed out, this large resistor is needed to keep the current constant, irrespective of the armature movement and thus it can be regarded as a current source. Note that as the armature moves towards the core, i.e the operating position, its impedance increases and without a large resistor in series with the relay, the current will decrease. The test circuit is shown in Fig.7.8.

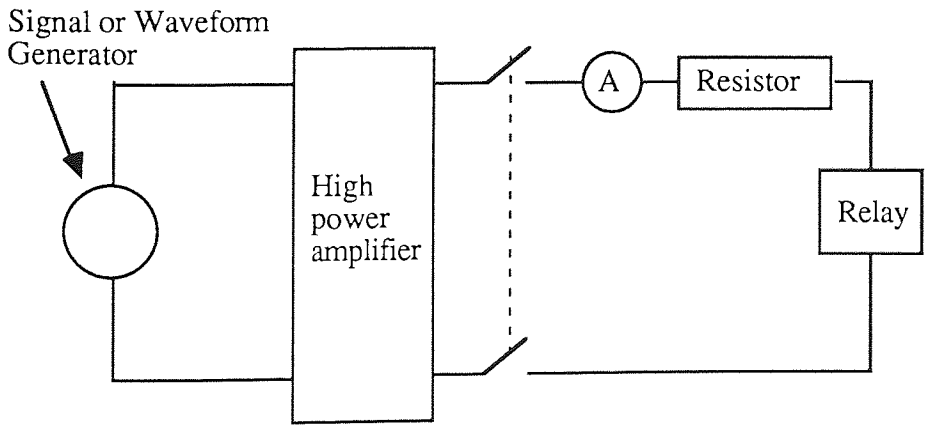

Figure 7.8. The test circuit to obtain the EM IOC relay characteristics

7.5.1. Effects of frequency

Fig.7.9 shows the variation of tripping current as a function of frequency. The simulation results are shown together with the experimental results. It was found that the tripping current increases with frequency as predicted in the simulation. In the experimental results however, the tripping current increases more rapidly than in the simulation results. This is due to the fact that in the simulation the current was taken as linearly related to the flux, independent of frequency. As frequency increased the hysteresis losses of the core, which increased with frequency, reduced the flux which results in the increase of tripping current. In addition, the relay constants used in the simulation were typical values and the constants of the relay tested may not be exactly similar with that used in the simulation. The important point to note is that the simulation results shows that although the losses are neglected, the tripping current is still affected by frequencies. This means that the tripping current is not only affected by the r.m.s. values of the current irrespective of the waveform as suggested by other models as described previously in section 7.1.

7.5.2. Effects of harmonics

The next test was designed to obtain the effect of harmonics on the tripping current of the relay. In order to demonstrate that it is the current waveform and not merely the r.m.s. value that affects the tripping current, a waveform similar to that of equation 7.1 was passed through the relay.

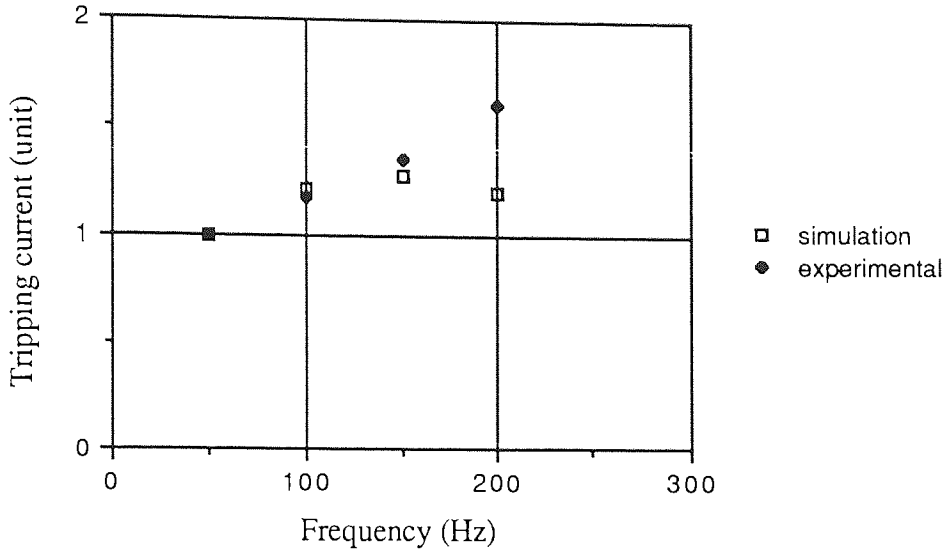

The tripping current at 50 Hz sinusoidal current is taken as 1 unit.

Figure 7.9. Comparison between experimental and simulation results of the tripping current as a function of frequency.

The test results are shown in Fig.7.10. Third and fifth harmonics (n = 3 and 5) were used for the test. The graph shows that as ∂_n was changed, so did the tripping current. Since ∂_n does not affect the r.m.s. nor the ampere-second value of the current but the waveform, then it is clear from this test that the tripping current depends on the current waveform as suggested by the simulation results. It is also important to note that at some particular values of ∂_n, the tripping current suddenly increased rapidly, as predicted in the simulation work, and rigorous collisions between the armature and the core were observed before the relay tripped. This experimental result suggests that the armature could be successfully attracted by the core but the core failed to hold it causing a rigorous vibration. The experimental results in Fig.7.10 also show that higher order harmonics had a less significant effect on the the variation of tripping current due to the phase angle ∂_n as was

predicted in the simulation.

Figure 7.11 shows the experimental results together with the simulation results, showing similar pattern. As ∂_3 increased so did the tripping current and that at a particular point, the tripping current increased rapidly before decreased again. The differences between the simulation and test results are due to the reasons discused in the previous section 7.5.1.

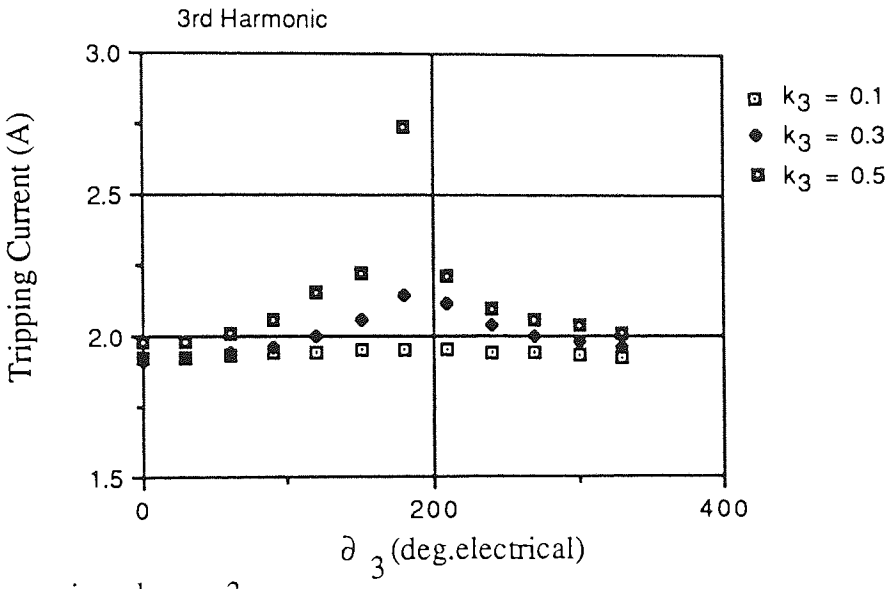

(a) Harmonic order n = 3

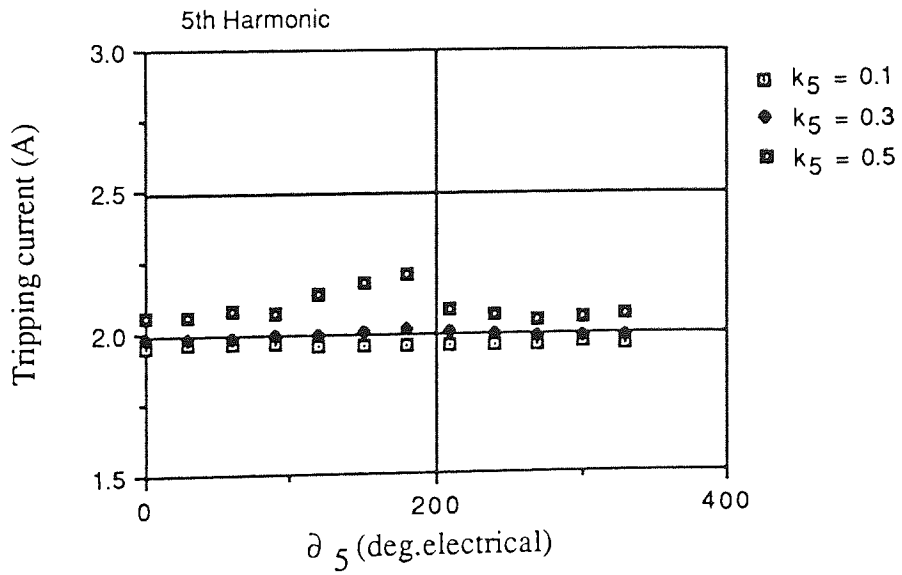

(b) Harmonic order n = 5

The current used was $i = I\{\sin(\omega_1 t) + k_n \sin(n\omega_1 t + \partial_n)\}$

Figure 7.10. Experimental results of the effect of harmonics on tripping current

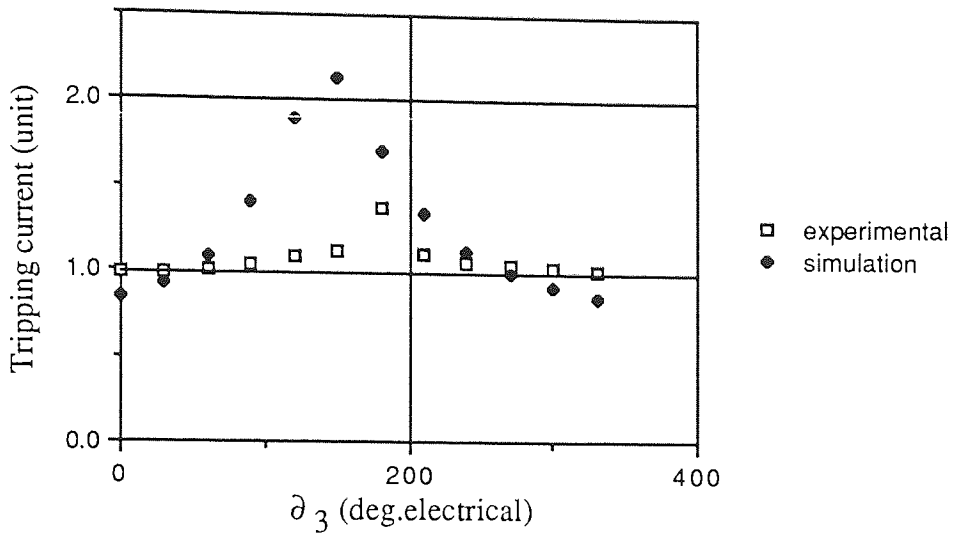

The current used was $i = I\{\sin(\omega_1 t) + 0.5\sin(n\omega_1 t + \partial_n)\}$, $n = 3$
The tripping current for the fundamental is taken as 1 unit.

Figure 7.11. Comparison of experimental and simulation results of the effect of harmonics on the tripping current

7.6. Summary

There are several important points that should be stressed here. Firstly, if only the attracting current is considered, i.e. the vibration of the armature is not taken into account, the attracting current is largely unaffected by harmonics. Hence Horton and Goldberg's model (37) can be accepted.

Since in practice it is the tripping current that should be considered, then the vibration of the armature should be taken into account. Both the simulation and experimental results showed that the tripping current of the relay was affected by harmonics. Moreover, the waveform also affected the tripping current, i.e. a current with a particular harmonic content might or might not affect the tripping current significantly depending on the relay constants and the waveform. For $n = 3$ and $k_3 = 0.5$ as shown in the experimental results

in Fig.7.9.a for example, the tripping current for $\partial_3 = 0^o$ did not differ very much with the sinusoidal waveform. This may lead to the conclusion that harmonics have no significant effect on the tripping current of the EM IOC relay. On the other hand, for $\partial_3 = 180^o$, the tripping current was affected significantly, around 35%, leading to a completely different conclusion. Since the current waveform, and not merely the harmonic content, affect the tripping current then it is clear that superposition cannot be applied to analyse the tripping current of this relay.

This work thus shows that EM IOC relays which are affected by harmonics in practice, has been verified theoretically.

CHAPTER 8. THE BASIC CONSTRUCTION AND OPERATION OF EM TOC RELAYS

8.1. Introduction

In this chapter, the theoretical reasons why the EM TOC relay can be affected by harmonics are presented. This is considered important since there are several somewhat contradictory views about how this relay is affected. An IEEE study (39) stated that an EM TOC relay using an induction disc as a rotor tends to operate faster if the current contains harmonics. The reason for this is because the speed of the disc is proportional to frequency. As a result, harmonics will cause EM TOC relays to have a shorter tripping time although the relay design may cause it to operate slower. On the other hand, based on their experiments, Jost et al (40) concluded that in a majority of cases, relays tend to operate slower, i.e. longer tripping time. A similar view was also expressed by Saramaga et al (51) based on their experiments on EM TOC relays. Chu et all (52) and Faucet and Keener (50) 's experimental results showed that harmonics may cause this relay to operate slower or faster. Unfortunately, the above works do not offer a thorough theoretical analysis. Saramaga et al (51), Horton and Goldberg (37) and Chu et al (52) derived the effects of harmonics on the driving torque of EM TOC relays. However, both Saramaga et al (51) and Horton and Goldberg (37) 's analysis are only limited to the pick up values of this relay and do not include the operating time, which is very important in selective overcurrent protection. In addition, Chu et al (52) stated that it is impossible to predict the tripping time of this relay from the the driving torque equations and that the only way of obtaining the effect of harmonics is by carrying out experiments. In their analysis however (51,52,37), it was shown that the superposition theory can be applied to calculate the driving torque produced if the current contains harmonics.

Due to the lack of theoretical background, in this work a similar method to that used previously to analyse the characteristics of RCCBs and EM IOC relays is used. Thus the

basic construction and operation of EM TOC relays are studied, then the effect of harmonics on the tripping mechanism, in this case the disc, is considered. The equations of the driving torque of an EM TOC relay using an induction disc as a rotor is derived. The effect of frequencies on the driving torque as well as the effect of harmonics on it are also studied. Since other works (51, 52, 37) showed that superposition can be applied to calculate the driving torque then it is important to obtain the effect of frequencies on the driving torque. In this chapter, only the equations are derived. The simulation and the experimental results will be given in chapter 9.

8.2. The basic construction of an EM TOC relay

This type of relay is designed for selective overcurrent protection. In this work, the attention is focussed on an EM TOC relay using an induction disc as the rotor which is rotated by a steady torque excerted upon it by a C shape pole electromagnet. In the UK, BS 142 covers this relay, which is referred to as a 'single input energising quantity measuring relays with dependent specified time'. When the energising quantity, in this case the current, exceeds the pick up values, the disc starts to rotate. The characteristics are such that the tripping time decreases if the current passing through the coil around the core increases.

The basic construction of a shaded pole induction disc type EM TOC relay is shown in Fig.8.1, where it can be seen that a part of the pole is shaded. It operates on the principle of the shaded pole motor. The flux from both the shaded and unshaded parts of the pole will produce an induced current in the disc, usually made of aluminium. The reaction of the fluxes and the induced currents will produce a steady driving torque that rotates the disc and at a particular position, the disc will actuate a switch. The disc movement is restrained by an adjustable spring, the torque which must be overcome before rotary motion can begin. Thus the spring will keep the disc at the rest position and also bring back the disc from the operating position to the rest position when the fault has been

cleared. The disc is shaped so that as it rotates, the driving torque increases and offsets the changing restraining torque of the return spring. The damping of the disc rotation is provided by a permanent magnet.

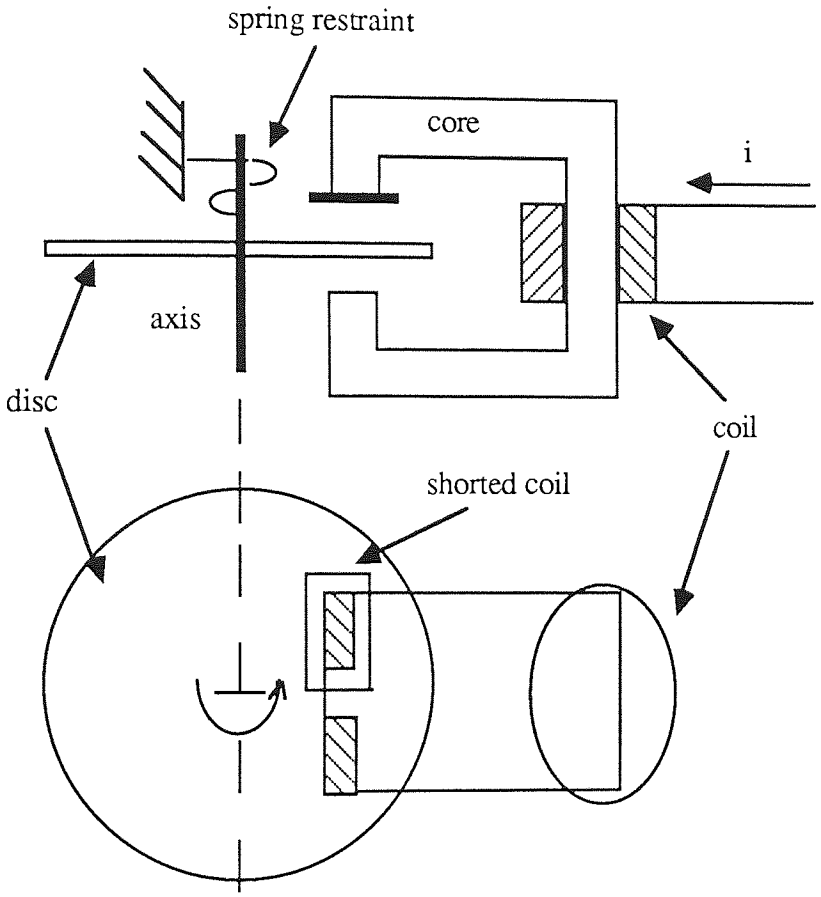

Figure 8.1. The basic construction of an EM TOC relay.

To vary the current setting of the relay, several current taps are provided. Selection of the current setting is carried out by using a plug setting bridge which has a single insulated plugs. The relay tripping time can be ajusted by moving the disc backstop which is controlled by rotating a wheel at the base of a graduated time multiplier scale. It is normally refered as the Time Multiplier Setting (TMS).

Depending on their characteristics, EM TOC relays are divided into several types such as inverse, very inverse, extremely inverse and IDMT. In this work, an IDMT relay was used in the laboratory work. The complete derivation of the driving torque T_d has been derived by Warrington (43) and also Horton and Goldberg (37), but is also given in appendix 5. The tripping time characteristic for a pure sinusoidal current has been discussed in detail by Warrington (43).

Thus it is the driving torque T_d that actuates the tripping mechanism, i.e the disc, and trips the relay and acts as the tripping parameter. The theoretical assessment of how the EM TOC relays are affected by harmonics will then be confined to how harmonics affect T_d and the disc.

8.3. The driving torque equations

As shown by Horton and Goldberg (37), for a pure sinusoidal current, provided the flux is linearly related to the current, the driving torque produced by a C shaped electromagnet with a shaded pole as shown in Fig.8.1 is :

$$T_{dn} = \frac{T(I_n)\, n \sin(\beta_n)}{\left[1 + (k\omega_1/S)^2 n^2\right]^{0.5} \left[1 + \{k\omega_1(1+a)/S\}^2 n^2\right]^{0.5}} \qquad (8.1)$$

where $T(I_n)$ and β_n are constants :

$$T(I_n) = 2 K N^2 I_n^2 k \omega_1 / S^2 \qquad (8.2)$$

$$\beta_n = \tan^{-1} \frac{n a k \omega_1 / S}{1 + \{(k\omega_1)^2 (1+a) n^2\}/S^2} \qquad (8.3)$$

It can be seen from the above equations that the torque has a steady value. Assuming that the EM TOC is a linear system as proposed by Horton and Goldberg (37), Chu et al (52) and Saramaga et al (51), the driving torque T_d if the current contains harmonics can be derived as follows :

$$i = \sum_{n=1}^{\infty} i_n \qquad (8.4)$$

$$i_n = \sqrt{2}\, I_n \sin (n\, \omega_1 t + \partial_n)$$

∂_n is the angle of the harmonics current with respect to the fundamental current i_1. The driving torque T_d is the sum of all the torques produced by each sinusoidal current waveform, hence :

$$T_d = \sum_{n=1}^{\infty} T_{dn} \qquad (8.5)$$

It follows that if the harmonic content of a current waveform and the relay constants are known, the pick up or the starting current of the relay for that particular current can be calculated.

8.4. Theoretical description of EM TOC relay characteristics

8.4.1. The use of curve fitting methods to obtain relay constants

The above work is extended so that it can be used to obtain relay constants through a simple test and to predict relay characteristics for any frequencies as well as for any shape of the waveform. To do that, equation (8.1) can be rearranged :

$$T_{dn} = \frac{C_T I_n^2 n^2 (C_2 - C_1)}{1 + n^2 C_1^2 + n^2 C_2^2 + n^4 C_1^2 C_2^2} \qquad (8.6)$$

where :

$$C_1 = k\omega_1 / R$$

$$C_2 = k\omega_1 (1+a) / S$$

$$C_T = 2 K N^2 k \omega_1 / S^2$$

The starting current at any frequency should produce the same torque T_{dn}, since it is the torque which is needed to overcome the restraining force of the spring at the beginning of the movement. Taking the starting current for the n^{th} harmonic as I_{stn}, then from equation (8.6) it can be derived that :

$$\frac{I_{stn}^2}{I_{st1}^2} = \frac{1 + n^2 C_1^2 + n^2 C_2^2 + n^4 C_1^2 C_2^2}{n^2 (1 + C_1^2 + C_2^2 + C_1^2 C_2^2)} \qquad (8.7)$$

From equation (8.7), if the starting current of the relay at the fundamental and several other frequencies is known, the constants C_1 and C_2 can be found. To achieve this, equation (8.7) can be rearranged as :

$$y = A_1 + A_2 x + A_3 x^2 \qquad (8.8)$$

where :

$$x = n^2$$

$$A_1 = 1/(1+C_1^2+C_2^2+C_1^2C_2^2)$$

$$A_2 = (C_1^2+C_2^2)/(1+C_1^2+C_2^2+C_1^2C_2^2)$$

$$A_3 = (C_1^2 C_2^2)/(1+C_1^2+C_2^2+C_1^2 C_2^2)$$

$$y = (I_{stn}^2 / I_{st1}^2) n^2$$

Equation (8.8) can then be solved using curve fitting methods. A_1, A_2 and A_3 can be found, followed by the calculation of C_1 and C_2. The derivation is given in appendix 6.

8.4.2. The equations that govern the disc movements

Equation (8.6) shows that when the current is increased, the driving torque increases and at a particular value the disc will start to rotate. The driving torque T_d which causes the disc to rotate will be opposed by the spring torque T_s and the braking torque T_b caused by the flux of the permanent magnet, $\emptyset_m$, the flux produced by the current, $\emptyset_{i,j}$, and friction. Note that due to the fluxes and the rotation of the disc, the flux produced by the current, $\emptyset_{i,j}$, will produce the flux braking torque, which is a self braking torque. The complete derivation of the braking torques is given in appendix 7.

Spring torque :

$$T_s = T_o + K_s x_a \qquad (8.9)$$

To offset the increasing torque of the spring due to angular displacement xa, the relay disc is shaped so that as it rotates, the driving torque increases (78, 79). Thus in equation 8.9, the constant K_s can be neglected.

Permanent magnet braking torque

$$T_{b,pm} = K_{b,pm} \, dx_a/d_t \qquad (8.10)$$

The braking torques produced by flux $\emptyset_{i,j}$:

$$T_{b,i1} = K_{b,i1} \, \emptyset_{i1}^2 \, dx_a/dt$$

$$T_{b,i2} = K_{b,i2}\, \emptyset_{i2}^2\, dx_a/dt$$

$$T_{b,i} = T_{b,i1} + T_{b,i2} \qquad (8.11)$$

Friction Braking Torque :

$$T_{b,f} = K_{b,f}\, dx_a/dt \qquad (8.12)$$

In order to get a negligible friction, a good bearing can be employed.

Hence, the total Breaking Torque is :

$$T_b = T_{b,pm} + T_{b,i} + T_{b,f}$$

$$= (K_{b,pm} + K_{b,f} + K_{b,i1}\, \emptyset_{i1}^2 + K_{b,i2}\, \emptyset_{i2}^2)\, dx_a/dt \qquad (8.13)$$

The movement of the disc is then governed by :

$$T_d - T_b - T_s = m_I\, d^2x_a/dt^2 \qquad (8.14)$$

8.4.3. Effect of frequency

As Saramaga (51) pointed out most of the braking torque is provided by the permanent magnet, thus equation (8.13) can be simplified as :

$$T_b = K_b\, dx_a/dt \qquad (8.15)$$

where K_b is the breaking constant. This simplification is supported, as will be seen later, by experimental results.

Equation (8.14) and (8.15) imply that although the time-current characteristics of EM TOC relays may be different for different frequencies, a similar torque is needed if the relay has similar tripping times at different frequencies. Consequently, the current I_n at

frequency $n\omega_1$ needed to produce the same tripping time as that of I_1 is :

$$I_n^2 = \frac{1 + n^2C_1^2 + n^2C_2^2 + n^4C_1^2C_2^2}{n^2 (1 + C_1^2 + C_2^2 + C_1^2C_2^2)} I_1^2 \qquad (8.16)$$

Thus, if C_1, C_2 and the time-current characteristic at the fundamental frequency are known, the characteristics at other frequencies can be found.

8.4.4. Effect of harmonics

Since the EM TOC relay can be regarded as a linear system, i.e superposition method can be used to calculate the driving torque, then the driving torque if the current contains harmonics is the sum of all the driving torques produced by each sinusoidal component of the waveform. Thus for a waveform which has a particular harmonic content, the driving torque will have a particular value, regardless of the waveform being applied.

To asses the driving torque for non-sinusoidal waveforms, combine equations (8.5) and (8.6) to obtain :

$$T_d = C_T \sum_{n=1}^{\infty} I_n^2 D_n \qquad (8.17)$$

where :

$$D_n = \frac{n^2 (C_2 - C_1)}{1 + n^2C_1^2 + n^2C_2^2 + n^4C_1^2C_2^2} \qquad (8.18)$$

It can be seen that the value of the driving torque is determined by the r.m.s. value of

each sinusoidal component of the current waveform, I_n.

Thus it can be concluded that if a current of say :

$$i = \sqrt{2}\, I_1 \sin(\omega_1 t) + \sqrt{2}\, I_3 \sin(3\,\omega_1 t + \partial_3)$$

is passed through the EM TOC relay, the value of ∂_3 does not affect the tripping time of the relay, which is only affected by I_1 and I_3. It should also be stressed, that this conclusion is correct even if the braking torques produced by the current fluxes are taken into account.

Since a known driving torque T_d should have a known tripping time, then equations (8.17) and (8.18) imply that if the constants C_1 and C_2 are known as well as the harmonic content, the value of any current waveform I which has similar T_d, and hence similar tripping time with I_1, can be found.

This is carried out by equating the driving torques that produce the same tripping times :

$$\sum_{n=1}^{\infty} I_n^2 D_n = I_1^2 D_1 \qquad (8.19)$$

The r.m.s. value of any current I which has the same tripping time as I_1 can thus be calculated.

From the above discussion, it can be concluded that the tripping time characteristics of an EM TOC relay can be found if the relay's constants and its characteristics at the fundamental frequency are known.

8.5. Summary

In this chapter the driving torque equations are developed and extended so that the effect of harmonics on the torque can be obtained. A simple method to obtain the relay constants by using a curve fitting method is also developed. However, the effect of harmonics calculation is based on the assumption that superposition theory to calculate the driving torque can be applied or only produce a negligible error and that the current and the flux is linearly related as suggested by other works (37,51,52), The important point to note is that unlike other models described in section 8.1., the effect of frequency and harmonics on the relay characteristics can be predicted with the help of the theory developed in this work.

CHAPTER 9. SIMULATION AND EXPERIMENTAL RESULTS OF THE EFFECT OF HARMONICS ON THE CHARACTERISTICS OF AN EM TOC RELAY

9.1. Introduction

In this chapter, the experimental results of the effect of harmonics on the operation of an EM TOC relay are presented. Firstly, the starting current of the relay for various frequencies was obtained in order to calculate the relay's constants according to the method developed in section 8.3. Then the tripping time for sinusoidal current at various frequencies was obtained and compared with the theoretical calculation. Then finally, the effect of harmonics on the tripping current was obtained. The main reason for studying the characteristics of the relay at various frequencies is to verify the theory to obtain the tripping time as described in section 8.4.3. In addition, as described in section 8.1, there was some contradictory views as to how frequency affects the relay characteristics.

To verify whether superposition theory can be applied, a current with a particular harmonic content, in this case a waveform which contains 10% 3^{rd} harmonic, was passed through the relay and the waveform was varied by varying the phase angle of the harmonic. The current was kept low, approximately 20% above the pick up value. If the superposition theory can be applied, then the variation of tripping time due to the variation of phase angle should be negligible. It was found that a large variation, around 35%, was obtained. It was then decided that the suggestion of calculating the driving torque using the superposition method (37,51,52) seems to be unacceptable, and that non-linearity needs to be taken into account.

The theoretical work is then extended to cover the non-linearity. The driving torque is derived without the use of the superposition method. In addition, the non-linearity of the core is also taken into account. The simulation of the effect of harmonics on the tripping

time was carried out on a computer and the results was compared with the experimental results.

9.2. Experimental results

9.2.1. Calculation of relay constants

A series of experiments were carried out to verify the theoretical work. A particular type of EM TOC relay using an induction disc as the rotor, in this case an inverse definite minimum time (IDMT) overcurrent relay was used in the test. Firstly, the time current characteristic of the relay was plotted for the fundamental frequency, the result is shown in Fig.9.1. Note, the higher the current, the shorter was the tripping time. Initially, the tripping time fell linearly with current but as the current was further increased, saturation of the core took place and the curve began to level off.

The next test was designed to obtain the starting current of the relay for sinusoidal current of several frequencies in order to calculate the relay constants. For a particular frequency, the current was increased gradually and the starting current, i.e the current able to start the rotation of the disc, was measured. The results are shown in table 9.1. The table shows that as frequency was increased, the starting current decreased but then it increased again. To find out C_1 and C_2, equation (8.8) was used followed by a curve fitting computation. A program to carry out the curve fitting was developed and is shown in appendix 8. In this program, the Chebyshef Polynomial constants were found using a subroutine provided by NAG ADFEX, a library routine available as described in reference (68). A brief review of curve fitting methods using the Chebyshef polynomial as well as the complete calculation is also included in appendix 8.

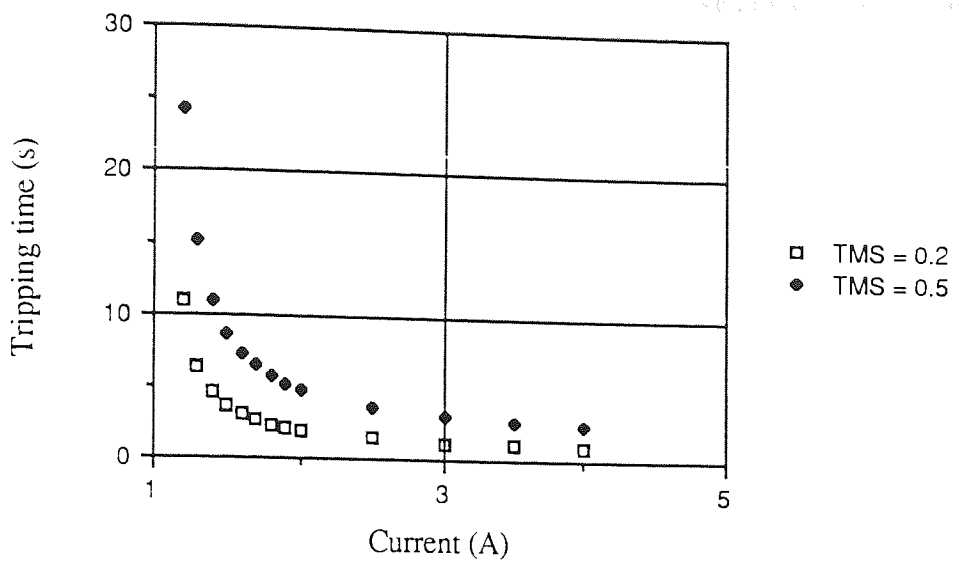

TMS : Time Multiplier Setting

The setting value of the relay was 1 A.

Figure 9.1. The EM TOC relay characteristic for fundamental frequency.

Frequencies (Hz)	Starting Current (A)
50	1.12
100	1.01
150	1.10
200	1.23
250	1.39
300	1.58
350	1.87

TMS (Time Multiplier Setting) was set at 0.5

The current setting was 1 A.

Table 9.1. Starting current at various frequencies for a typical EM TOC relay

The values of A_1, A_2 and A_3 can then be calculated followed by C_1 and C_2. From the above computation, it was found that :

$$C_1 = 0.3113$$

$$C_2 = 0.9799$$

Since the constants are already known, then the prediction of the effect of frequency on the tripping characteristics may be carried out.

9.2.3. Effect of frequency

Fig.9.2 shows the tripping time characteristics of the relay for sinusoidal waveform of various frequencies, both experimentally and theoretically. The theoretical predictions were made using equation (8.16). The figure shows that the theoretical results are very close to the experimental results for low values of overcurrent. At higher values, where saturation takes place, the flux can no longer be assumed to be linearly related to the current and discrepancies between the test and theoretical results become apparent. However, up to approximately 2.0 A, i.e 100 % above the rated current, the theoretical results are still very close to the test results.

It should be pointed out however, that as shown in Fig.9.2, as frequency was increased, it did not necessarily mean that the disc would rotate faster resulting in a shorter tripping time as predicted theoretically by other studies (39). The tripping time for other frequencies can be higher or lower as shown by the experimental and theoretical (calculated) results. As shown in the theoretical description in section 8.2, the driving torque, and thus the tripping time depends very much on both the frequency of the current and the relay constants.

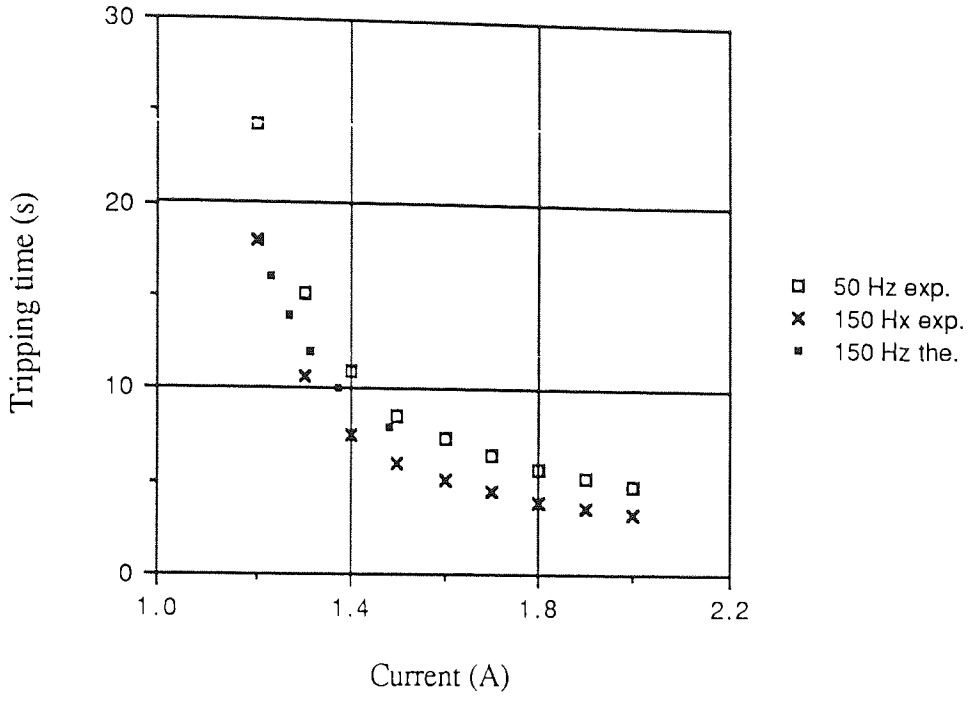

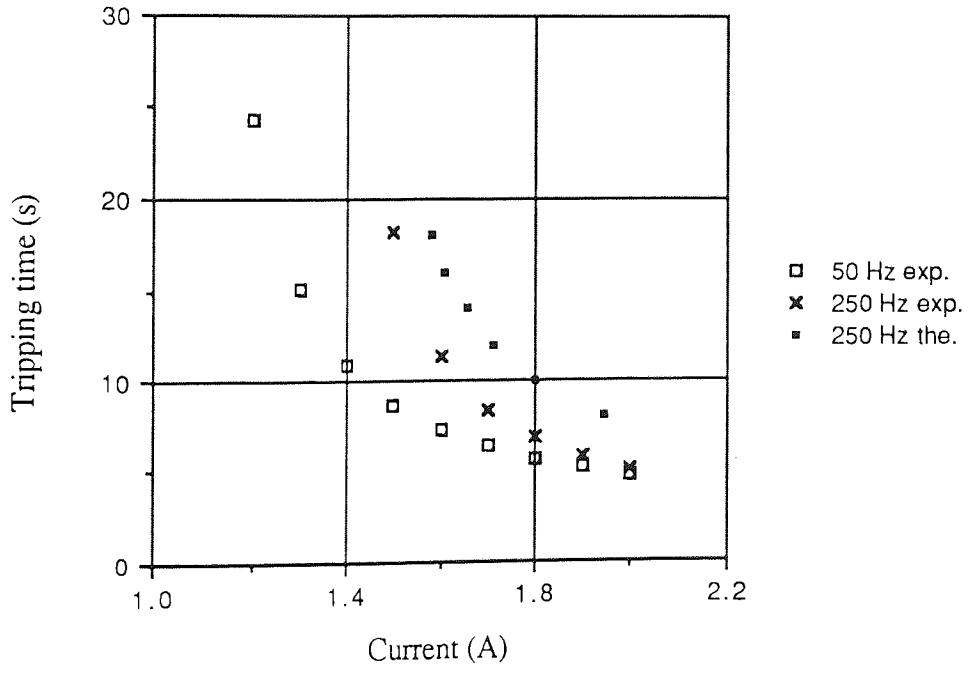

TMS (Time Multiplier Setting) is set at 0.5

Rated tripping current 1 A.

Figure 9.2. Comparison between experimental (exp.) and theoretical (the.) results of EM TOC relay characteristics at various frequencies.

9.2.4. Effects of harmonics

This test was designed to obtain the effect of harmonics on the tripping time of the relay. As discussed, the tripping time should only be affected by the harmonics content of the current. A current of :

$$i_{1,3} = I\{\sin(\omega_1 t) + k_3 \sin(3\omega_1 t + \partial_3)\}$$

was passed through the relay and k_3 was varied. $I_{1,3}$, the r.m.s. value of $i_{1,3}$, was kept low at 1.2 A to avoid saturation of the core. ∂_3 was varied from 0^o to 360^o, and the tripping time was measured. The results are shown in Fig.9.3.a, they show that the tripping time is greatly affected by ∂_3. While the tripping time of the relay at the fundamental frequency of 1.2 A was 24.3 seconds, the value for $I_{1,3}$ varied from 19 to 32 seconds for $k_3 = 0.1$. For a higher harmonic content, e.g for $k_3 = 0.2$, the variation was even larger, varying from 15 to 60 seconds. For a higher current, the variation was smaller as shown in Fig.9.3.b.

The above test suggests that the tripping time of the EM TOC relay is greatly affected by the current waveform especially at lower overcurrent values. It also implies that the driving torque is also dependent upon the current waveform. Additionally, this result shows that the relay should not be assumed to be a linear system since the discrepancies obtained from the test are quite significant even though the test was carried out at low current (1.2 A) and low harmonic content ($k_3 = 0.1$).

To analyse the effect of current waveform on the tripping time, the theoretical work is extended further.

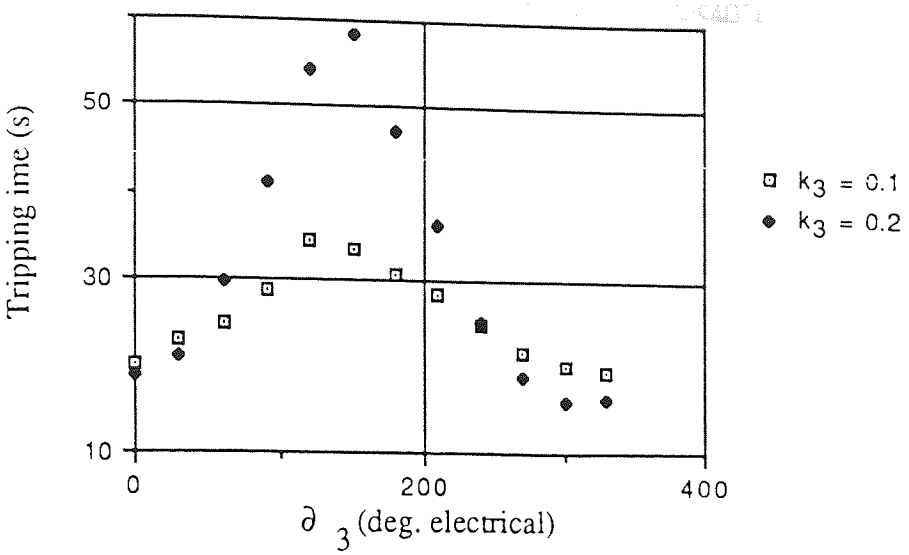

The r.m.s. value of $i_{1,3}$ was kept at 1.2 A.

(a) The effect of phase angle on tripping time for different harmonic content

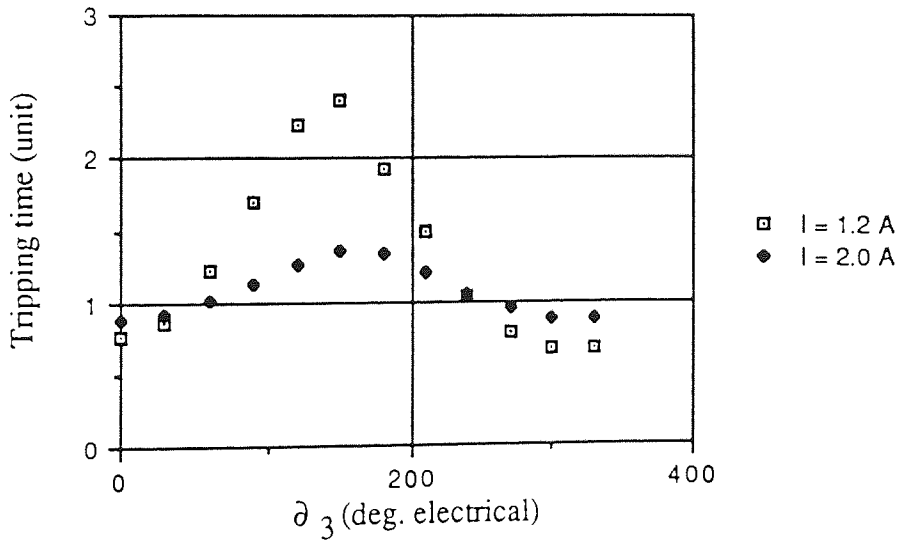

$k_3 = 0.2$
The tripping time of the fundamental of the two current (1.2 A and 2 A) are taken as 1 unit.

(b) The effect of low (1.2 A) and high (2 A) currents on the variation of tripping time

TMS (Time Multiplier Setting) was set at 0.5
The current setting was 1 A.
The current waveform used was $i_{1,3} = I \{\sin(\omega_1 t) + k_3 \sin(3\omega_1 t + \partial_3)\}$
Tripping time for the fundamental current was 24.32 s

Figure 9.3. The effect of harmonics on the tripping time of an EM TOC relay.

9.3. Extension of the theoretical work concerning non-linearity

As described previously in chapter 8, the two assumptions made concerning linearity are :

a. The system is assumed to be a linear system, i.e. superposition can be applied to calculate the driving torque, resulting in equations (8.4) and (8.5).

b. The flux is assumed to be linearly related to current, resulting in equation (8.1).

Since the experimental results show that even a small harmonic content may affect the tripping time significantly, the above assumptions will be considered further in the next section.

9.3.1. The use of superposition method

Firstly the system will not be regarded as a linear system and thus superposition method to calculate the driving torque will not be used. The derivation of the driving torque should take into account the interaction between all flux and induced current in the disc. Appendix 9 shows this derivation. It was found that the driving torque was not a steady torque. A current which contains a third harmonic component will have a driving torque of :

$$T_{d\ 1,3} = T_1 + T_2 \sin (2\ \omega_1 t + \partial_{2T}) + T_4 \sin (4\ \omega_1 t + \partial_{4T}) \qquad (9.1)$$

The constants T_1, T_2, T_4, ∂_{2T}, and ∂_{4T} depend not only on the relay design, but also on the phase angle between the third harmonic and the fundamental. If it is regarded as a linear system, then the last two terms in equation (9.1) disappear and :

$$T_{d\ 1,3} = T_1 \qquad (9.2)$$

It has to be pointed out that although the driving torque is not a steady torque as described

by equation (9.1), it is a periodic waveform which consists of a constant value T_1, and two sinusoidal torques with frequency $2\omega_1$ and $4\omega_1$. Since the tripping time of an EM TOC relay is in the order of tens of seconds, the sinusoidal torque with the frequencies indicated should have no effect on the disc since it will only see the average of the driving torque, i.e. T_1. Thus this first effect should not affect the tripping time of the relay.

9.3.2. Non-linearity of the core

At low current and due to the large air gap, the B-H curve of the core is considered to be linear and thus the current was assumed to be linearly related to the flux. However, a degree of non-linearity may exist. A model was set up to show how this non-linearity may cause a significant change in the tripping time. Non-linearity in the core of the IDMT relay used in the experimental work may cause a slight distortion in the flux waveform, i.e the flux waveform is not exactly the same shape as that of the current. There are several methods for evaluating the non linear properties of a core (44,45), although few gave much attention to the waveform distortion itself. One of the models, developed by Emmanuel and Chandra (46), showed how flux waveform can be constructed from the current waveform.

In this work, the model is based on the simplified version developed in reference (46). The following assumptions were made :

a. The hysteresis loss is neglected, since in this work, the hysteresis does not affect the tripping time differences caused by ∂_n.

b. The B-H curve is taken as a series of straight lines as shown in Fig.9.4.

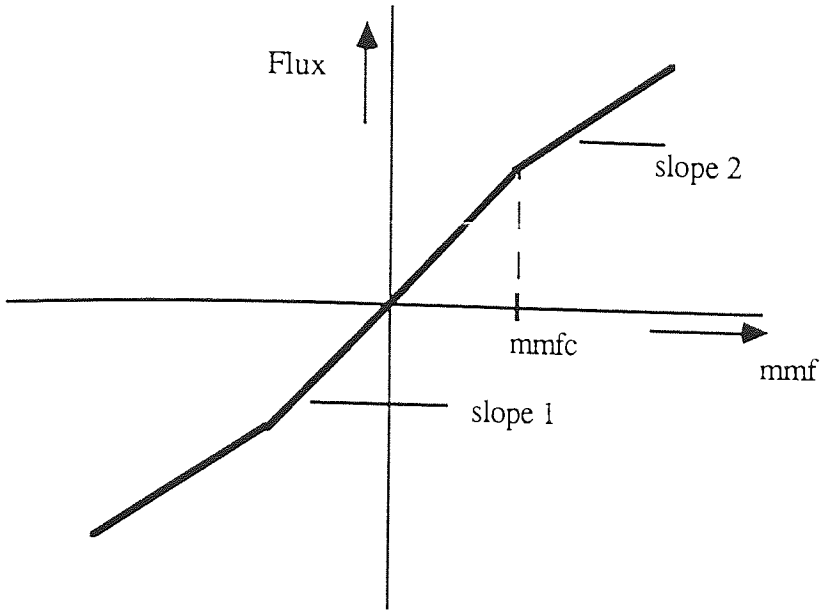

Figure 9.4. The B-H characteristic

9.2.3. Model analysis using a typical EM TOC relay

An exercise was carried out using the constants of the IDMT relay used in the experimental work which has been obtained in section 9.2.1. Firstly the distortion of the fundamental sinusoidal current waveform due to the non-linear effects of the core must be found. To simplify the calculation, instead of evaluating the distorted flux waveform, the flux is taken as being linearly related to the current and thus the driving torque equation as expressed by equation 8.1 is still valid. However, to include the non-linearity of the B-H curve, the current waveform is distorted in a similar way to the flux. To do this, the B-H curve in Fig.9.4 is changed appropriately, i.e. the slope 1 is taken as 1.0. Thus in this model analysis, the x axis in Fig.9.4 represents the undistorted current and the y axis represents the distorted current waveform due to the non-linearity of the B-H curve of the core.

For this exercise, the non-linear characteristics of the core were assumed to be ;

- linear up to the setting current of the relay, i.e 1 A r.m.s. Thus the instantaneous current waveform up to a value of $1\sqrt{2}$ A is not distorted, thus slope 1 in Fig.9.4 is

taken as 1.0 up to $1\sqrt{2}$.

- Above $1\sqrt{2}$ A, a slope of 0.8 is taken for slope 2.

Refer to Fig.9.4 for slopes 1 and 2. Due to this non-linearity, the current waveform will be slightly distorted. The distortion however is affected by the phase angle between the harmonic and the fundamental as will be discussed later when describing Fig.9.6.

To obtain the effect of harmonics, several features must be considered. Firstly, the distorted waveform produced as a result of the interaction of the sinusoidal waveform and the non-linearity should be found. The distorted current waveform is then analysed using the 24 ordinate method (62) which gives the fundamental and harmonics of the distorted current waveform. The driving torque T_d produced by the distorted current waveform can be found using equations (8.5) and (8.6).

Since C_1 and C_2 can be found using the curve fitting method for the starting current, the value of driving torque T_d can be expressed in per unit of C_T, the results are given in Fig.9.5. The tripping time as a function of current for the test results is also shown. Thus at this stage, the relationship between the current, the driving torque and the tripping time has already been obtained.

The next step is to evaluate the tripping time for a non-sinusoidal current waveform. The method is similar to that for a sinusoidal waveform. Firstly, the distorted waveform produced by a non-sinusoidal current due to the non linearity of the core is found. Then as shown above, the driving torque T_d can be found and expressed in terms of C_T. Since a known driving torque produces a known tripping time, then by referring to Fig.9.5, the tripping time of any current waveform can be obtained.

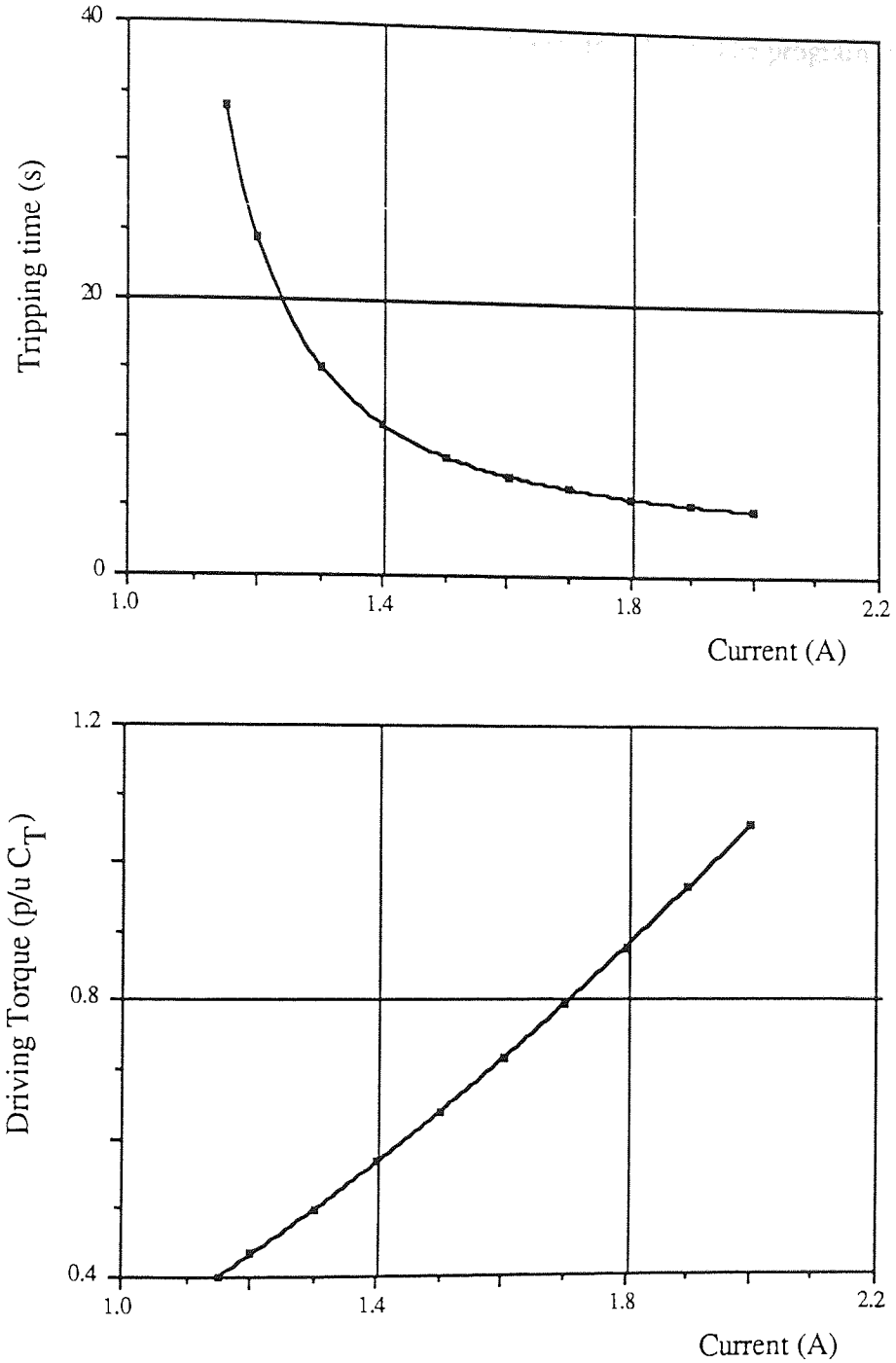

Figure 9.5. Tripping-time, current and driving torque relationship.

Calculated values of C_1 and C_2 : $C_1 = 0.3113$; $C_2 = 0.9799$

As an exercise, a current of ; $i = I \{\sin(\omega_1 t) + k_3 \sin(3\omega_1 t + \partial_3)\}$ was used which is similar to that used in the previous laboratory test. The current i was kept at 1.2 A, i.e. I (peak) = 1.69. As in the experiment, ∂_3 was varied from 0 to 360 deg. and k_3 was also

varied. The rated current of the relay was taken as 1 Amp. The program to compute the flux waveform distortions is given in Appendix 10.

Fig.9.6 shows the current waveforms, with and without distortion. The figure shows that at $\partial_3 = 0°$, the waveform is almost undistorted, while for $\partial_3 = 180°$, a slight distortion is present. The distortion is so small that it may lead to the conclusion that the tripping time will not be affected, although the simulation and experimental results show that this is not true.

Fig.9.7 shows the results of the driving torque and the tripping time variation calculations. This figure shows that a small non-linearity, in this case taken as a 20% drop of slope 2 w.r.t slope 1, may cause a large variation of tripping time due to the variation of phase angle ∂_3. In addition, the tripping time for a pure sinusoidal current lies between the maximum and minimum tripping times of the non-sinusoidal current if ∂_3 is varied. This theoretical analysis shows a similar pattern and accords well with the experimental results. The simulation results also show that the effect of waveform is less significant for higher overcurrent values.

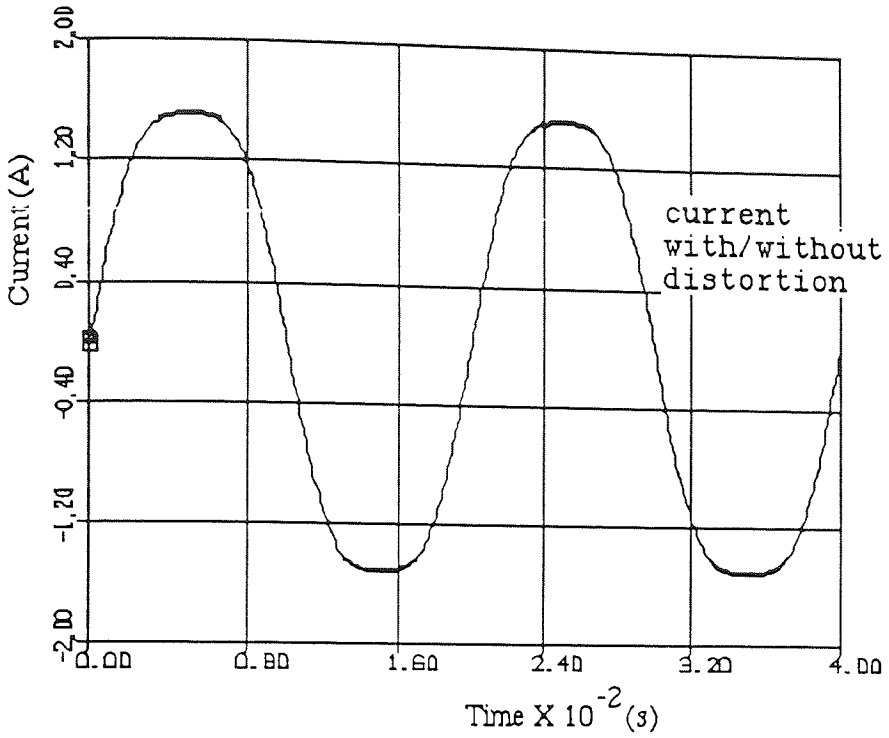

(a) The current waveform for phase angle $\partial_3 = 0$ deg.

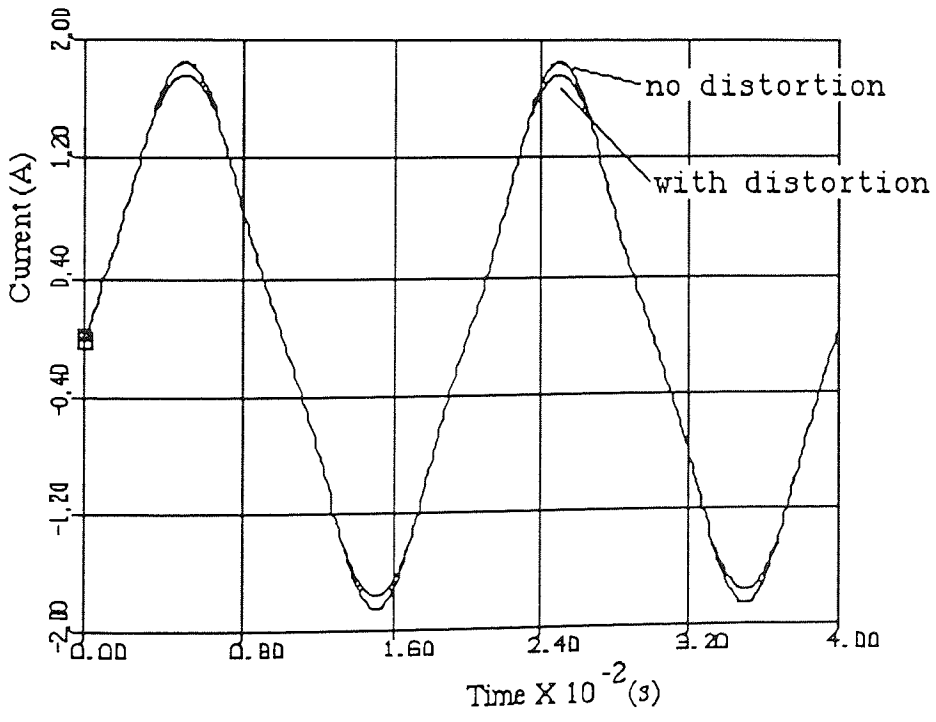

(b) The current waveform for phase angle $\partial_3 = 180$ deg

The current used was $i = I \{\sin(\omega_1 t) + 0.1 \sin(3\omega_1 t + \partial_3)\}$

Figure 9.6. The effect of ∂_3 on current waveforms.

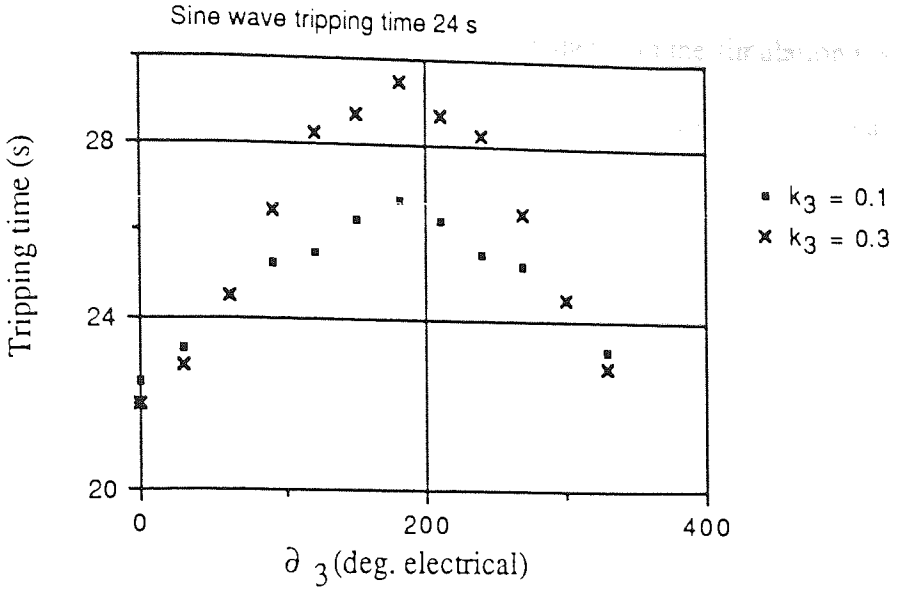

(a) The tripping time for I = 1.2 A

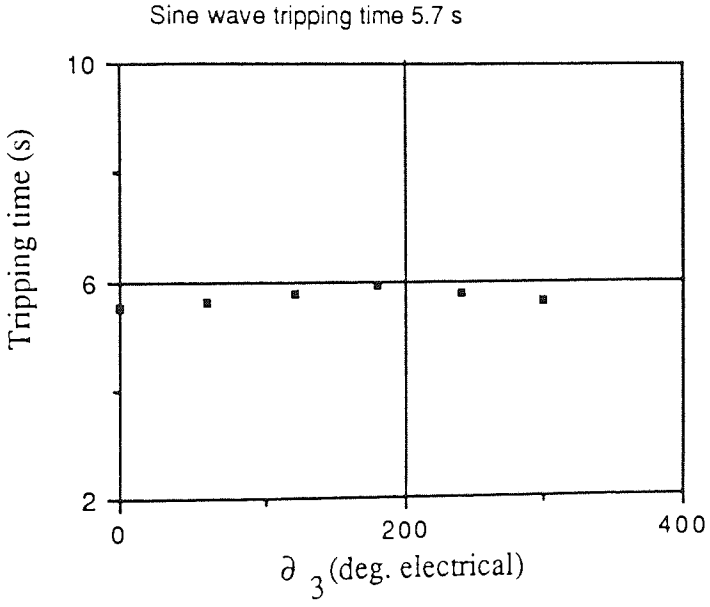

(b) The tripping time for I = 1.8 A, $k_3 = 0.3$

The current used was $i = I \{ \sin(\omega_1 t) + k_3 \sin(3\omega_1 t + \partial_3) \}$

Figure 9.7. Simulation results of the effect of harmonics on the tripping time of a typical EM TOC relay

Figure 9.8. shows the experimental results together with the simulation results. It can be seen that both curves follow a similar pattern, i.e it increases as ∂_3 increases from 0^o to approximately 180^o and then decreases. The tripping time of the fundamental also lies between the maximum and minimum values of the curves. The difference due to the assumption taken for the non-linearity of the core and that the losses, which are frequency dependent, is neglected in the simulation.

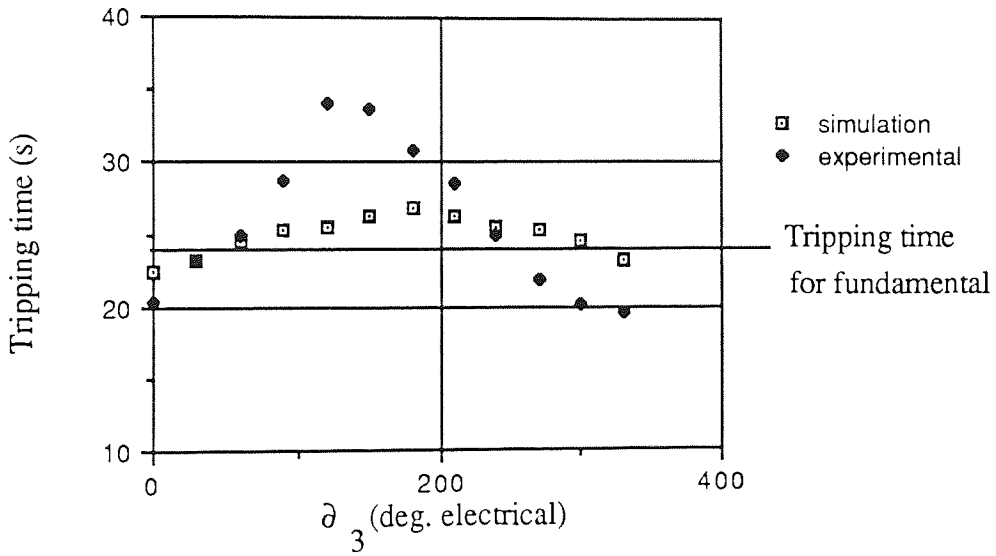

The current used was $i = 1.69 \{ \sin(\omega_1 t) + 0.1 \sin(3\omega_1 t + \partial_3) \}$

Figure 9.8. Comparison between simulation and experimental results of the effect of harmonics on the tripping time.

The important point to note here is that a small non-linearity of the core, taken in the simulation as a 20% drop in the second slope w.r.t slope 1, may cause significant differences in the tripping time. This is caused by the characteristics of the relay. As shown in Fig.9.5, a small difference in the driving torque in the low overcurrent region may cause significant differences in the tripping time. Thus the combination of a small non-linearity which causes a slight distortion and a small difference in the driving torque

may cause a large difference in the tripping time especially in the low overcurrent region. This is very important since EM TOC relays such as the IDMT relay used in the test, are used for selective protection, hence the tripping time characteristic plays an important role.

9.3. Summary

There are several important points that should be stressed here. First of all both the simulation and experimental results show that the tripping time characteristics of the relay for sinusoidal waveforms varies with frequencies. The tripping time can be lower or higher depending on the relay constants.

Concerning the effect of harmonics then it should be stressed that a particular harmonic content may or may not affect the tripping time of the relay significantly. Furthermore, the effect can be either to increase or decrease the relay tripping time. It depends on the relay constants, current waveform and non-linearity of the core. The experimental results in Fig.9.3.a shows for example, that a current which contains 3^{rd} harmonic may have lower tripping time compared with the tripping time of the fundamental current for ∂_3 between 300^o to 360^o and 0^o to 30^o. For ∂_3 around 60^o and 270^o, the tripping time is similar with the tripping time of the fundamental current, while for ∂_3 between 90^o and 240^o it is higher.

This work thus shows that the tripping time of the relay, which is practically affected by harmonics and frequencies, can be verified theoretically.

CHAPTER 10. CONCLUSION, DISCUSSION AND FURTHER WORK

10.1. Contributions of this work

The major thrust of this work on RCCB and protection relays relates to the way those relays should be analysed to assess the effect of harmonics on their performance. This leads to the theoretical explanation of the effect of harmonics on their characteristics which is not explained satisfactorily elsewhere.

While it has been known that harmonics may affect the tripping current of EM IOC relays in practice, other models as described in section 6.1 showed that theoretically, harmonics should have no effect at all as long as the current and the flux are linearly related. This work shows, that although that assumption is made, theoretically harmonics still affect the tripping current of EM IOC relay. The effect depends on the relay constants and the current waveforms. It has been shown, both theoretically and experimentally, that a current with a particular harmonic content may or may not affect the tripping current, depending on the current waveform. This work thus shows that EM IOC relays, which are affected by harmonics in practice, can be verified theoretically.

As described in section 8.1, while it was suggested by other work that the tripping time of EM TOC relays for a current which contain higher harmonic frequencies tends to be higher then their tripping time for fundamental, other experimental results showed that it is not always the case. This work offers theoretical explanation as to why the tripping time at various frequencies can be lower or higher than the tripping time for the fundamental. This work also gives a theoretical explanation as to why the tripping time for a current with a particular harmonic content may have lower, similar or higher tripping time compared with that of the fundamental as shown in the experimental results. The characteristics depend on the relay constants, current waveform and the non-linearity of the B-H curve of the core.

It has also been shown that harmonics affect the tripping current of RCCBs. The effect depends on RCCB constants and the current waveforms and thus a current with a particular harmonic content may have a different tripping current due to a different waveform. This work also relates the effect of harmonics on RCCBs and the human body. It is shown that effectiveness of RCCBs in protecting people against electrocution, especially ventricular fibrillation which is the cause of death, still has to be studied since the effect of harmonics on ventricular fibrillation is not clear.

It has been shown that the shape of the waveform and relay constants have a significant influence on the way harmonics affect RCCBs and protection relays. Thus in assessing the effect of harmonics, not only the harmonic content, but also the shape of the waveform should be known. The method developed provides a useful tool and the basic methodology to analyse the effects of harmonics on the relays in general.

In addition to the conclusion above, it is important to mention the various conclusions obtained for each piece of protection equipment studied. Concerning the RCCB, it can be concluded that :

1. A fault, introduced only once at a random fault angle (ωt_o) and at no load condition for sinusoidal residual current, will rarely measure the maximum total tripping time which can be encountered in practise.
2. If random tests are performed to obtain the maximum total tripping time of a RCCB for a sinusoidal waveform with a 2 ms interval resolution, the random test should be repeated 30 times, where one can expect to hit the maximum tripping time at least once with 95 % confidence. In addition, the maximum value should be taken as the RCCB tripping time and not the average.
3. A longer total tripping time, in excess of the standard limit, may be obtained in electronic RCCBs if they are switched onto a standing fault.

4. Harmonics affect the tripping current of RCCBs. The effect depends on the waveform of the residual current and the RCCB constants, and not merely on the r.m.s. value of the harmonics content.

Concerning the two protection relays studied, it can be concluded that :

1. The main characteristics of EM IOC and EM TOC relays are affected by harmonics and determined by both the waveform and relay constants and not merely by the r.m.s. or Ampere second values of the current. Thus two waveforms having the same harmonic content may have completely different characteristics due to different phase angles.
2. Relay characteristics are a function of frequency but do not represent how the relay will behave if the sinusoidal currents at given frequencies are summated.

10.2. Implications of this work

The results of this study has several implications on other areas which need to be taken into account, i.e.:

10.2.1. If a testing standard which includes harmonics is to be published, then the waveform of the current should be taken into consideration, and not merely the harmonic content.

10.2.2. In the measurement of harmonics, information concerning the waveform such as the phase angle between each harmonic and the fundamental (∂_n), should also be taken into account.

10.2.3. The above findings also imply that the work concerning the effect of harmonics on CTs should also consider the waveform distortion.

10.3. Suggestions for further works

10.3.1. The study of the behaviour of RCCBs and protection relays due to non-periodic

waveforms, such as inrush current, surge, etc. This is considered an important area since these types of waveform are present in the supply.

10.3.2. Since the trend today is towards the use of electronic protection relays, both digital and analog, the method developed here should be applied to such relays to assess how appropriate it is in such an application. Fuller et al 's test results (49) on electronic relays shows that they are also affected by harmonics.

10.3.3. It seems that RCCB circuits, especially the CBT deserves more investigation into their behaviour in response to a sinusoidal waveform since in some tests, the RCCB fails to react to the fault the first time the residual current exceeds the threshold value.

10.3.4. Since RCCB and relay constants significantly affect the performance of these devices, these constants deserves more measurement and study.

List of References

1. BIEGELMEIER, G.: 'Tripping sensitivities and tripping times of residual current operated circuit breakers', Elektrotechnik und Maschinenbau (FRG), Vol 98, No 9, 1981, pp 373-379. OA translation No 2508 by ECRC-UK

2. BIEGELMEIER, G.: 'Basic considerations on protective measures against electric shock in low voltage installations', IEE Conference publication 251, London 5-6 June 1985.

3. IEC report 479-1(1984) and -2 (1987), 'Effects of current passing through the human body', IEC, Switzerland.

4. COURT, M.: 'An Evolutionary history of the RCCB', Electrical Review, Vol 215 , No 18, 7 December 1984, page 38-40.

5. 15th edition of the IEE Wiring Regulation, including all amendments up to 10th January 1986.

6. BS 4293:1983,: 'Residual Current Operated Circuit Breakers'.

7. 15th edition of the IEE Wiring Regulation, including all amendments up to June 1987.

8. FERRIS, L.P., KING, B.G., SPENCE, P.W., WILLIAM, H.B.: 'Effect of electric shock on the heart', Electrical Engineering, Vol 55, May 1936, page 498-515.

9. DALZIEL, C.F.: 'Dangerous electric currents', AIEE Transaction, Vol 65, August/ September 1946, page 579-585.

10. DALZIEL, C.F., LEE, W.R.: 'Reevaluation of lethal electric currents', IEEE Transaction on Industry and General Application, Vol IGA-4 No5 Sept/Oct. 1968, page 467-476.

11. DALZIEL, C.F., LEE, W.R.: 'Lethal electric currents', IEEE Spectrum, Vol 6, No 2, February 1969.

12. HAMMAM, M.S., BAISHIKI, R.S.: 'A Range of body impedance values for low voltage, low source impedance systems of 60 Hz', IEEE Transaction on Power Apparatus and Systems, Vol PAS 102, No 5, May 1983.

13. BIEGELMEIER, G., LEE, W.R.: 'New considerations on the threshold of ventricular fibrillation for ac shocks at 50-60 Hz', IEE Proceeding, Vol 127, Part A, March 1980, page 103-110.

14. NOWAK, K.: 'Fifteen years of current operated earth leakage protection in the VDE Regulations', Der Elektromeister und Deutsche Elektrohandwerk, December 1973, Vol 48, No 4, pp 1772-1774. SMRE translation No 6547

15. MORLEY, L.A, TRUTT, F.C., NOVAK, T.: 'Sensitive ground fault protection for mines, phase 1 - ac utilization', Pensylvania state University, NTIS PB 85 - 185767.

16. MORE, G.E.: 'ELCB', The Safety Practitioner, March 1983 page 4-6.

17. TRUTT, F.C., MORLEY, L.A., RUFT, D.J.: 'Sensitive Ground Fault Protection', IEEE-IAS- 1983 Mexico, 3-7 October 1983.

18. DALZIEL, C.F.: 'Transistorized, residual current trip device for low voltage circuit breaker', AIEE transaction, February 1963, page 973 - 983.

19. DALZIEL, C.F.: 'Improvement in Electrical safety', AIEE transaction, Vol 81, May 1962, page 121-127.

20. DALZIEL, C.F.: 'Transistorized ground fault interupter reduces shock hazard', IEEE Spectrum, January 1970, page 55-62.

21. MITTRA, D.K., BASU, S.K.,. MONDAL, R.K.: 'Novel fail-safe earth fault protection schemes for underground coalmines using restricted neutral system of power supply', IEE Proceeding part C, Vol 129, No 1, January 1982, page 35-40.

22. GROSS, T.A.O.: 'Ground fault protective systems with variable rate integration of fault signals', US Patent No 4,024,435 May 17, 1977.

23. HASELER, P.: 'Consumer Units', Electrical Equipment, April 1987, page 18-20.

24. EMANUEL, A.E., DOUGHERTY, J.W.: 'Sensitive Ground Fault Interupter performance in the presence of direct current', IEEE Transaction on Power Delivery, Vol. PWRD-1, No 1, January 1986, page 111-117.

25. KIDD, A.L.: 'Discriminating RCCBs for installation protection', Wiring Installation and Supplies, Issue 24, 1985.

26. BRIDGES, J.E.: 'Impact of recent development in biological safety criteria', IEEE Transaction on Power Delivery, Vol PWRD-2, No 1, January 1987, page 238-248.

27. ROESCH, H.: 'Current Operated ELCBs, for AC and pulsating DC fault currents', Siemens Power Engineering Vol.3, 1981, No 8-9, page 252-5.

28. The Electricity Council : 'Savety of Immersion Heater', report No IMG 251,15 November 1983.

29. The Electricity Council: 'Report on the Working party on Residual Current Devices', report No IMG 295, 20 November 1984.

30. WRIGHT, A.: 'Current Transformers, their transient and steady state performance', Chapman and Hall Ltd, London, 1968.

31. SASTROSUBROTO, A.S., FEATHERSTONE, A.M.: 'An examination of the tripping time characteristics of Residual Current Circuit Breakers which may give rise to failures', 23rd University Power Engineering Conference, Nottingham, UK, 20-22 September 1988.

32. FEATHERSTONE, A.M., SASTROSUBROTO, A.S.: 'The Simulation and Mathematical modelling of harmonic disturbances on electro-heat protection equipment', International Seminar on Mathematical Modelling in Electroheat, Leningrad, USSR, 20-24 June 1989.

33. SASTROSUBROTO, A.S., FEATHERSTONE, A.M.: 'Probability evaluation of Residual Current Circuit Breaker testing method', 24th University Power Engineering Conference, Belfast, UK, 19-21 September1989.

34. LAUERER, F.: 'Unfalverhütung bei stromverbraucheranlagen durch empfinliche fehlerstrom-schutzschalter', B.A.U, West germany,1972

35. LINDERS, J.R.: 'Electric wave distortions: Their hidden cost and containment', IEEE Transaction on Industrial Applications, Vol.IA-15, No 5, Sept./Oct. 1979, page 459-71.

36. IEEE Load characteristic task force,: 'The effects of power system harmonics on power system equipments and loads', IEEE Transaction on Power Apparatus and System, Vol. PAS-104, No 9, Sept. 1985, page 2555-63.

37. HORTON, W.F. and GOLDBERG, S.: 'The effects of harmonics on the operating points of electromechanical relays', IEEE Transaction on Power Apparatus and System, Vol. PAS-104, May 1985, page 1178-88.

38. GEC Measurements, 'Protective relay application guide', UK, 1975.

39. IEEE Wave distortion group: 'The impact of sine wave distortions on protective relays', IEEE Transaction on Industrial Applications, Vol. IA-20, No 2, March/April 1984, page 335-43.

40. JOST, F.A., MENZIES, D.F. and SACHDEV, M.S.: 'Effects of system harmonics on power system relays', CEA, System planning and operation section, Power system protection comitte spring meeting, USA, March 1974.

41. PEEK, R.L., WAGAR, H.N.: 'Switching relay design', Van Nostrand, UK, 1955.

42. KARO, D., DHAR, P.: 'The calculation of the dynamic characteristic of electromagnet relay with the aid of an analogue computer', International Conference on CAD, Southampton, 15-18 April 1969.

43. WARRINGTON, A.R.C.: 'Protective relays', Chapman and Hall Ltd, UK, 1968.

44. GREENE, J.D., GROSS, C.A., BIRDWELL, G., CHAKRAVARTHI, K.R.: 'Non sinusoidal excitation of transformers", Proc. of the IEEE 17th symp. on system theory, Auburn, USA 24-26 March 1985.

45. MEISEL, J.: 'Current Instrument Transformer Error Calculations', Proc. AIEE, December 1963, page 1082-1085.

46. EMANUEL, A.E., CHANDRA, H.N.: 'Current Transformer accuracy on asymetrically triggered thyristor circuits', IEEE Transaction on Power Apparatus and Systems, Vol. PAS-99, No 1, Jan/Feb. 1980, page 92-98.

47. IEEE Power system relaying committe: 'Fault induced wave distortion of interest to relay engineers', IEEE Transaction on Power Apparatus and Systems, Vol. PAS-104, No 12, December 1985, page 3574-3584.

48. IEEE Power system relaying committe: 'Sine wave distortions in power systems and the impact on protective relaying', 1985 report.

49. FULLER, J.F., FUCHS, E.F., ROESLER, D.J.: 'Influence of Harmonics on Power Distribution System Protection', IEEE Transaction on Power Delivery, Vol.3, No 2, April 1988, page 549-557.

50. FAUCET, M.A, KEENER, C.A.: 'Harmonics may delay relay operation', Electrical World, April 9, 1938, page 80.

51. SARAMAGA, D.E., MENZIES, R.W., SWIFT, G.W.: 'Effect of harmonics current on induction disc relay operating torque', IEEE PES Summer meeting, Vancouver, Canada, July 1973, paper No C73351-4.

52. CHU, H.Y., LIN, F.J, HUANG, C.L.: 'Harmonics effects of watthour meter type induction disc overcurrent relay', IEEE Electronicom 85, 7-9 October 1985, USA.

53. SASTROSUBROTO, A.S., FEATHERSTONE, A.M.: 'The simulation of electromechanical overcurrent relays with respect to harmonics', 23rd University Power Engineering Conference, Nottingham, UK, 20-22 September 1988.

54. SASTROSUBROTO, A.S., FEATHERSTONE, A.M.: 'The effects of harmonics on the operating poiunts of electromechanical overcurrent relays', 24th University Power Engineering Conference, Belfast, UK, 19-21 September1989.

55. SASTROSUBROTO, A.S., FEATHERSTONE, A.M.: 'Continuous simulation model of electromechanical instantaneous type relays with respect to harmonics', 3rd European Simulation Congress, Edinburgh, UK, 5-8 September1989.

56. MC GRAW-EDISON Team,: 'Harmonic considerations for electrical distribution feeders', report for Oak Ridge National Laboratory, US Department of Energy, March 1988.

57. CRUCQ, J.M., ROBERT, A.: 'Statistical approach for harmonic measurements and calculations', 10th International conference on Electricity Distribution (CIRED), Brighton, UK, 8-12 May 1989.

58. Engineering Guidance G.5/3: 'Limits for harmonics in the United Kingdom Electricity Supply system', Electricity Council, September 1976.

59. BS 5406 : 1988,: 'Disturbances in supply systems caused by household appliances and similar electrical equipment'.

60. GRETSCH, R., DE VRE, R,: 'Standardization of measurement methods for harmonics', 10th International conference on Electricity Distribution (CIRED), Brighton, UK, 8-12 May 1989.

61. IEC publication 555-2, : 'Disturbances in supply systems caused by household appliances and similar electrical equipment, part 2 : Harmonics', July 1988.

62. SHEPPERD et al, 'Higher electrical engineering', Pitman, 1970

63. DALZIEL, C.F.: 'Effect of frequency on Let Go Currents', AIEE Transaction, December 1943, Vol. 62, page 745-750.

64. BERNSTEIN, T.: 'Evaluation of the electric shock hazard for the Nova XR 5000 stun gun', University of Wisconsin - Madison USA, January 22nd 1985.

65. GEDDES, L.A., BAKER, L.E., 'Response to passage of electric current through the body', Journal of the Association for the advancement of Medical Instrumentation, Vol 5, No 1, January 1971, page 13 - 18.

66. DALZIEL, C.F.: 'Effect of waveform on Let Go currents', AIEE Transaction, Vol 62,1943, page 739-744.

67. BS 142:1982, 'Electrical protection relays'.

68. NAG Library manual, 1980.

69. Mitchell and Gauthier Associates, 1981, Advanced Continuous Simulation Language user guide/reference manual.

70. VINCENT, W.R.: 'Harmonics and electrical noise in distribution systems', Electric Power Research Institute, USA, 1985.

71. GEERTS, G., ROBERT, A.,: 'Harmonics statistical measurements in public networks from November 85 to November 86', LABORELEC, report number 1-GG-AR/1310/8701.

72. VDE 0664, 'Residual current-operated protective devices' part 1, October 1985, translated by British Standard Institution.

73. MEIR, P.: 'DC sensitive RCCBs', Electrical Review, Vol 216, No 17, 31May 1986, page 24-26.

74. ROESCH, H.: 'Construction and function of Earth-leakage circuit breakers, requirements on its magnet components', Journal of Magnetism and Magnetic Material, No 9, 1978, page 150-156.

75. GLASSBURN, W.E., SONNEMANN, W.K.: 'Principles of induction type relay design', AIEE Transaction, Vol 72, part III, February 1953, page 23-27.

76. HEISING, C.R., PATTERSON, R.C.: 'Reliability expectations for protective relays', IEE Fourth International Conference on Developments in Power system protection, University of Edinburgh, UK, 11-13 April 1989, Conference publication No 302, page 23-27.

77. BRADLEY, D.A., GRINDROD, S.J.: 'The influence and measurement of harmonics on an industrial system', IEE third international conference on Sources and effects of power system disturbances, Conference publication No 210, page 136-141.

78. SONNEMANN, W.K.: 'A new inverse time overcurrent relay with adjustable characteristics', AIEE Transaction, Vol 72, part III, February 1953, page 360-368.

79. LAI, L.L.: 'Simulation of power station protection equipment', PhD thesis, ASTON University, 1984.

80. BAGHZOUZ, Y., TAN, O.W.: 'Harmonic analysis of induction watthour meter performance', IEEE Transaction on Power Apparatus and Systems, Vol PAS-104, No 2, February 1985, page 399-406.

81. FROBERG, C.E.: 'Numerical mathematics', The Benyamin/Cummings Publishing Co, Menlo Park, California, USA, 1985.

82. ARRILAGA, J., BRADLEY, D.A., BODGER, P.S.: 'Power system harmonics', John Wiley & Sons, 1985

83. BAITCH, T.L.: 'Network harmonics distortion limits : A review of the world scene and specifically of Australia's harmonic limitation standard', IEEE International conference on harmonics in power systems, 22-23 October 1984, Worcester, Massachusetts, USA.

84. ORR, J.A., CYGANSKI, D.: 'Data collection and statistical analysis techniques for power system harmonics', IEEE International conference on harmonics in power systems, 22-23 October 1984, Worcester, Massachusetts, USA.

85. MARSHALL, A.J.: 'A demonstration of current waveform distortion with inadequate test equipment', GEC Measurements, UK.

86. FUCHS, E.F., ROESLER, D.J., ALASHAB, F.: 'Sensitivity of home appliances to harmonics and fractional harmonics of the power system's voltage. Part 1. Transformer and Induction machines', IEEE International conference on harmonics in power systems, 22-23 October 1984, Worcester, Massachusetts, USA.

87. STEEL, J.G., SWIFT-HOOK, D.T.: 'Statistics of Circuit Breaker performance', Proc. IEE Vol. 117, No 7, July 1970, page 1337 - 1345.

88. KELLY, J., WALLACE, J.E.: The analytical design and evaluation of electromagnets, AIEE Trans. Part I, Vol. 75, 1956 (January 1957 section), page 675- 680.

89. GOLDBERG, S., HORTON, W.F.,: 'Induction watthour meter accuracy with non-sinusoidal currents', IEEE Transaction on Power Delivery, Vol. PWRD-2, No. 3, July 1987, page 683-690.

90. HIRANO, T., WADA, H.,: 'Effects of waveform distortion on characteristics of induction watthour meter', Electrical Engineering in Japan, Vol. 89, No. 4, 1969, page 29-39.

91. FINKE, G.B., MA, B.M.: 'A new type of differential transformer core for ground fault circuit interupters', IEEE Transactions on Magnetics, Vol.MAG-17, No.6, November 1981, page 3157-3159.

92. PFEIFER, F., KUNZ, W.: 'Crystaline and amorphous alloys for sophisticated electronic devices', IEEE Transactions on Magnetics, Vol.MAG-18, No.6, November 1982, page 1406-1411.

93. HYINK, R.: 'An analysis of the dynamics of an electromechanical system', AIEE Trans. Part I, Vol. 79, September 1960, page 267-271.

94. GEC Measurements, : 'Protective relay application guide', 1975, UK.

95. SASTROSUBROTO, A.S., FEATHERSTONE, A.M., NORRIS, W.T.: 'The performance of residual current devices', Aston University, Electric Power Group Note, FE/EEEAP/3/89.

96. BS 7071 : 1989, 'Portable residual current devices'.

97. SASTROSUBROTO, A.S., FEATHERSTONE, A.M., NORRIS, W.T.: 'Measuring the tripping time of Residual Current Devices (RCDs) used for protecting people', Submitted to the IEE Proceedings-C, Generation, Transmission and Distribution, now being revised.

APPENDIX 1. THE WAVE FORM GENERATOR FOR RELAY TESTING

In order to test the tripping current of protection relays and RCCBs for non-sinusoidal waveforms, a current source with controlled harmonic content was designed.

A.1.1. The block diagram

Basically, the generator is as shown below. It consists of a software package (S1) written in BASIC, which produces a set of digital signals which represents the required waveform. Another package S2 (written in machine language) is used to read and send the data to the output terminal of the computer. This digital data is then converted to an analog signal. Since the data is to represent a periodic waveform, it can be read repetitively, thus producing a continuous voltage output. The analog output can then be amplified, passed through the relay in series with a 'large' resistor (compared with the relay impedance) to produce a current source. Fig.A.1.1 shows the block diagram.

A.1.2. Measurements and frequency analysis results

Before the waveform generator is used for the experiment, the waveform was analysed using a frequency analyser. The pictures below show some measurement results. Digital data are produced every 0.5 deg or every 27μs (for a 50 Hz sinusoidal waveform), giving a smooth 50 Hz sinusoidal waveform as shown in Fig.A.1.2.

Figures A.1.3.a shows a waveform which contain 50% third harmonic, and figure A.1.3.b shows the frequency analysis.

All the figures show that the waveform output is acceptable since the unwanted harmonic content is at least 40 dB below the expected output.

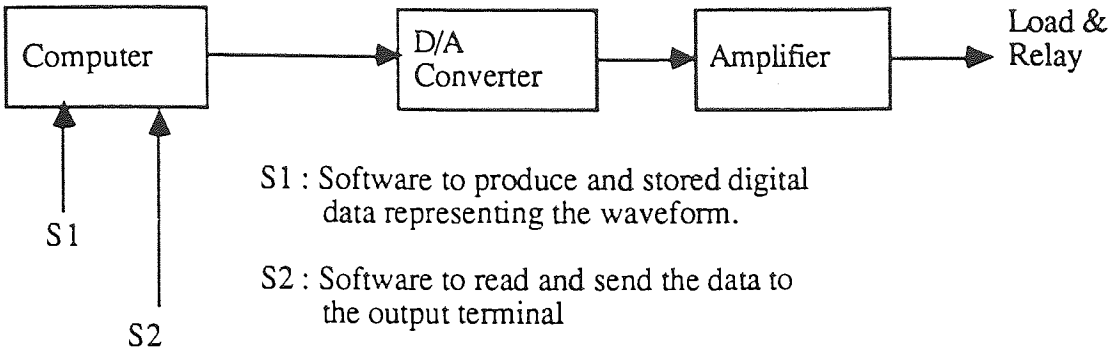

Figure A.1.1. Block diagram of the waveform generator

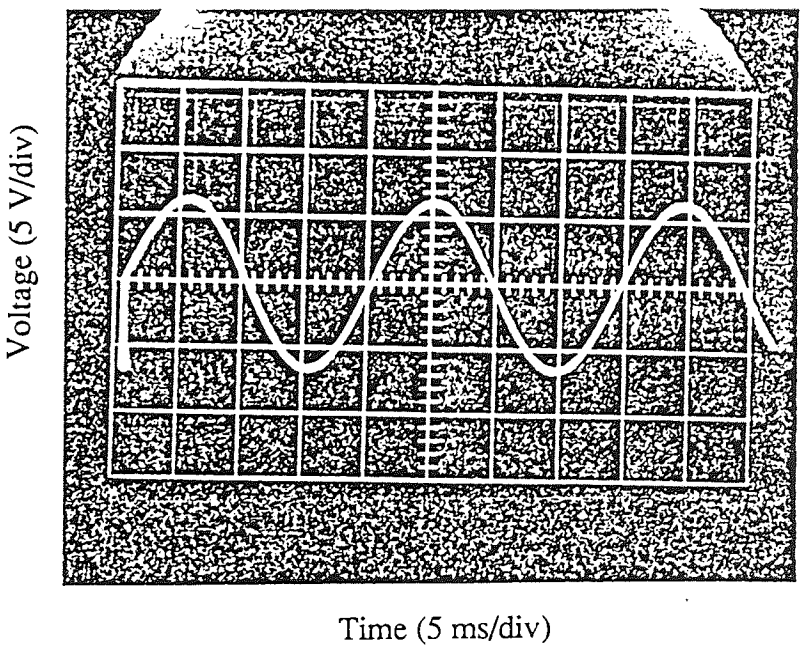

Figure A.1.2. Pure 50 Hz sinusoidal output of the waveform generator

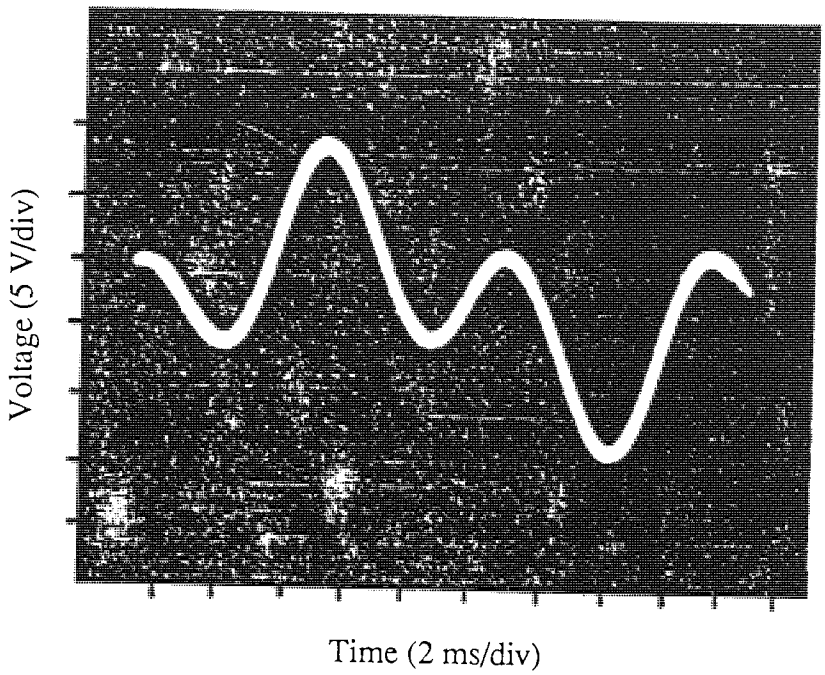

(a) The waveform

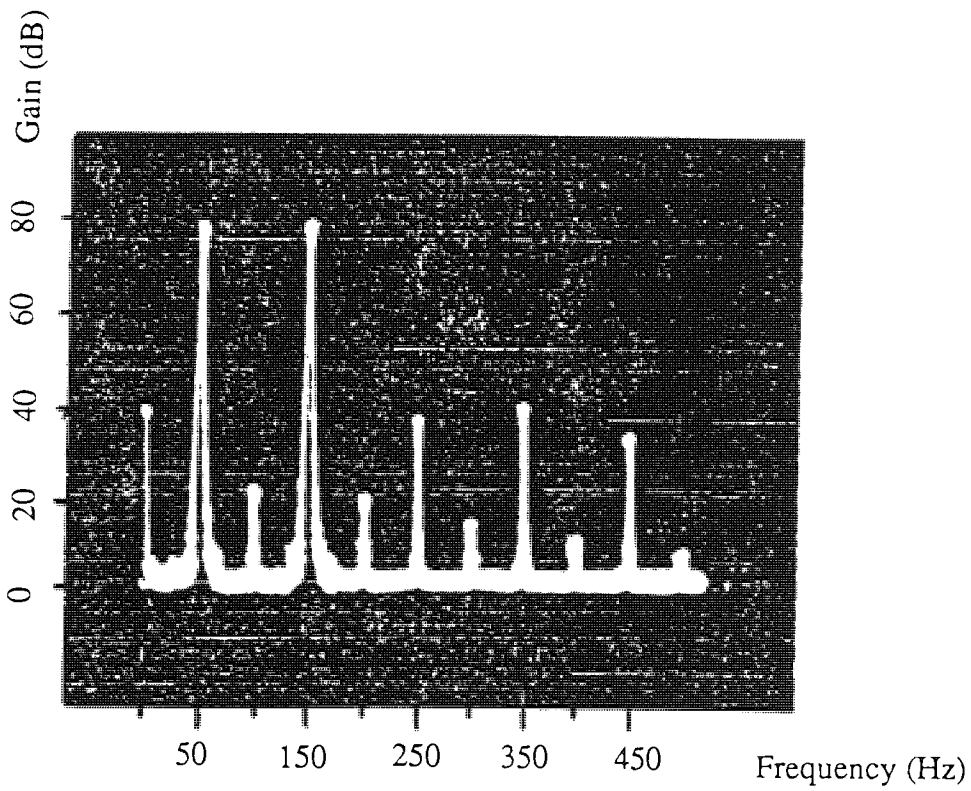

(b) The frequency analysis

Figure A.1.3. Output of the generator with 50% third harmonic content (w.r.t. the total r.m.s. content)

APPENDIX 2. PROGRAM FOR RCCBs CHARACTERISTICS COMPUTATION

A.2.1. R.M.S. calculation program

Flow chart Diagram :

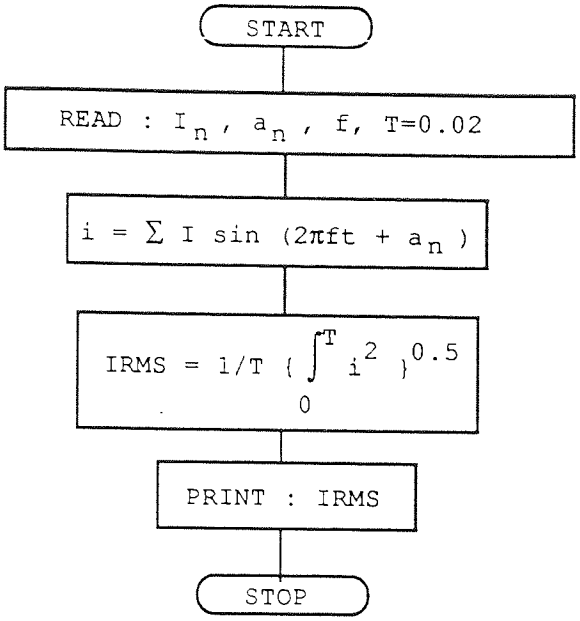

Program is kept under : 'EX10.CSL'

A.2.2. Computation of RCCB tripping current

Flow chart Diagram :

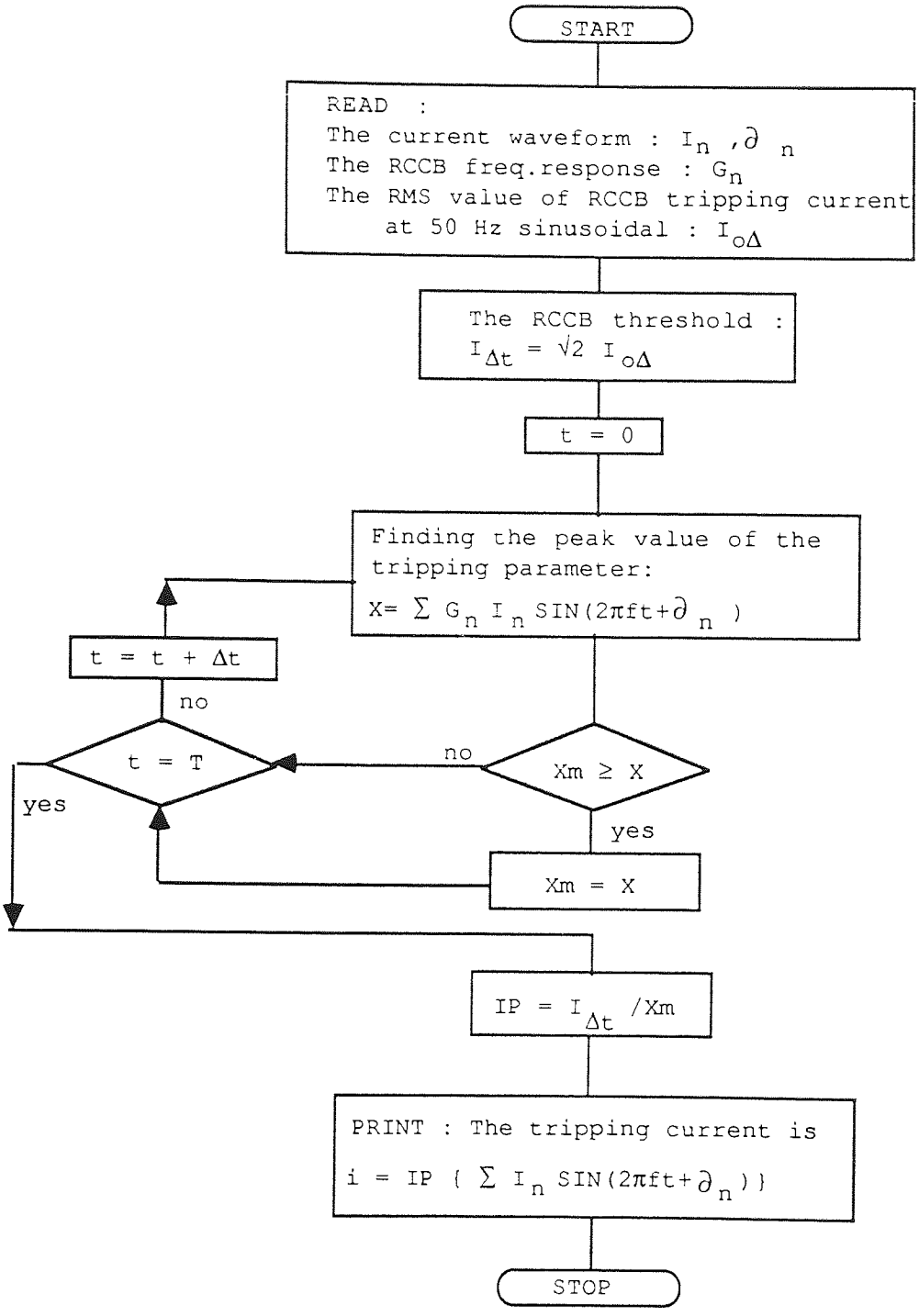

Program is kept under : 'RCCB.BAS'

APPENDIX 3. DERIVATION OF ALL EQUATIONS THAT GOVERN THE RELAY ARMATURE MOVEMENT

A.3.1. The similarity between the hinged and atracted armature types of EM IOC relays

Refer to the attracted armature type EM IOC relay in Fig.A.3.1, the air gap reluctance is :

$$S_g = 2 (X_o/2) / (\mu_o a) = X_o / (\mu_o a) \qquad (A.3.1)$$

Since X_o may vary with time as the armature is attracted while μ_o and a are constant, then X_o may be replaced with (X_o-x), where x/2 is the armature travel. Hence :

$$S_g = (X_o-x) / (\mu_o a) \qquad (A.3.2)$$

Now refer to the hinged armature type EM IOC relay in Fig.A.3.2, for a length of d_z, the air gap reluctance is :

$$dS_g = x / (\mu_o w dz) \qquad (A.3.3)$$

the air gap permeance is :

$$dP_g = \mu_o w dz/x \qquad (A.3.4)$$

From Fig.A.3.2, it can be found that :

$$x = (X_o/ Z_4) z \qquad (A.3.5)$$

The substitution of (A.3.4) to (A.3.3) gives an air gap permeance of :

$$dP_g = \mu_o w (Z_4 / X_o) (dz/z) \qquad (A.3.6)$$

Air gap permeance for area a_{34} is :

$$P_{g34} = \int_3^4 dP_g$$

$$= \mu_o w (Z_4 / X_o) \ln (Z_4 / Z_3) \qquad (A.3.7)$$

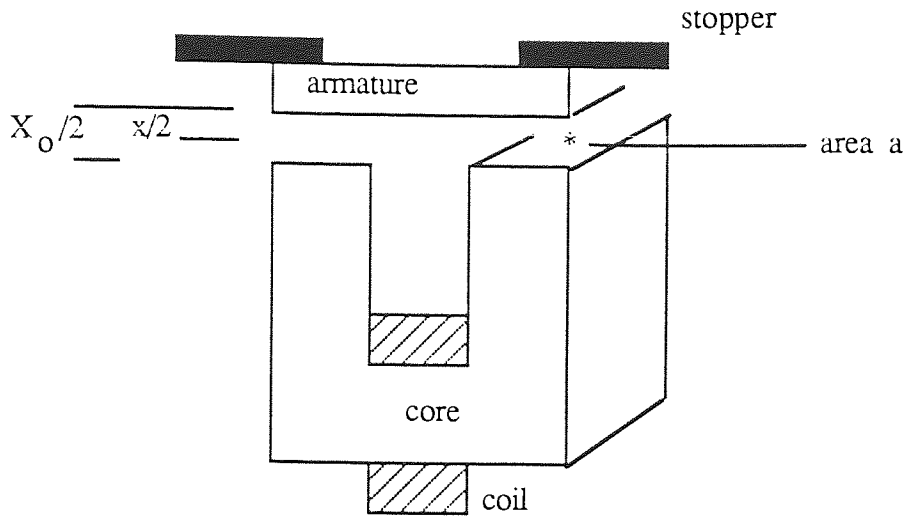

Figure A.3.1. An attracted armature type EM IOC relay.

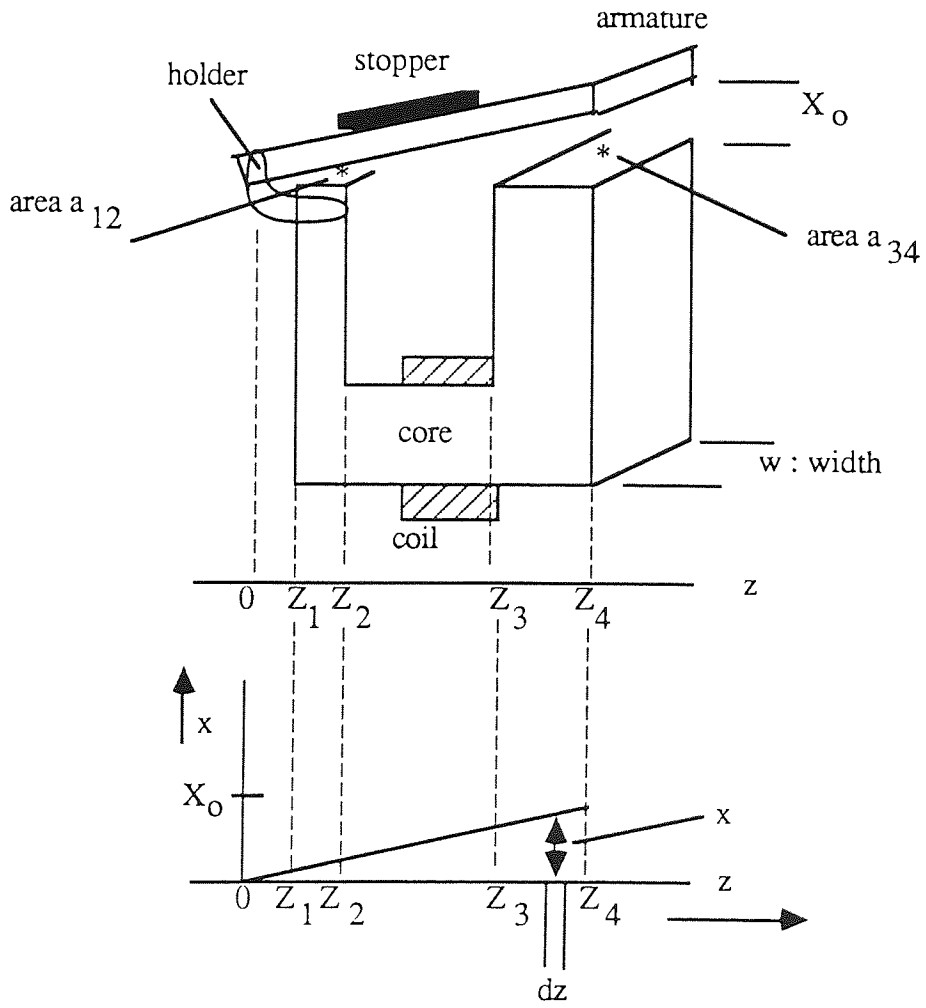

Figure A.3.2. A hinged armature type EM IOC relay showing the armature axis

The air gap reluctance for area a_{34} is :

$$S_{g34} = \frac{X_o}{\mu_o w Z_4 \ln (Z_4 / Z_3)} \qquad (A.3.8)$$

Multiply (A.3.8) by (Z_4-Z_3 / Z_4-Z_3) gives :

$$S_{g34} = \frac{X_o (Z_4-Z_3)}{\mu_o w (Z_4-Z_3) Z_4 \ln (Z_4 / Z_3)} \qquad (A.3.9)$$

$$\text{Taking } k_{34} = \frac{Z_4 \ln (Z_4 / Z_3)}{Z_4 - Z_3} \qquad (A.3.10)$$

since $a_{34} = w (Z_4-Z_3)$, then (A.3.9) can be rewritten as :

$$S_{g34} = X_o / (\mu_o a_{34} k_{34}) \qquad (A.3.11)$$

Similarly, for an air gap area a_{12}, the reluctance is :

$$S_{g12} = X_o / (\mu_o a_{12} k_{12}) \qquad (A.3.12)$$

The total air gap reluctance is :

$$S_g = (X_o / \mu_o) \left(\frac{1}{a_{12} k_{12}} + \frac{1}{a_{34} k_{34}} \right) \qquad (A.3.13)$$

Taking a' as the effective area where

$$a' = \frac{1}{a_{12} k_{12}} + \frac{1}{a_{34} k_{34}} \qquad (A.3.14)$$

then the total air gap reluctance can be expressed as :

$$S_g = X_o / (\mu_o a') \qquad (A.3.15)$$

Since μ_o and a' are constants determined by the relay design while X_o may vary as the armature is attracted toward the core, X_o may be replaced with (X_o-x) where x is the armature travel. Then (A.3.15) can be expressed as :

$$S_g = (X_o-x)/(\mu_o a') \qquad (A.3.16)$$

NB: a' is the effective air gap area.

Since (A.3.2) and (A.3.16) are similar, it follows that both hinged and attracted armature type EM IOC relays can be treated in the same way.

A.3.2. Armature movement of an unshaded type EM IOC relay

Refer to Fig.A.3.3. The air gap has a constant permeability μ_o, and the energy in it is :

$$W = (1/2) \int_{vol.} B.H \, dv$$

$$= (1/2) \int_{vol.} (B^2 / \mu_o) (a \, dx) \qquad (A.3.17)$$

This energy will appear as a mechanical work, i.e the attraction of the armature by a pulling force F_p.

$$W_{mech} = \int F_p \, dx \qquad (A.3.18)$$

Equating the last two equations, we obtain :

$$F_p = (1/2) (B^2 / \mu_o) a$$

$$= \Phi_g^2 / (2 \mu_o a) \qquad (A.3.19)$$

since $\Phi_g = B.a$

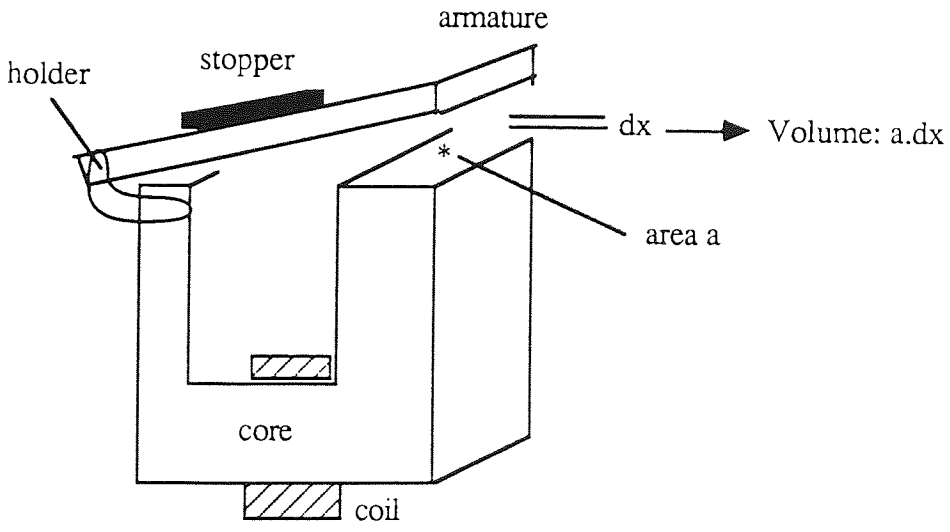

Figure A.3.3. A hinged armature type EM IOC relay showing the core area

From Fig.6.2, redrawn here as Fig.A.3.4, the total reluctance is :

$$S_{tot} = S_c + \frac{S_l\,(S_o+S_g)}{S_l + (S_o+S_g)} \qquad \text{(A.3.20)}$$

$$= S_c + S_{log} \qquad \text{(A.3.21)}$$

by taking :

$$S_{log} = \frac{S_l\,(S_o+S_g)}{S_l + (S_o+S_g)} \qquad \text{(A.3.22)}$$

Hence, the total flux generated by an ampere turn of Ni is :

$$\Phi_c = Ni\ /\ (S_c + S_{log}) \qquad \text{(A.3.23)}$$

where S_l, S_c and S_o are determined by the relay design, while the air gap reluctance S_g can be calculated by using equation (A.3.2) or (A.3.16).

The air gap flux can then be derived as :

$$\Phi_g = \frac{S_l}{S_l + (S_o+S_g)}\,\Phi_c \qquad \text{(A.3.24)}$$

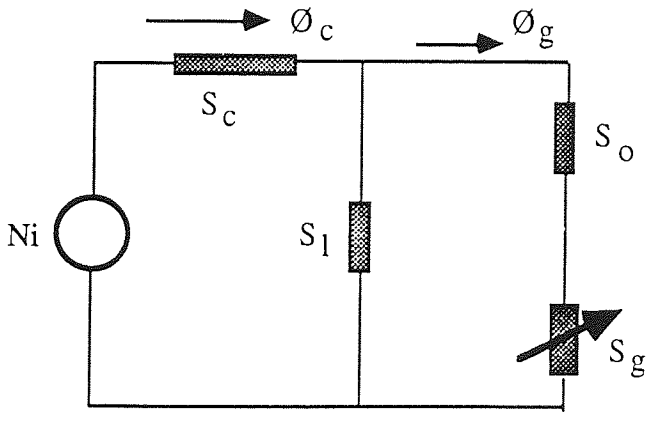

Figure A.3.4. The magnetic circuit of a relay.

Knowing Φ_g, the pulling force F_p can be derived by using (A.3.19). The restraining forces consists of the spring force F_s and the friction force F_f, where :

$$F_s = F_o + K_s x \qquad \text{(A.3.25)}$$

$$F_f = K_f \, dx/dt \qquad \text{(A.3.26)}$$

Total force F will determine the armature movement according to :

$$F = m \, dx/dt \qquad \text{(A.3.27)}$$

Since $F = F_p - F_s - F_f$, it follows that the armature movement is governed by :

$$F_p - F_s - F_f = m \, dx/dt \qquad \text{(A.3.28)}$$

A.1.3. Armature movement of a shaded relay

Suppose a part of the relay is shaded as shown in Fig.A.3.5. a_1 is the unshaded area while a_2 is the shaded area. Taking Φ_{c1} as the flux in the unshaded pole and Φ_{c2} as the flux in the shaded area, then Φ_{c1} and Φ_{c2} will produce air gap flux Φ_{g1} and Φ_{g2} respectively. All reluctances in conjunction with Φ_{c1} and Φ_{c2} are S_{li}, S_{ci}, S_{gi}, S_{oi}, S_{logi} and S_{toti}. Index i can be either 1 or 2.

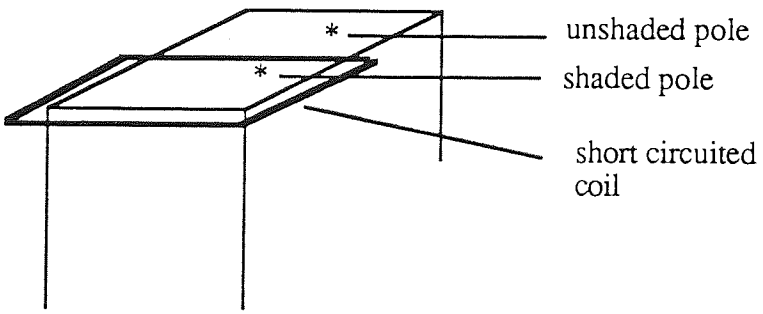

Figure A.3.5. A shaded pole of a relay.

Since an induced current i_{sc} flows through the short circuited coil, then by taking $i = (\sqrt{2}\, I) \sin(\omega_1 t)$, we obtain :

$$\Phi_{c1} = \frac{Ni}{S_{c1} + S_{log1}} \qquad \text{(A.3.29)}$$

$$\Phi_{c2} = \frac{Ni - i_{sc}}{S_{c2} + S_{log2}} \qquad (A.3.30)$$

where :

$$i_{sc} = G_s \frac{d}{dt} \Phi_{c2}$$

$$= j\,\omega_1\, G_s\, \Phi_{c2} \qquad (A.3.31)$$

Combining (A.3.30) and (A.3.31), we obtain :

$$Ni = \{(S_{c2} + S_{log2}) + j\,\omega_1\, G_s\}\, \Phi_{c2} \qquad (A.3.32)$$

in vectorial form :

$$Ni = \left[\{(S_{c2}+S_{log2})^2 + (\omega_1\, G_s)^2\}^{0.5} \tan^{-1}\{(\omega_1\, G_s)/(S_{c2}+S_{log2})\}\right]\Phi_{c2} \qquad (A.3.33)$$

Equations (A.3.29) and (A.3.33) can be rewritten as :

$$\Phi_{c1} = \frac{N(\sqrt{2}\, I)\sin \omega_1 t}{S_{c1} + S_{log1}} \qquad (A.3.34)$$

$$\Phi_{c2} = \frac{N(\sqrt{2}\, I)\sin(\omega_1 t + \gamma)}{\{(S_{c2}+S_{log2})^2 + (\omega_1\, G_s)^2\}^{0.5}} \qquad (A.3.35)$$

where :

$$\gamma = -\tan^{-1}\frac{\omega_1\, G_s}{S_{c2}+S_{log2}} \qquad (A.3.36)$$

Knowing Φ_{c1} and Φ_{c2}, the related Φ_{g1} and Φ_{g2} can be calculated using (A.3.24). The pulling forces F_{p1} and F_{p2} can be found from (A.3.19). Since ;

$$F_p = F_{p1} + F_{p2} \qquad (A.3.37)$$

it follows that the armature movement can then be analysed from equation (A.3.28).

APPENDIX 4. SIMULATION OF THE RELAY ARMATURE MOVEMENT

A.4.1. Evaluating the attracting current

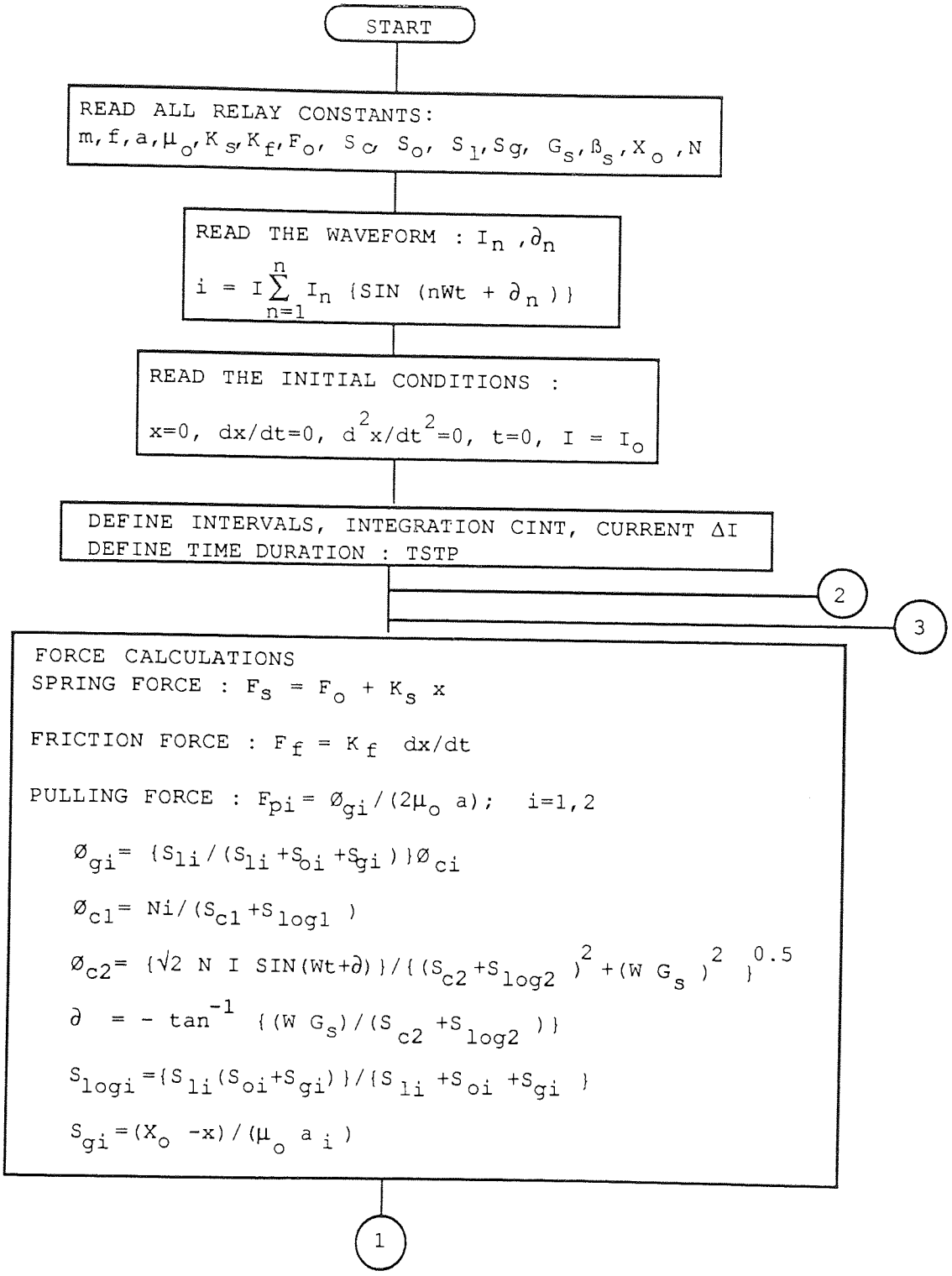

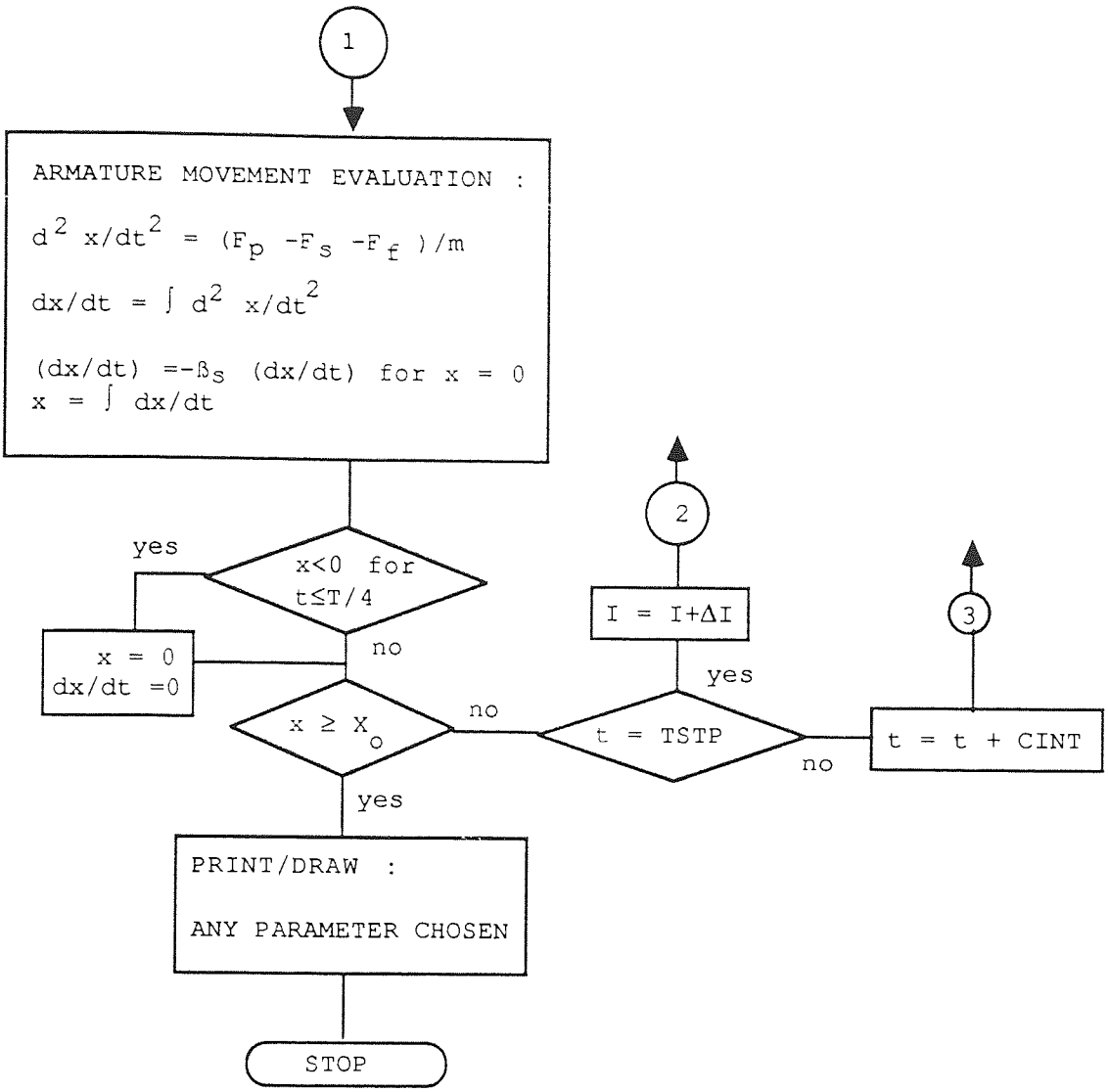

Program is kept under : 'IOC.CSL'

A.4.2. Evaluating the tripping current

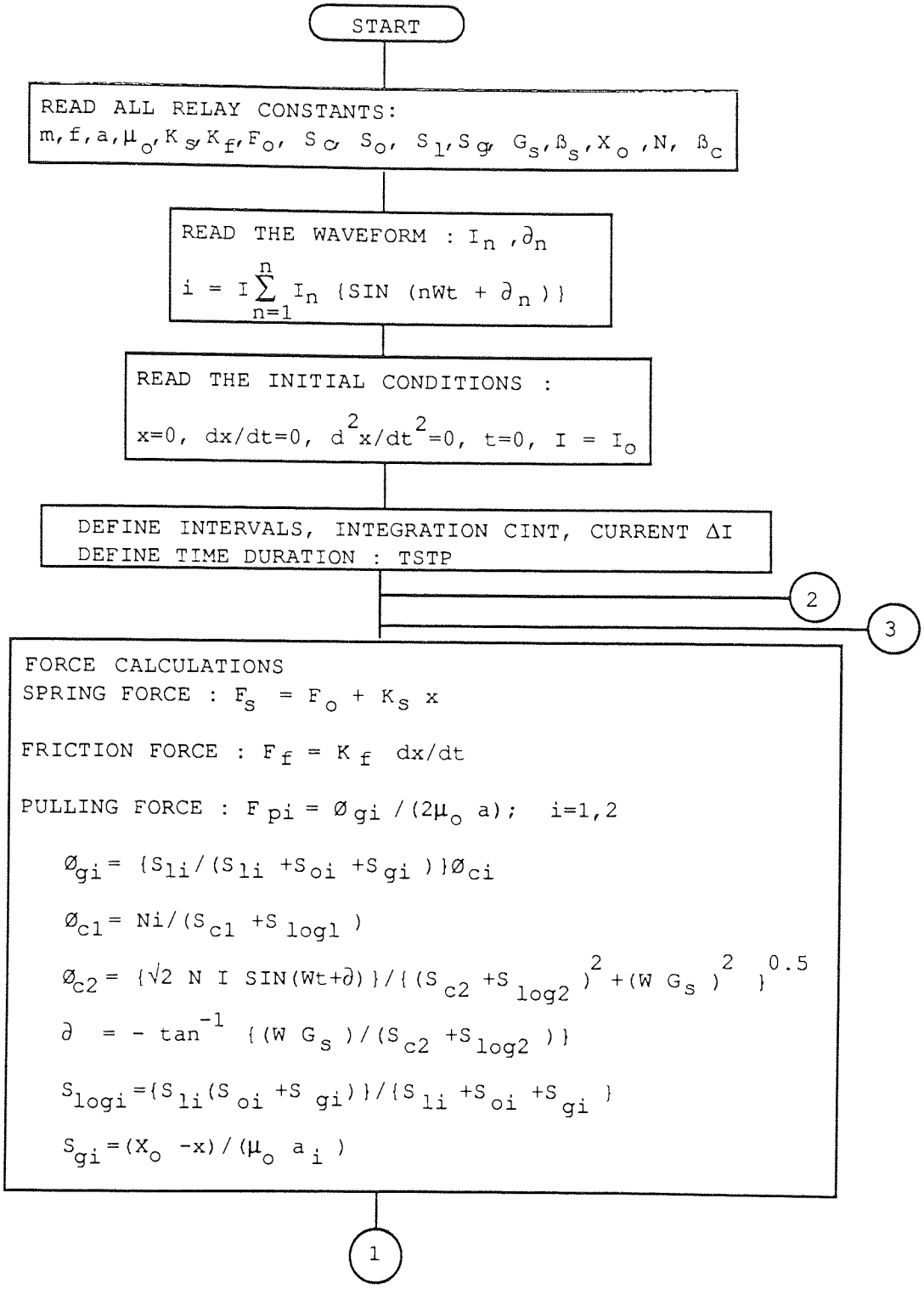

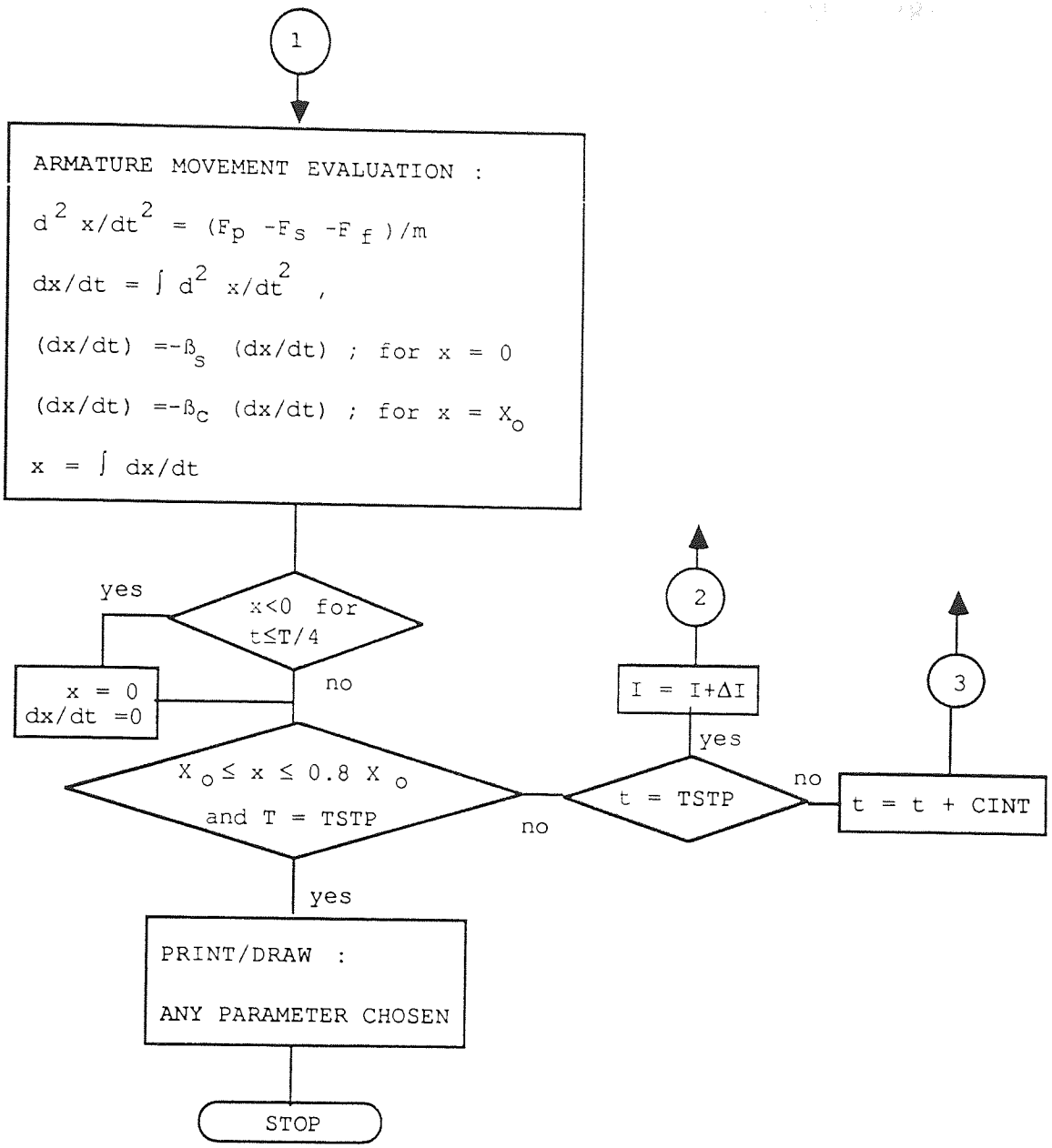

Program is kept under : 'NEWIOC.CSL'

APPENDIX 5. THE DRIVING TORQUE Td FOR A SINUSOIDAL CURRENT

The analysis is based on the diagram shown in Fig.8.1. Assuming that flux is linearly related to current. Let :

S_1 = Reluctance of flux path 1, the unshaded part of the pole.
S_2 = Reluctance of flux path 2, the shaded part of the pole.
i_{d1} = Induced disc current due to $\phi_{i,1}$
i_{d2} = Induced disc current due to $\phi_{i,2}$
i_{sc} = Induced current in the shorted turn
R_{sc} = Resistance of the shorted turn

Then :

$$\phi_{i,1} = (Ni + i_{d1})/S_1 \qquad (A.5.1)$$

$$\phi_{i,2} = (Ni + i_{d2} - i_{sc})/S_2 \qquad (A.5.2)$$

$$i_{sc} = (1/R_{sc})\, d\phi_{i,2}/dt \qquad (A.5.3)$$

$$i_{d1} = - k\, d\phi_{i,1}/dt \qquad (A.5.4)$$

$$i_{d2} = - k\, d\phi_{i,2}/dt \qquad (A.5.5)$$

where k is a constant of the disc. Assuming that one half of the pole is shaded such that $S_1 = S_2 = S$, and let $1/R_{sc} = k\, a$, where a is a constant dependent upon the disc, then :

$$(S + k\, d/dt)\, \phi_{i,1} = Ni \qquad (A.5.6)$$

$$(S + k\,(1+a)\, d/dt)\, \phi_{i,2} = Ni \qquad (A.5.7)$$

let $i = \sqrt{2}\, I \sin(\omega_1 t)$

where ω_1 is the fundamental angular frequency and I is the r.m.s. value.

Equations (A.5.6) and (A.5.7) can be written as :

$$Ni = \left[\{ S^2 + (\omega_1 k)^2 \}^{0.5} \angle \tan^{-1} (\omega_1 k/S) \right] \phi_{i,1}$$

and

$$Ni = \left[\{ S^2 + (\omega_1 k(1+a))^2 \}^{0.5} \angle \tan^{-1} \{ (\omega_1 k/S)(1+a) \} \right] \phi_{i,2}$$

It follows that ;

$$\phi_{i,1} = \frac{\sqrt{2}\, NI \sin(\omega_1 t + \alpha_1)}{S^2 \left[1 + (\omega_1 k/S)^2 \right]^{0.5}} \qquad (A.5.8)$$

$$\phi_{i,2} = \frac{\sqrt{2}\,NI\sin(\omega_1 t + \alpha_2)}{S^2\left[1 + \{(\omega_1 k/S)(1+a)\}^2\right]^{0.5}} \qquad \text{(A.5.9)}$$

where

$$\alpha_1 = -\tan^{-1}(\omega_1 k/S)$$

$$\alpha_2 = -\tan^{-1}\{(\omega_1 k/S)/(1+a)\}$$

The electromechanical torque developed in the disc is produced by the interaction of each flux with the current produced by the other flux.

$$T_d = K(i_{d1}\,\phi_{i,2} - i_{d2}\,\phi_{i,1}) \qquad \text{(A.5.10)}$$

where K is a constant.

Combining equations (A.5.8), (A.5.9), and (A.5.10), and taking the angular frequency as $n\omega_1$ it can be found that the driving torque for any sinusoidal current is :

$$T_{dn} = \frac{2K N^2 I_n^2 k\,\omega_1\,n\sin(\beta_n)}{S^2\left[1 + (k\omega_1/S)^2 n^2\right]^{0.5}\left[1 + \{k\omega_1(1+a)/S\}^2 n^2\right]^{0.5}} \qquad \text{(A.5.11)}$$

where $\beta_n = \alpha_{1n} - \alpha_{2n}$

$$= \{-\tan^{-1}(n\,\omega_1 k/S)\} - \{-\tan^{-1}(n\,\omega_1 k(1+a)/S)\}$$

and after some trigonometric manipulation, we get :

$$\beta_n = \tan^{-1}\frac{n\,a\,k\,\omega_1/S}{1 + \{(k\omega_1)^2(1+a)n^2\}/S^2}$$

as shown in equation 8.3.

APPENDIX 6. THE EQUATIONS FOR THE PREPARATION OF CURVE FITTING

Consider equation (8.1), written here as (A.6.1) :

$$T_{dn} = \frac{2\,K\,N^2\,\omega_1\,I_n^2\,k\,n\,\sin(\beta_n)}{S^2\left[1+(k\omega_1/S)^2\,n^2\right]^{0.5}\left[1+\{k\omega_1(1+a)/S\}^2\,n^2\right]^{0.5}} \qquad (A.6.1)$$

Let :

$$C_1 = k\omega_1/S$$

$$C_2 = k\omega_1(1+a)/S$$

$$C_T = 2\,K\,N^2\,k\,\omega_1/S^2$$

then (A.6.1) can be rewritten as :

$$T_{dn} = \frac{C_T\,I_n^2\,n\sin(\beta_n)}{\left[1+C_1^2\,n^2\right]^{0.5}\left[1+C_2^2\,n^2\right]^{0.5}} \qquad (A.6.2.a)$$

$$T_{dn} = \frac{C_T\,I_n^2\,n\sin(\beta_n)}{\left[1+n^2\,C_1^2+n^2\,C_2^2+n^4\,C_1^2\,C_2^2\right]^{0.5}} \qquad (A.6.2.b)$$

and (8.3), written here as (A.6.3) :

$$\beta_n = \tan^{-1}\frac{n\,a\,k\,\omega_1/S}{1+(k\omega_1)^2(1+a)n^2/S^2} \qquad (A.6.3)$$

can be rewritten as :

$$\beta_n = \tan^{-1}\frac{n\,(C_2-C_1)}{1+C_1\,C_2\,n^2} \qquad (A.6.4)$$

since $C_2 - C_1 = k\,\omega_1\,a/S$

From (A.6.4), sin β_n can be calculated :

$$\sin \beta_n = \frac{n\,(C_2 - C_1)}{\left[1 + n^2 C_1^2 + n^2 C_2^2 + n^4 C_1^2 C_2^2\right]^{0.5}} \qquad \text{(A.6.5)}$$

Combining equations (A.6.2.b) and (A.6.5), we obtain :

$$T_{dn} = \frac{C_T I_n^2 n^2 (C_2 - C_1)}{1 + n^2 C_1^2 + n^2 C_2^2 + n^4 C_1^2 C_2^2} \qquad \text{(A.6.6)}$$

which is the driving torque equation.

Now consider equation (8.7) written here as (A.6.7) :

$$\frac{I_{stn}^2}{I_{st1}^2} = \frac{1 + n^2 C_1^2 + n^2 C_2^2 + n^4 C_1^2 C_2^2}{n^2 (1 + C_1^2 + C_2^2 + C_1^2 C_2^2)} \qquad \text{(A.6.7)}$$

Taking :

$$n^2 = x$$

$$\frac{I_{stn}^2}{I_{st1}^2} = y'$$

$$C_1^2 = C_3$$
$$C_2^2 = C_4$$

then equation (A.6.7) can be rewritten as :

$$y' = \frac{1 + C_3 x + C_4 x + C_3 C_4 x^2}{x (1 + C_3 + C_4 + C_3 C_4)} \qquad \text{(A.6.8)}$$

again, let :

$$C_3 + C_4 = K_1$$
$$C_3 C_4 = K_2$$
$$y' x = y$$

then we obtain :

$$y = \frac{1}{1+K_1+K_2} + \frac{K_1}{1+K_1+K_2} x + \frac{K_2}{1+K_1+K_2} x^2 \qquad \text{(A.6.9)}$$

which can be rewritten as :

$$y = A_1 + A_2 x + A_3 x^2$$

The curve fitting method can then be used to obtain the constants A_1, A_2 and A_3.

APPENDIX 7. THE BREAKING TORQUE EQUATIONS

The movement of the disc is governed by the driving torque and three restraining torques, i.e the spring, the friction, the braking torques. The first two restraining torques are easily obtained, the last one however is more complicated. In this section, the equations for the braking torque are derived.

A.7.1. Permanent magnet breaking torque

$$T_{b,pm} = K_{b,pm}' \, \Phi_m \, i_m \qquad (A.7.1)$$

where Φ_m is the permanent magnet flux and i_m is the induced current in the disc due to Φ_m and the disc rotation. Taking the angular disc velocity as $v_a = dxa/dt$, then :

$$i_m = v_a \, \Phi_m / R_m \qquad (A.7.2)$$

R_m is the disc resistance.

Combining equations (A.7.1) and (A.7.2), we obtain :

$$T_{b,pm} = (K_{b,pm}' \, \Phi_m^2 / R_m) v_a \qquad (A.7.3.a)$$

$$= K_{b,pm} \, v_a \qquad (A.7.3.b)$$

Note, Φ_m and R_m are constants.

A.7.2. The breaking torque due to the flux produced by the current

As described in appendix 5, there are two fluxes produced by the current in the main winding. Due to these fluxes and the disc rotation, each flux induces a disc current. The interaction between them produces the self braking torque.

From equations (A.5.8) and (A.5.9), the fluxes are :

$$\phi_{i,1} = \frac{\sqrt{2}\, NI \sin(\omega_1 t + \alpha_1)}{S^2 \left[1 + (\omega_1 \, k/S)^2\right]^{0.5}} = \sqrt{2}\, \Phi_{i,1} \sin(\omega_1 t + \alpha_1) \qquad (A.7.4)$$

$$\phi_{i,2} = \frac{\sqrt{2}\, NI \sin(\omega_1 t + \alpha_2)}{S^2 \left[1 + \{(\omega_1 \, k/S)(1+a)\}^2\right]^{0.5}} = \sqrt{2}\, \Phi_{i,2} \sin(\omega_1 t + \alpha_2) \qquad (A.7.5)$$

and the disc currents due to the disc rotation are :

$$i_1 = v_a \sqrt{2}\, \Phi_{i,1} \sin(\omega_1 t + \alpha_1) \qquad \text{(A.7.6)}$$

$$i_2 = v_a \sqrt{2}\, \Phi_{i,2} \sin(\omega_1 t + \alpha_2) \qquad \text{(A.7.7)}$$

The average braking torque due to the fluxes and disc currents are :

$$T_{b,i1} = \omega_1/2\pi \int_0^{2\pi/\omega_1} (K_{b,i1}\, \phi_{i,1}\, i_1)\, dt = K_{b,i1}\, \Phi_{i,1}^2\, v_a \qquad \text{(A.7.8)}$$

$$T_{b,i2} = \omega_1/2\pi \int_0^{2\pi/\omega_1} (K_{b,i2}\, \phi_{i,2}\, i_2)\, dt = K_{b,i2}\, \Phi_{i,2}^2\, v_a \qquad \text{(A.7.9)}$$

The angular velocity $v_a = dx_a/dt$

The above are the equations as shown in (8.11).

APPENDIX 8. THE CURVE FITTING METHOD

The curve fitting program used is the one developed by NAG for computing a two dimensional curve, E02 ADF. By inputing the data, degree of polynomial equation and the weighting factor, the program will then compute the Chebyshef polynomial constants of the curve that fits this data.

For a two degree equation as shown in (A.6.8), the program will compute all constants of the equation :

$$y = 0.5\, Ch_0\, T_0(X) + Ch_1\, T_1(X) + Ch_2\, T_2(X) \qquad (A.8.1)$$

where :

$$T_0(X) = 1$$
$$T_1(X) = X$$
$$T_2(X) = 2X^2 - 1$$

Ch_i are Chebyshef constants, i = 0,1,2

X is the 'normalised' x, where x is the data, and :

$$X = (2x - x_{max} - x_{min})/(x_{max} - x_{min}) \qquad (A.8.2)$$

x_{max} and x_{min} are the maximum and minimum values of x respectively. It is thus clear, that the value of X lies between 0 and 1.

Equation (A.8.1) can be converted to a standard polynomial equation of the form;

$$y = A_1 + A_2 x + A_3 x^2$$

The program to compute the Chebyshef constants and change them to standard polynomial constants then evaluates the relay constants C_1 and C_2 is given below.

A.8.1. Program to prepare test results data (starting current & harmonic number) for computation using NAG

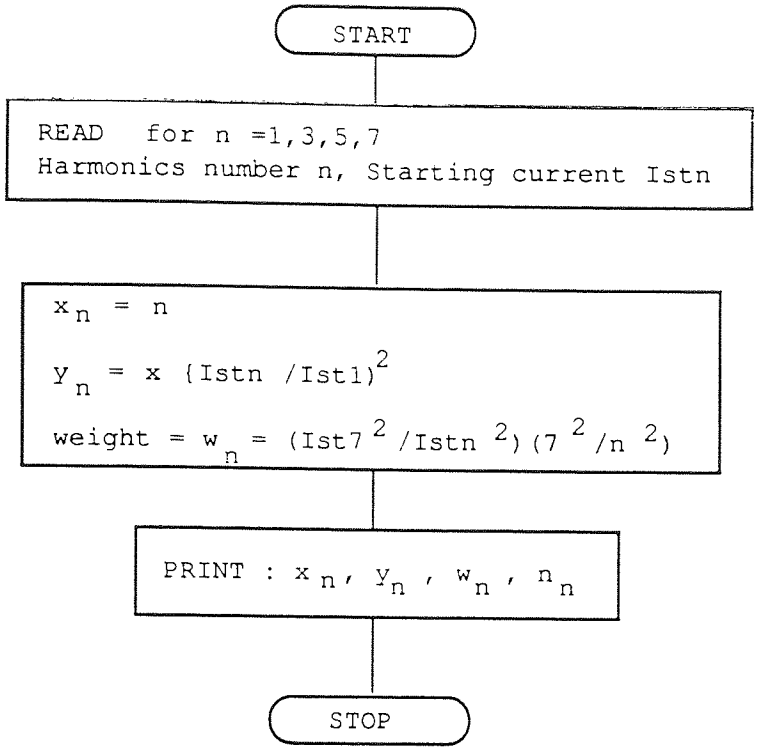

Program is kept under : 'DATACHEF.FOR'
Result is kept under : 'RDATACHEF.DAT'

A.8.2. Program to compute Chebyshef constants

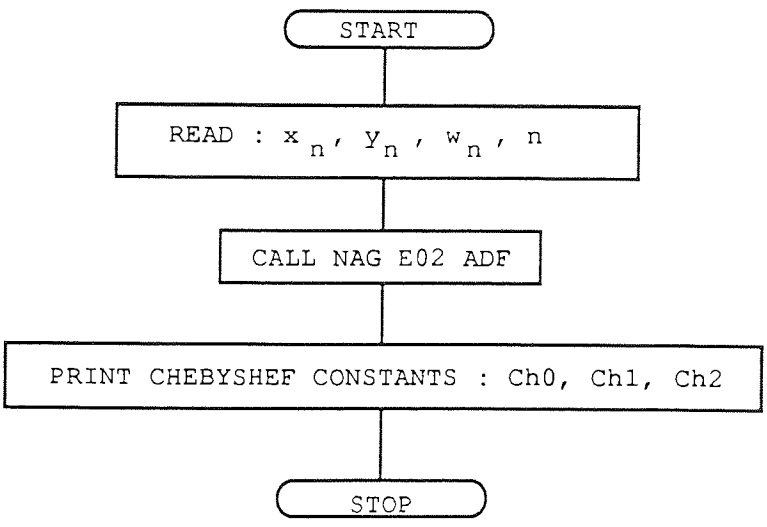

Program is kept under : 'CHEF1.FOR'
Input is read from : 'RDATACHEF.DAT'
Result is kept under : 'NEWRCHEF,DAT'

A.8.3. Program to change Chebyshef constants into standard polynomial constants and to evaluate relay constants C_1 and C_2.

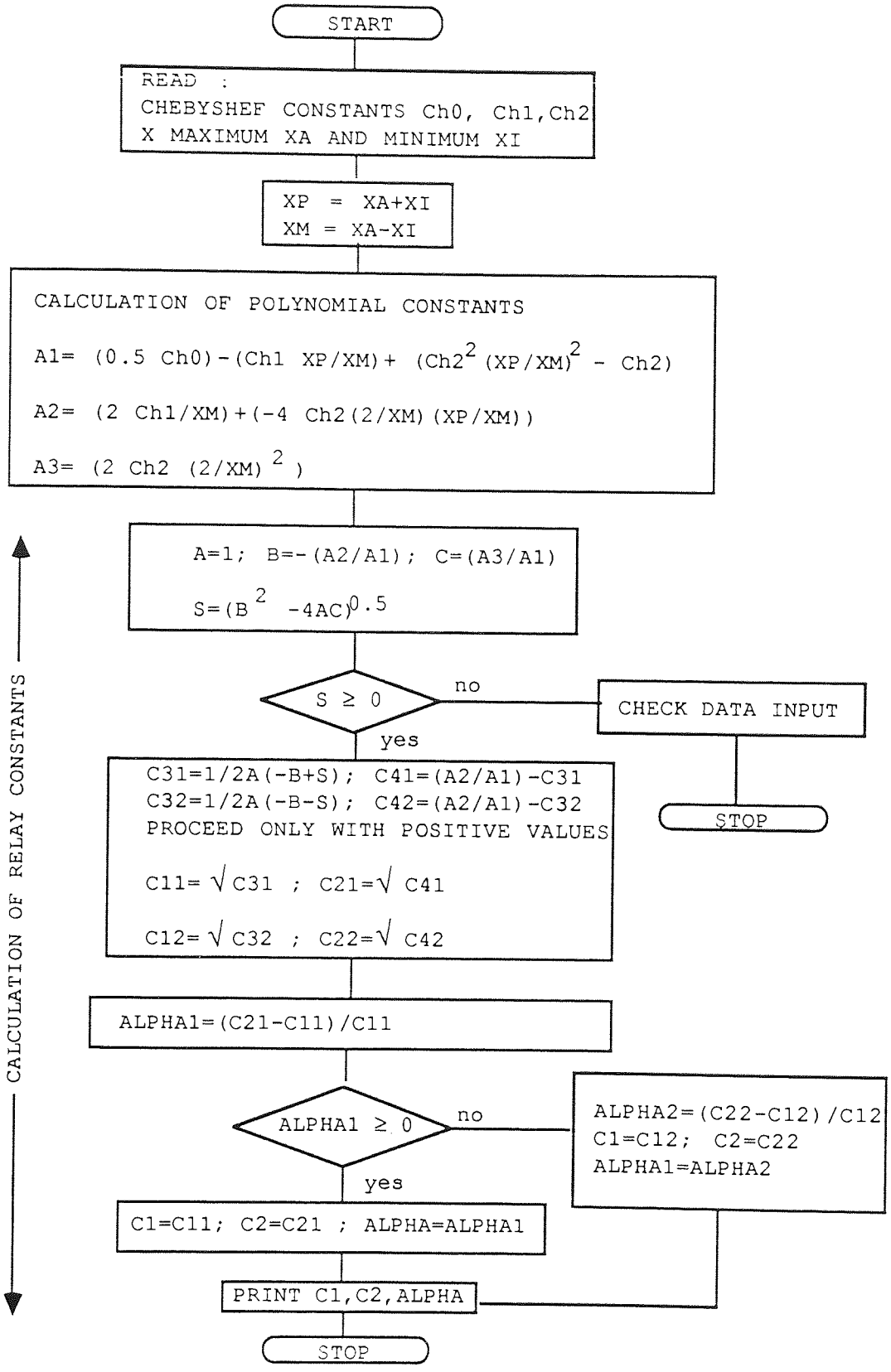

Program is kept under : 'POLCHEFC1.FOR'
Input is read from : 'NEWRCHEFC.DAT'
Result is kept under : 'NEWRPOLCHFC.DAT'

A.8.4. Program to evaluate the tripping time for non-sinusoidal current (for harmonic number 2 to 7)

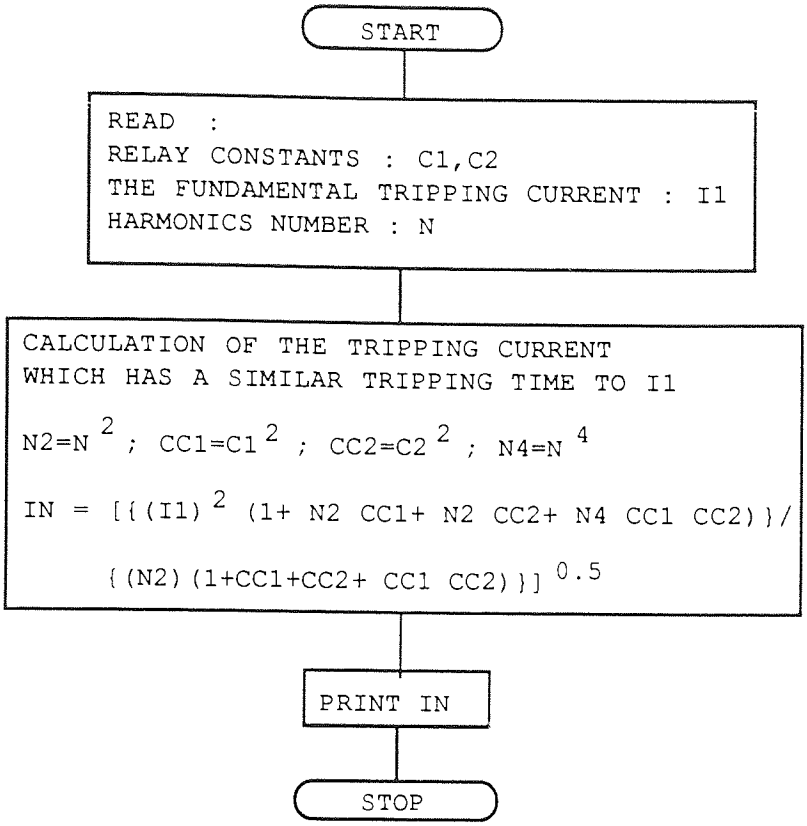

Program is kept under : 'ISTN1.FOR'
Input is read from : 'NEWRPOLCHEFC.DAT'

APPENDIX 9. THE DRIVING TORQUE FOR A NON LINEAR RELAY SYSTEM

If a non-sinusoidal current is passed through an EM TOC relay winding, then as shown in appendix 3, it will produce two fluxes, each has a phase angle with respect to the current. These two fluxes will then induce two disc currents;

$$i = \sum_{n=1}^{\infty} i_n \; ; \text{ where } i_n = \sqrt{2}\, I_n \sin(n\omega_1 t) \qquad \text{(A.9.1)}$$

the fluxes produced by the current i are :

for the unshaded pole ;

$$\phi_{i,1} = \sum_{n=1}^{\infty} \phi_{in,1} \; ; \text{ where } \phi_{in,1} = \sqrt{2}\, \Phi_{in,1} \sin(n\omega_1 t + \partial_{1n}) \qquad \text{(A.9.2)}$$

for the shaded pole ;

$$\phi_{i,2} = \sum_{n=1}^{\infty} \phi_{in,2} \; ; \text{ where } \phi_{in,2} = \sqrt{2}\, \Phi_{in,2} \sin(n\omega_1 t + \partial_{2n}) \qquad \text{(A.9.3)}$$

The induced disc currents are :

$$i_{d1} = \sum_{n=1}^{\infty} i_{n,d1} \; ; \text{ where } i_{n,d1} = -\, k \sqrt{2}\, \phi_{in,1}\, n\omega_1 \cos(n\omega_1 t + \partial_{1n})$$

$$i_{d2} = \sum_{n=1}^{\infty} i_{n,d2} \; ; \text{ where } i_{n,d2} = -\, k \sqrt{2}\, \phi_{in,2}\, n\omega_1 \cos(n\omega_1 t + \partial_{2n}) \qquad \text{(A.9.4)}$$

The driving torque is :

$$T_d = K\,(i_{d1}\, \phi_{i,2} - i_{d2}\, \phi_{i,1})$$

As an illustration, the driving torque for a current that contains third harmonics will be shown.

Consider the two fluxes as :

$$\phi_{i,1} = \phi_{i1,1} + \phi_{i3,1}$$

$$= \sqrt{2}\, \Phi_{i1,1} \sin(\omega_1 t + \partial_{11}) + \sqrt{2}\, \Phi_{i3,1} \sin(3\omega_1 t + \partial_{13})$$

$$\phi_{i,2} = \phi_{i1,2} + \phi_{i3,2}$$

$$= \sqrt{2}\, \Phi_{i1,2} \sin(\omega_1 t + \partial_{21}) + \sqrt{2}\, \Phi_{i3,2} \sin(3\omega_1 t + \partial_{23})$$

These two fluxes produce two induced disc currents ;

$$i_{d1} = i_{1,d1} + i_{3,d1}$$

$$= \sqrt{2}\, I_{1,d1} \sin(\omega_1 t + \partial_{11}) + \sqrt{2}\, I_{3,d1} \sin(3\omega_1 t + \partial_{13})$$

$$i_{d2} = i_{1,d2} + i_{3,d2}$$

$$= \sqrt{2}\, I_{1,d2} \sin(\omega_1 t + \partial_{21}) + \sqrt{2}\, I_{3,d2} \sin(3\omega_1 t + \partial_{23})$$

The driving torque is :

$$T_{d\ 1,3} = (\phi_{i1,2}\, i_{1,d1} + \phi_{i3,2}\, i_{3,d1}) + (\phi_{i1,2}\, i_{3,d1} + \phi_{i3,2}\, i_{1,d1})$$

$$- (\phi_{i1,1}\, i_{1,d2} + \phi_{i3,1}\, i_{3,d2}) - (\phi_{i1,1}\, i_{3,d2} + \phi_{i3,1}\, i_{1,d2})$$

After a series of algebraic manipulation, the result is

$$T_{d\ 1,3} = T_1 + T_2 \sin(2\, \omega_1 t + \partial_{2T}) + T_4 \sin(4\, \omega_1 t + \partial_{4T})$$

where T_j and ∂_{jT} are constants; j = 1,2,4

APPENDIX 10. THE DRIVING TORQUE COMPUTATION FOR A NON LINEAR CORE

A.10.1. Program to evaluate the distortion of the flux waveform

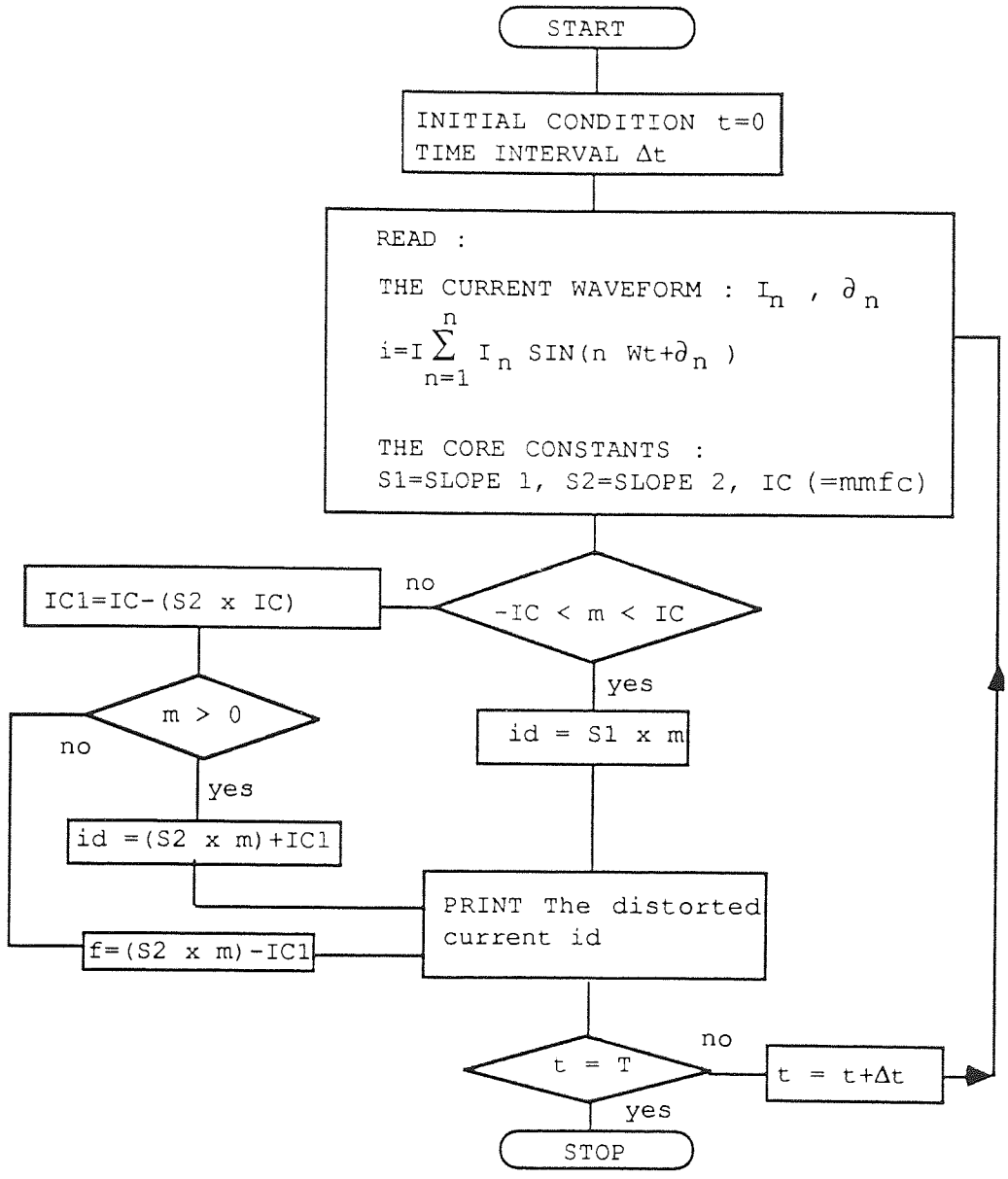

Program is kept under : 'NONLIN-31.FOR'
Result is kept under : 'RNONLIN-3.DAT'

A.10.2. Harmonic analysis of the flux waveform

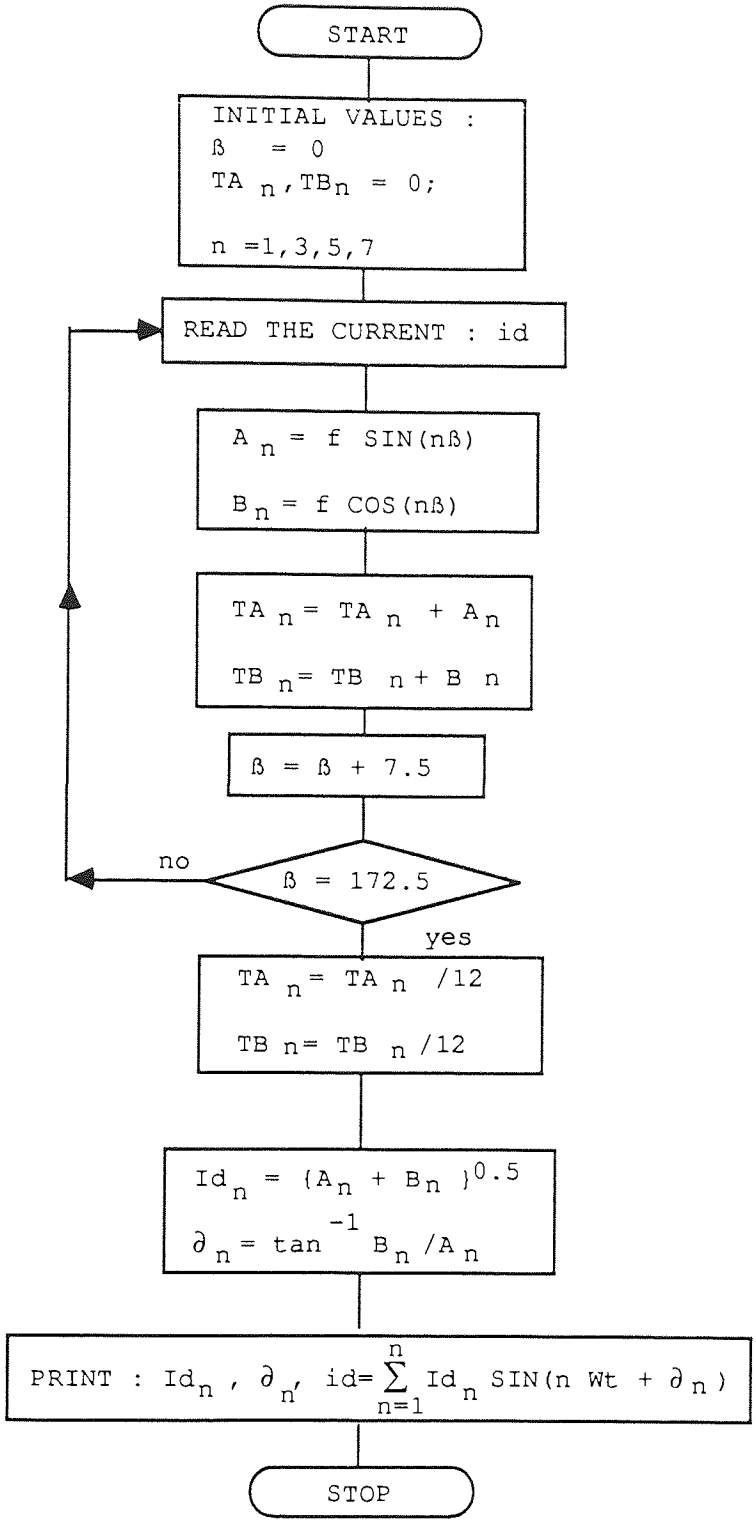

Program is kept under : 'HARMEVA.FOR'
Input is read from : 'RNONLIN-3.DAT'
Result is kept under : 'NEWRHARMEVA.DAT'

A.10.3. Program to compute the driving torque

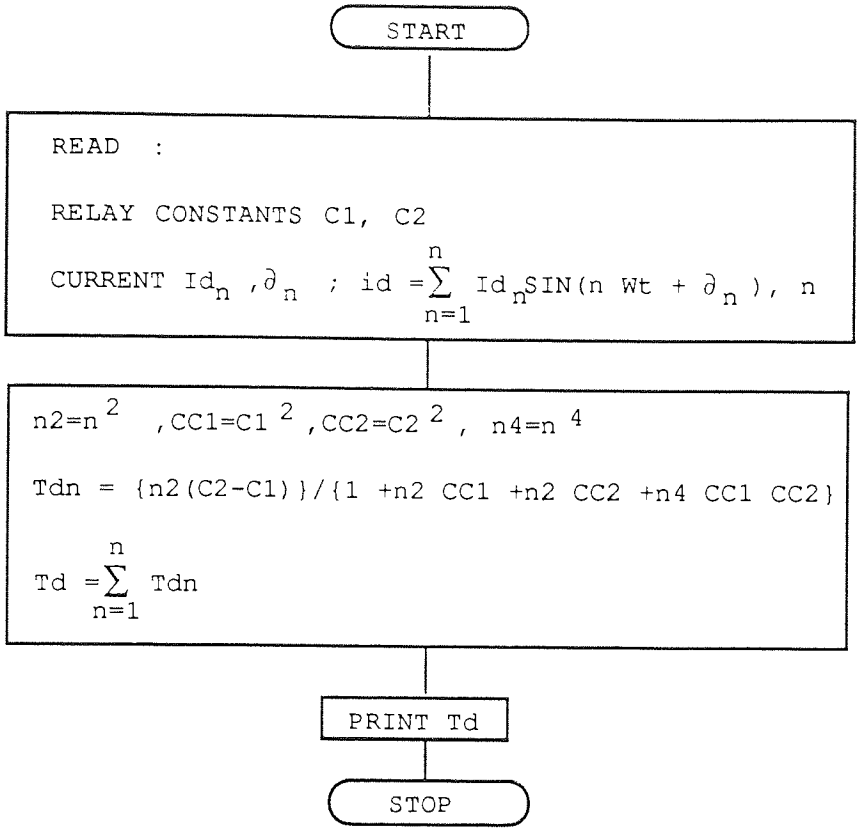

Program is kept under : 'TORQUE.FOR'
Input is read from : 'NEWRPOLCHEFC.DAT' (constants C_1 and C_2)
and 'NEWRHARMEVA.DAT' (current waveform)

APPENDIX 11. PAPERS PUBLISHED

All the six papers published as the results of this study are presented in this appendix.

1. SASTROSUBROTO, A.S., FEATHERSTONE, A.M.: 'An examination of the tripping time characteristics of Residual Current Circuit Breakers which may give rise to failures', 23rd University Power Engineering Conference, Nottingham, UK, 20-22 September 1988.

2. SASTROSUBROTO, A.S., FEATHERSTONE, A.M.: 'The simulation of electromechanical overcurrent relays with respect to harmonics', 23rd University Power Engineering Conference, Nottingham, UK, 20-22 September 1988.

3. FEATHERSTONE, A.M., SASTROSUBROTO, A.S.: 'The Simulation and Mathematical modelling of harmonic disturbances on electro-heat protection equipment', International Seminar on Mathematical Modelling in Electroheat, Leningrad, USSR, 20-24 June 1989.

4. SASTROSUBROTO, A.S., FEATHERSTONE, A.M.: 'Continuous simulation model of electromechanical instantaneous type relays with respect to harmonics', 3rd European Simulation Congress, Edinburgh, UK, 5-8 September1989.

5. SASTROSUBROTO, A.S., FEATHERSTONE, A.M.: 'The effects of harmonics on the operating poiunts of electromechanical overcurrent relays', 24th University Power Engineering Conference, Belfast, UK, 19-21 September1989.

6. SASTROSUBROTO, A.S., FEATHERSTONE, A.M.: 'Probability evaluation of Residual Current Circuit Breaker testing method', 24th University Power Engineering Conference, Belfast, UK, 19-21 September1989.

AN EXAMINATION OF THE TRIPPING TIME CHARACTERISTICS OF RESIDUAL CURRENT CIRCUIT BREAKERS (RCCBs) WHICH MAY GIVE RISE TO FAILURES.

A.S. Sastrosubroto and A.M. Featherstone

Aston University

Content has been removed for copyright reasons

THE SIMULATION OF ELECTROMECHANICAL OVERCURRENT RELAYS WITH RESPECT TO HARMONICS.

A.S. Sastrosubroto and A.M. Featherstone

Aston University

Content has been removed for copyright reasons

THE SIMULATION AND MATHEMATICAL MODELLING OF HARMONIC DISTURBANCES ON ELECTRO-HEAT PROTECTION EQUIPMENT

A.M.Featherstone and A.S.Sastrosubroto

Aston University

Content has been removed for copyright reasons

THE EFFECTS OF HARMONICS ON THE OPERATING POINTS OF ELECTROMECHANICAL OVERCURRENT RELAYS

A.S. Sastrosubroto and A.M. Featherstone

Aston University

Content has been removed for copyright reasons

PROBABILITY EVALUATION OF RESIDUAL CURRENT CIRCUIT BREAKER (RCCB) TESTING METHOD

A.S. Sastrosubroto and A.M. Featherstone

Aston University

Content has been removed for copyright reasons